ENHANCEMENT OF THE INTERFACIAL TRANSFER OF IODINE BY CHEMICAL REACTION

by

Juliette Roseanne Ling

A thesis submitted in conformity with the requirements for the degree of
Master of Applied Science
Graduate Department of Chemical Engineering and Applied Chemistry
University of Toronto

Enhancement of the Interfacial Transfer of Iodine by Chemical Reaction

Juliette Roseanne Ling, M.A.Sc. Thesis, 1997, Graduate Department of Chemical Engineering and Applied Chemistry, University of Toronto

Enhancement of the interfacial transfer of iodine by chemical reaction was studied by developing a mechanistic model to simulate the interfacial transfer of iodine, and then testing the model experimentally. The reactions considered were those of iodine with thiosulphate, iodide, and hydroxide ions and radiolytic reactions. Two separate systems were studied; one for evaporation and one for absorption of iodine. It was found that impingement had a significant effect on interfacial transfer, promoting absorption into solution and impeding evaporation from solution. Also, the overall mass transfer coefficient of iodine was dependent upon the concentration of $I_2(g)$ in the system and/or the equilibrium constant of the reaction, depending on the reaction involved. As well, radiolytic reactions enhanced the interfacial transfer of iodine, and the degree of enhancement was dependent upon the dose rate of the radiation field present and the pH of the solution.

I would like to thank the following people for their contribution to the completion of this project:

Dr. Evans, for his guidance and supervision

the members of the Environmental and Nuclear Engineering Group, especially Fariborz, Sevana, Tutun, Mark, Phil and Nawal, for their advice, assistance and encouragement

my family, for their support and tolerance

and my sister Nicole, for everything

Most of all, I would like to thank God for surrounding me with all these people, who have been there for me when I was most in need of comfort and support.

NOMENCLATURE

A	gas-liquid interfacial surface area (cm^2)
$C_{X,eq}$	concentration of X at equilibrium (M)
$C_{X,i}$	concentration of X at the gas-liquid interface (M)
D	diffusivity (cm^2/s)
δ_g	thickness of the gas side film (cm)
δ_l	thickness of the liquid side film (cm)
F	flow rate of air (cm^3/s)
φ	the enhancement factor
φ_{max}	the maximum enhancement factor
H	iodine water/air equilibrium partition constant
$[I_2]_{gasin}$	concentration of iodine gas entering the reaction vessel (M)
$[I_2]_{aq}$	aqueous concentration of iodine (M)
k_b	reverse reaction rate constant of a reversible reaction
k_f	forward reaction rate constant of a reversible reaction
k_g	gas phase mass transfer coefficient (cm/s)
k_l	liquid phase mass transfer coefficient (cm/s)
k_l'	enhanced liquid phase mass transfer coefficient (cm/s)
k_r	rate constant of a second order irreversible reaction
k_r'	pseudo first order rate constant of a reaction
K_{eq}	equilibrium constant of a reversible reaction
K_{OG}	overall mass transfer coefficient based on the gas side (cm/s)
K_{OL}	overall mass transfer coefficient based on the liquid side (cm/s)
N	rate of mass transfer (mol/s)
P_{amb}	partial pressure of the ambient water vapour
P_{sat}	saturation partial pressure of water at temperature T
s	fractional rate of surface renewal, as defined by the surface renewal theory

$t_{c,l}$	contact time, as defined by the penetration theory
V_l	volume of the liquid phase (cm^3)
V_g	volume of the gas phase (cm^3)

LIST OF TABLES

1. INTRODUCTION

Interfacial mass transfer, which is the transfer of material from one phase to another, is of particular importance in industry. It occurs in many facets of engineering, including separation and recovery operations, chemical manufacturing processes, electrochemical deposition processes, distillation and gas chromatography. It has long been recognised that the efficiency of many of these processes can be improved by enhancing mass transfer. This can be accomplished by changing the design of the system, adjusting operating conditions, or by chemical reaction.

This study is concerned with gas-liquid interfacial transfer. There are many different types of gas-liquid mass transfer equipment. Examples of these are packed and plate columns, trickle bed reactors, scrubbers, agitated vessels and bubble columns. These pieces of equipment are all designed with the idea of promoting the rate of gas absorption or desorption. Large surface area to volume ratios, long residence times and fluid agitation are factors that are common to almost all gas-liquid mass transfer equipment. It was early in the twentieth century that the almost limitless potential of chemical reaction to enhance mass transfer was recognised. Specifically, it was observed that rapid chemical conversion of a molecule in a liquid phase could greatly reduce the time required for its transfer from an interface to the bulk fluid, thereby increasing its liquid phase mass transfer coefficient.

In this study, the effect of various chemical reactions on the interfacial transfer of iodine was studied. The objectives were: (1) to measure the enhancement as a function of the concentration of the reactants, (2) to create a mechanistic model to simulate these systems and (3) to extend this model to predict the extent of enhancement due to radiolytic reactions.

The reactions that were investigated in this research were those between iodine and thiosulphate ions, iodide ions and hydroxide ions. Iodine was an ideal choice for this study because it is volatile, is easily measured, and the kinetics of the reactions had already been determined. There was also some industrial significance in the choice of iodine for this study. Iodine-131, in the form of caesium iodide, is a fission product produced in nuclear reactors. Under conditions that could arise inside the containment structure of a reactor, some of this caesium iodide might be converted to iodine via radiolytic reactions. If the mass

volatilisation of radioiodine may be accelerated, increasing the amount of gas phase iodine potentially available for release to the environment. Conversely, the high concentrations of thiosulphate in the sprays that might be used in some containment structures could also enhance interfacial transfer, thereby improving the scrubbing efficiency of these sprays. It was therefore worthwhile to investigate whether or not the mass transfer of iodine is enhanced by chemical reaction, and, if it is, under what conditions.

The study was divided into two main parts: (1) experimental collection of mass transfer data and (2) computer simulation of mass transfer with chemical reaction. The first part was performed for simple systems in which iodine gas was either absorbed into solution or evaporated from solution, in the absence and in the presence of various chemical reactions. The system basically consisted of a flow of gas impinging onto a stagnant pool. The methods used for determining the aqueous concentration of iodine in the system were radioactive tracing and ultra-violet spectrophotometry. The extent of the enhancement of mass transfer was measured by comparing mass transfer parameters in the presence of chemical reaction to those for physical absorption alone. The second part of the study was done by using the FACSIMILE program to model the mass transfer of iodine in the presence of the chemical reactions that were investigated in the first part. This was done to verify that the model worked. Once this was accomplished, the model was extended to include mass transfer in the presence of a radiation field.

In this document, the basic principles behind mass transfer are outlined in chapter 2. Chapter 3 provides a review of published literature on the effect of chemical reactions on the rate of mass transfer. Chapter 4 gives a detailed description of the experimental procedures followed in performing the experimental part of the project, and chapter 5 provides details on the computer modelling part of the project. Chapter 6 presents the results of the study, together with a discussion of these results. Finally, conclusions are made in chapter 7.

2.1 DIFFUSION EQUATIONS

Diffusion is the random motion of particles in a fluid. The driving force for diffusion is concentration gradients within the fluid. The equations governing one-dimensional diffusion of a species A are

$$\frac{\partial a}{\partial t} = D_A \frac{\partial^2 a}{\partial x^2} \qquad 2\text{-}1$$

$$R = -D_A \frac{\partial a}{\partial x} \qquad 2\text{-}2$$

where a is the concentration of A as a function of space and time and R is the flux of A across a unit area perpendicular to the direction of diffusion. Equation 2-1 is Fick's second law of diffusion, and can be derived from the continuity equation by assuming constant density and diffusivity, and a stagnant fluid. For a gas, A, being absorbed into a liquid, equation 2-2 defines the rate of absorption of A, where x is the distance from the gas-liquid interface. For a system in which diffusion is accompanied by chemical reaction, equation 2-2 is unchanged but equation 2-1 becomes

$$\frac{\partial a}{\partial t} = D_A \frac{\partial^2 a}{\partial x^2} - r_A(x,t) \qquad 2\text{-}3$$

where r_A is the rate at which A is consumed by the reaction. Solutions to equations 2-1, 2-2 and 2-3 are given in most mass transfer texts [1, 2, 3].

2.2 GAS-LIQUID INTERFACIAL MASS TRANSFER PRINCIPLES

A molecule diffusing from the gas phase to the liquid phase or vice versa is said to undergo interphase mass transfer. The rate of mass transfer across the gas-liquid interface is given by equations 2-4 and 2-5 [2, 3, 4].

$$= -V_g \frac{d}{dt} C_g = k_g A(C_g - C_{g,i}) \quad 2\text{-}5$$

In these equations, C_l and C_g denote the bulk concentrations in the liquid and gas phases respectively, $C_{l,i}$ and $C_{g,i}$ denote the liquid and gas interfacial concentrations and k_l and k_g are the liquid and gas phase mass transfer coefficients. If the mass transfer system is closed, equilibrium will be achieved. At this stage, the concentrations in the gas and liquid phases will be related by equation 2-6. Subscript eq indicates equilibrium concentrations and H is the liquid-gas equilibrium partition coefficient.

$$\frac{C_{l,eq}}{C_{g,eq}} = H \quad 2\text{-}6$$

It is experimentally difficult to measure concentrations at the interface, and therefore it is more useful to describe the rate of diffusion in terms of bulk concentrations. Equations 2-7 and 2-8 give the rate of mass transfer in terms of the concentrations of the diffusing species in the bulk gas and bulk liquid phases.

$$N = V_l \frac{d}{dt} C_l = K_{OL} A(C_l - HC_g) \quad 2\text{-}7$$

$$= K_{OG} A(\frac{C_l}{H} - C_g) \quad 2\text{-}8$$

The terms K_{OL} and K_{OG} denote the overall mass transfer coefficients using, respectively, the liquid and gas side as the basis, and are defined by equations 2-9 and 2-10.

$$\frac{1}{K_{OL}} = \frac{1}{k_l} + \frac{H}{k_g} \quad 2\text{-}9$$

$$\frac{1}{K_{OG}} = \frac{1}{Hk_l} + \frac{1}{k_g} \quad 2\text{-}10$$

In this study, K_{OL} will be the parameter used to describe mass transfer, and hence all subsequent reference to the overall mass transfer coefficient will pertain to K_{OL}.

It is generally believed that in interfacial mass transfer, there exists two films which impede mass transfer, and hence the rate of mass transfer is dependent upon transfer through these two films. The films are located immediately above and below the mass transfer interface; one in the gas phase and one in the liquid phase. Many theories have been proposed to explain the phenomenon of mass transfer inside these two films, but only three are widely accepted today [2, 3, 4].

The first theory is the stagnant film theory. This theory postulates that the films are stagnant, and transfer through them occurs by diffusion only. For a molecule diffusing through one of these stagnant films, the thickness of the film is important. In the case of the gas phase film, if the thickness of the film is δ_g, and the diffusivity of the diffusing species in the gas phase is D, then the gas phase mass transfer coefficient is given by equation 2-11.

$$k_g = \frac{D}{\delta_g} \qquad 2\text{-}11$$

Equation 2-11 can be applied to the liquid phase by replacing subscript g with subscript l and defining D as the diffusivity in the liquid phase.

The second mass transfer theory is the penetration theory. In this theory, it is proposed that transfer through a film results from contact between the bulk phase and the film. The length of time for which contact occurs is an important parameter in determining the transfer rate. If, for the liquid phase film, the contact time is $t_{c,l}$, then the liquid phase mass transfer coefficient is given by equation 2-12.

$$k_l = 2\sqrt{\frac{D}{\pi t_{c,l}}} \qquad 2\text{-}12$$

As with the film theory, equation 2-12 can be applied to both the liquid phase and the gas phase by using the appropriate values of D and t_c.

The third theory is Danckwerts surface renewal theory. This theory is similar to the penetration theory in that it also proposes contact between the bulk and film. However, in the surface renewal theory, it is proposed that fluid in the film is continually replaced by fresh liquid from the bulk. This replacement may be a result of a combination of factors including

is given by equation 2-13, which, as with the other theories, can also be applied to the gas phase.

$$k_l = \sqrt{Ds} \qquad 2\text{-}13$$

In equation 2-13, s is the fractional rate of surface renewal.

The parameters δ, t_c and s are all difficult to measure directly, and can only be estimated from mass transfer rates. They are highly dependent on experimental conditions, including temperature, pressure, fluid flow rate and geometry of the system.

Although the three mass transfer models are very different, they are all based on plausible theories. For example, the stagnant film theory suggests that the mass transfer coefficient is directly proportional to diffusivity, whereas the other two models suggest that the mass transfer coefficient is related to the square root of the diffusivity. However, in many empirical correlations k_l is proportional to $D^{2/3}$, 2/3 being between ½ and 1. Sherwood, Pigford and Wilke [3] compared the three models in terms of mass transfer enhancement, and concluded that all three models are adequate in predicting mass transfer enhancement due to chemical reaction.

2.4 LIQUID AND GAS PHASE LIMITATIONS

As with any rate, the rate of mass transfer depends on the slowest step in the process. If mass transfer through the liquid phase boundary is slower than transfer through the gas phase film, then the rate of mass transfer will depend more on the liquid phase than on the gas phase, and vice versa.

If the stagnant film theory is used, then the ratio of diffusivity to film thickness will determine which film is rate limiting. The film for which this ratio is smaller will be the rate limiting film. If the penetration theory is used, then the ratio of diffusivity to contact time will determine which film is rate limiting, and if the surface renewal theory is used, the product of diffusivity and fractional rate of surface renewal will determine which film is rate limiting. In extreme cases, it is possible for the mass transfer rate to be limited by one of the phases to such an extent that the rate depends totally on that one phase. In these cases, the

k_g/H, then K_{OL} will depend on k_g only, and the rate of mass transfer will be gas phase limited. If, on the other hand, k_g/H is infinitely large compared to k_l, then K_{OL} will be equal to k_l, and the rate of mass transfer will be totally liquid phase limited.

2.5 THE ENHANCEMENT OF MASS TRANSFER BY CHEMICAL REACTION

If mass transfer occurs in the presence of chemical reaction in the liquid phase, then equation 2-4 has to be modified to account for the enhancement of mass transfer by the reaction. Equation 2-14 defines the new rate of mass transfer, k_l' being the enhanced liquid phase mass transfer coefficient.

$$N = k_l'(C_l - C_i) \qquad 2\text{-}14$$

The extent of the enhancement is measured by the enhancement factor, φ, defined as the ratio of the liquid phase mass transfer coefficient in the presence of chemical reaction to the liquid phase mass transfer coefficient for physical absorption alone [2, 3, 4].

$$\varphi = \frac{k_l'}{k_l} \geq 1 \qquad 2\text{-}15$$

The enhancement factor is a function of the rate constant of the reaction and the concentration of reactant.

There are many different types of chemical reactions, and different conditions under which each reaction takes place. In this study, first order reactions will be considered with respect to reversibility of reaction and rate of reaction. Reactions will be categorised as slow, fast or instantaneous and either irreversible or reversible. Second order and pseudo-first order reactions will also be discussed.

2.5.1 FIRST ORDER REACTIONS

Consider gas A being absorbed into a liquid and undergoing irreversible reaction in the liquid to form B.

$$A \rightarrow B$$

reaction occurs, and hence, most of the reaction will occur in the bulk layer. In this case, the absorption process will be the same as for physical absorption without reaction, and mass transfer will not be enhanced. If the reaction is fast enough, then most of the reaction will occur in the liquid phase film and mass transfer will be significantly enhanced. Using the surface renewal model, an equation for approximating a value of the enhancement factor is given by

$$\varphi = \sqrt{\left(1 + \frac{Dk_r}{k_l^2}\right)} \qquad 2\text{-}16$$

Using the stagnant film theory, the enhancement factor is given by

$$\varphi = \sqrt{\frac{Dk_r}{k_l^{\,2}}} \qquad 2\text{-}17$$

If the reaction is instantaneous, then all of the reaction will occur in the liquid phase film. If k_r is large enough, then both equations 2-16 and 2-17 predict that the enhancement of the liquid side mass transfer can be practically infinite [2, 3].

The above discussion for slow reactions would still apply if the reaction was reversible rather than irreversible.

$$A \leftrightarrow B$$

However, for an instantaneous, reversible first order reaction with finite equilibrium constant K_{eq}, the enhancement is limited. The maximum value that the enhancement factor can attain is given by equation 2-18 [3].

$$\varphi_{max} = 1 + K_{eq} \qquad 2\text{-}18$$

2.5.2 SECOND ORDER REACTIONS

For an irreversible second order reaction of the form

$$A + \beta B \rightarrow \gamma C$$

the maximum value of φ is given by equation 2-19 [2, 3].

$$\varphi_{max} = \frac{D_A \beta [A]_i}{} \qquad 2\text{-}19$$

In this equation, $[B]_{initial}$ is the initial concentration of reactant B and $[A]_i$ is the concentration of A at the interface. For second order reversible reactions of the form

$$A + \beta B \leftrightarrow \gamma C$$

the derivation of an equation for the enhancement factor is complicated. However, combining appropriate forms of equations 2-4 and 2-15, φ may be obtained from equation 2-20.

$$\varphi = \frac{N_A}{k_l(A_i - A_{initial})} \qquad 2\text{-}20$$

2.5.3 PSEUDO FIRST ORDER REACTIONS

In special cases, the behaviour of second order reactions can be approximated by first order kinetics. Consider the following irreversible reaction:

$$A + B \rightarrow C$$

The rate of the reaction is $r = k_r[A][B]$. If the concentration of B is approximately constant, then the rate of the reaction can be approximated by $r \approx k_r'[A]$, where k_r' is equal to $k_r[B]$. In mass transfer theory, the condition that must be satisfied for a second order reaction to be considered pseudo first order is

$$\varphi_{max} >> \sqrt{M} \qquad 2\text{-}21$$

where φ_{max} is given by equation 2-19 and M is given by equation 2-22 [2].

$$M = \frac{D_A k_r [B]_{initial}}{k_l^2} \qquad 2\text{-}22$$

The enhancement of mass transfer by chemical reaction has been studied both theoretically and experimentally for many different systems. Due to the empirical nature of many of the parameters used to describe mass transfer, most of these studies have been based on experimental verification of theoretically derived models. In addition to the different mass transfer systems investigated, many different analytical methods have been used to quantify mass transfer enhancement, ranging from comparison of mass transfer rates to calculation of dimensionless parameters based on mass transfer coefficients.

3.1 EVIDENCE FOR THE ENHANCEMENT OF MASS TRANSFER BY CHEMICAL REACTION

Enhancement of mass transfer by chemical reaction has been observed experimentally by a number of authors. Many of these used plots of φ against $\sqrt{M}$ to study mass transfer enhancement. For example, Brian, Vivian and Habib [5] studied the effect of the hydrolysis of chlorine on the absorption of chlorine into water in a wetted-wall column. They plotted φ against $\sqrt{M}$ and compared predictions based on the penetration theory to experimental results. The conclusions that they made were: (1) the model predictions agreed well with the experimental results and (2) the hydrolysis of chlorine enhances the absorption of chlorine into water, with enhancement factors ranging from 1.3 to 3. Because hydrochloric acid suppresses the hydrolysis reaction of chlorine, absorption of chlorine into 0.2N hydrochloric acid was studied to obtain data for the physical absorption of chlorine unaccompanied by chemical reaction.

Another simpler method of studying mass transfer enhancement involves combining equations 2-4, 2-12 and 2-15. Using this method, Takahashi, Hatanaka and Konaka [6] studied the effect of reaction on the rate of absorption of chlorine using a stopcock absorber. They analysed mass transfer enhancement by plotting the rate of absorption against the inverse square root of the contact time for the absorption of chlorine into a number of liquids. The slopes of the plots were proportional to the product of the enhancement factor and the

absorption of chlorine into water was approximately 30% greater than that for physical absorption alone. Since the concentration of chlorine at the interface would have decreased due to the reaction between chlorine and water, the enhancement factor must have been greater than one if the slope of the plot increased. This demonstrates the mass transfer enhancement of chlorine due to the reaction between chlorine and water. Takahashi et al also showed that the reaction between chlorine and sodium hydroxide also enhances the mass transfer of chlorine, and the enhancement increases as the concentration of sodium hydroxide increases.

Reaction in the bulk liquid can be divided into three different categories [2]: very slow reaction, slow reaction and fast reaction. For very slow reaction the enhancement factor is one, and mass transfer occurs as physical absorption only. For slow reaction with rate constant k_r, the rate of absorption increases without an increase in the enhancement factor only if the condition $\sqrt{M} << 1$ is met, where M is given by equation 2-22. For fast reaction, the enhancement factor is greater than one. These three categories provide another useful method of studying the enhancement of mass transfer by chemical reaction. Hix and Lynn [7] performed a study on the enhancement of the absorption of sulphur dioxide into solution by reaction with hydrogen sulphide. They were able to conclude that the reaction between hydrogen sulphide and sulphur dioxide was a slow reaction and so did not cause enhancement of the liquid phase mass transfer coefficient of sulphur dioxide. However, the rate of absorption was increased due to the decrease in the concentration of H_2S in the bulk solution.

A study involving mass transfer with chemical reaction from gas bubbles was done by Johnson, Hamielec and Houghton [8]. The system used in their study involved mass transfer of carbon dioxide from single gas bubbles into aqueous solutions of monoethanolamine. As in previous studies, the experimental results were compared to model predictions based on theory. They analysed their data by comparing the Sherwood number to $Re^{1/2}Sc^{1/3}$. The Sherwood number was used to demonstrate mass transfer enhancement because it is directly proportional to the liquid phase mass transfer coefficient. The experimental plot of Sh against $Re^{1/2}Sc^{1/3}$ shows that for the same value of $Re^{1/2}Sc^{1/3}$, Sh increased as the mole % of

therefore enhanced by reaction with monoethanolamine, and the enhancement was greater for higher mole % of monoethanolamine.

3.2 EXPERIMENTAL METHODS OF DETERMINING MASS TRANSFER COEFFICIENTS

It is more difficult to determine liquid and gas phase mass transfer coefficients than to determine overall mass transfer coefficients. This is because of the difficulty in measuring physical quantities at the mass transfer interface as opposed to measuring properties in the bulk phases.

The most obvious method of determining overall mass transfer coefficients is by direct measurement of bulk concentrations and relevant parameters, and subsequent substitution into equation 2-7. Whitmore and Corsi [9] used this method to determine overall mass transfer coefficients for volatile organic compounds found in sewers. The experiments were performed by introducing volatile tracer into wastewater in the sewer and collecting bulk gas and liquid phase samples for analysis. The concentrations of the volatile tracer in the gas and liquid bulk phases were determined by analysis of the samples with a Hewlett-Packard gas chromatograph and mass selective detector. The experimental uncertainty in this method of determining the overall mass transfer coefficient was approximately a factor of two.

An indirect method of determining gas phase mass transfer coefficients was suggested by Danckwerts [2]. By absorbing a gas into a solution with which the gas undergoes instantaneous, irreversible reaction, it should be possible to determine the gas phase coefficient. The rate of absorption would be proportional to $k_g C_g$, where C_g is the bulk gas phase concentration.

Another indirect method of calculating gas phase mass transfer coefficients involves using empirical correlations. Trabold and Obot [10] performed experiments on the evaporation of water with impinging air jets and provided an equation for calculating the mass transfer coefficient of water from the experimental data. Danckwerts [2] suggested that,

can be calculated from the gas phase mass transfer coefficient of water using equation 3-1.

$$\frac{k_{g,H_2O}}{D^n_{air,H_2O}} = \frac{k_{g,x}}{D^n_{air,x}} \qquad 3\text{-}1$$

In equation 3-1, the value of n is one if the film theory is used, and ½ if the penetration theory is used. In most empirical correlations, n is taken to be ⅔.

3.3 ENHANCEMENT OF THE MASS TRANSFER OF IODINE BY CHEMICAL REACTION

Iodine is important in nuclear technology because it is produced in nuclear reactors and is a potential hazard to humans. Hence, a number of studies have been done on the rates of transfer of iodine between the liquid and gas phases. An experimental study on the rates of evaporation of chlorine, bromine and iodine from aqueous solutions was performed by Polissar [11]. In his experiments, samples were periodically taken from a beaker containing the aqueous solution under investigation. Using a titrimetric method of analysis, the concentrations of the halogen in the samples were determined. In the case of iodine, he also performed experiments to investigate the effect that reaction with iodide ions has on the rate of evaporation of iodine. He analysed the results by plotting the concentration of the halogen in the system against time and evaluating the rate of evaporation. For solutions of free iodine and solutions in which the concentration of potassium iodide was less than 0.006 M, he found that the rates of evaporation were approximately constant and equal. For solutions in which the concentration of potassium iodide was between 0.066 M and 0.361 M, as the concentration of potassium iodide increased, the rate of evaporation decreased. Polissar concluded that the diminished rate of evaporation at higher potassium iodide concentrations was due to a decrease in the amount of free iodine available for evaporation, resulting in a decrease in the driving force for mass transfer. For solutions in which the concentration of potassium iodide was 1.00 M and greater, the concentration of total iodine in the solution actually increased. Polissar explained this increase by the rate of evaporation being so small that the oxygen reaction more than compensated for the decrease in concentration. When

effect that the reaction between iodine and iodide ions might have had on the mass transfer coefficient. However it was possible, using his experimental results, to estimate values of $K_{OL}A/V$ from the slopes of the plots. Table 3.1 shows a summary of the estimated values of $K_{OL}A/V$, based on Polissar's data, for the evaporation of iodine from solution.

Table 3.1: summary of $K_{OL}A/V$ values calculated from Polissar's data [11] for the evaporation of iodine from triiodide solutions

Total Iodide Concentration (M)	**$K_{OL}A/V$ (s^{-1})**
0	2×10^{-4}
0.0005	2×10^{-4}
0.0014	3×10^{-4}
0.0024	4×10^{-4}
0.006	7×10^{-4}
0.06	11×10^{-4}
0.0096	13×10^{-4}
0.15	27×10^{-4}
0.25	46×10^{-4}

Comparing the values obtained for $K_{OL}A/V$, it can be seen that for the evaporation of iodine from solutions in which the iodide concentration was 0.0005 M or less, the overall mass transfer coefficient was unaffected by the presence of iodide ions. As the concentration of iodide ions increased above 0.0005 M however, the overall mass transfer coefficient also increased, demonstrating significant enhancement of iodine mass transfer. No upper limit on the mass transfer coefficient was observed, and so a value for the gas phase mass transfer coefficient could not be estimated. Values of φ could not be calculated without knowledge of the gas phase mass transfer coefficient, but an estimation of the enhancement factor was possible using equation 3-2.

$$\varphi = \frac{k_l'}{k_l} = \frac{\left(\frac{1}{K_{OL}} - \frac{H}{k_g}\right)_{rxn}}{\left(\frac{1}{K_{OL}} - \frac{H}{k_g}\right)_{no\ rxn}} \qquad 3\text{-}2$$

In equation 3-2, H/k_g is constant for both the numerator and the denominator. Assuming the evaporation of iodine from the 0.25 M iodide ion solution to be close to gas phase limitation, an upper bound on H/k_g was estimated to be 220 s/cm. Substituting this value of H/k_g into equation 3-2 and using the data for the evaporation of iodine from a solution containing 0.15 M iodide ion, the enhancement factor was estimated to be 30 for the evaporation of iodine from a solution containing 0.15 M iodide ions. In reality, the enhancement factor is larger than this value because the actual maximum value of H/k_g is less than 220 s/cm.

Because sodium thiosulphate sprays are used inside containment structures, the effect of the reaction between iodine and thiosulphate ions on the transfer of iodine inside containment is important. Taylor [12] investigated the effect of various reactions, including the reaction between iodine and thiosulphate ions, on the absorption of iodine into solution. His absorption apparatus consisted of a disc-type laboratory column. By comparing K_{OG} values, he found that for the absorption of iodine into sodium thiosulphate and iodide solutions of concentration greater than 0.08 M, the absorption of iodine was gas phase limited. For the absorption of iodine into water, the absorption was appreciably limited by the liquid phase. The overall reactions between iodine and thiosulphate ions and between iodine and iodide ions are given in reactions 3-3 and 3-4.

$$I_2 + 2S_2O_3^{2-} \rightarrow 2I^- + S_4O_6^{2-} \qquad 3\text{-}3$$

$$I_2 + I^- \leftrightarrow I_3^- \qquad 3\text{-}4$$

Reaction 3-3 and the forward reaction of 3-4 are fast, second order reactions, reaction 3-3 being almost instantaneous. If reactions 3-3 and 3-4 are assumed to be pseudo-first order reactions, then using equations 2-16 and 2-19, upper limits on the enhancement factor can be estimated for both. Since k_r is large for both reaction 3-3 and the forward reaction of 3-4, the maximum enhancement factor will be large for both reactions for high reactant concentration. Taylor's observation that the enhancement was the same for both reactions for reactant concentrations above 0.08 M suggests that at these concentrations maximum enhancement had already been achieved and mass transfer was indeed limited by the gas side.

3.4 PREDICTION OF REACTION RATE CONSTANTS FROM RATES OF MASS TRANSFER

Using Danckwerts' [2] method of categorizing reactions by their rate, it should be possible to estimate the rate constant of a reaction at some intermediate rate of reaction. For a gas A being absorbed into a liquid and undergoing an irreversible, second order reaction with a solute B dissolved in the liquid, Hix and Lynn [7] suggested a method of calculating the rate constant, k_r, of the reaction. In a sieve-tray absorber, the mass balance equation is

$$Q_L C_{Ainit} + k_l \frac{A}{V}(C_{Ai} - C_{Ao}) = Q_L C_{Ao} + H_L k_r C_{Ao} C_{Bo} \qquad 3\text{-}5$$

where Q_L is the volumetric flow of liquid to the tray and H_L is the holdup volume of liquid in the tray, C_{Ao} and C_{Bo} are the bulk concentrations, and C_{Ai} and C_{Ainit} are the interfacial and initial concentrations of A respectively. For this system, the rate of absorption per unit volume is given by equation 3-6,

$$\frac{dA}{dt} = k_l' \frac{A}{V}(C_{Ai} - C_{Ao}) = \frac{(C_{Ao} - C_{Ainit})}{\tau} + k_r C_{Ao} C_{Bo} \qquad 3\text{-}6$$

where τ is the residence time of liquid in the tray. If the reaction is too slow, then the last term on the right of equation 3-6 is negligible. If the reaction is too fast, then most of the reaction will occur in the film and C_{Ao} will be negligible. If, however, the reaction is slow enough that the enhancement factor is one, and yet the rate of absorption is increased due to a decreased amount of A in the bulk, then by rearranging equation 3-6, an equation for k_r can be obtained.

$$k_r = \frac{\frac{dA}{dt} - \left(\frac{C_{Ao} - C_{Ainit}}{\tau}\right)}{C_{Ao} - C_{Bo}} \qquad 3\text{-}7$$

Hix and Lynn used this method to calculate the rate constant for the reaction between sulphur dioxide and hydrogen sulphide, and reported that their results were in fair agreement with previous measurements of the same rate constant.

In this chapter, a detailed description of all the experiments performed during this study is provided. The experiments described are: (i) the evaporation of water, (ii) the absorption of iodine gas into sodium thiosulphate solutions, (iii) the evaporation of iodine from solutions containing iodine, iodide ions and triiodide ions, and (iv) the absorption of iodine gas into iodide ion solutions. See appendix A for specifications on the equipment and chemicals used.

Certain terms and parameters are relevant to more than one type of experiment and will be defined now.

The reaction vessel: for experiments involving evaporation, this term refers to the flask containing the solution being evaporated. For experiments involving absorption of iodine gas, this term refers to the flask containing the absorbing solution. The volume of liquid contained in the flask never exceeded 100 mL, and, at the liquid level, the diameter of the flask was measured with a vernier calliper to be 7.3 cm. A diagram of the reaction vessel is shown in figure 4.1.

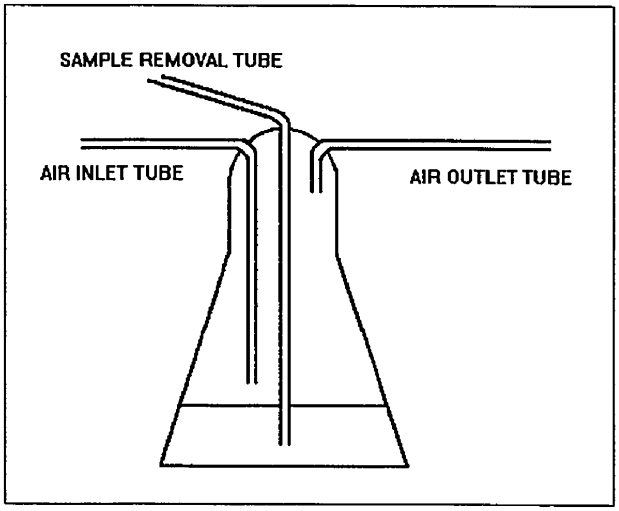

Figure 4.1: the reaction vessel used in experiments

absorption of iodine gas into solution, and refers to the flask containing the source of iodine gas.

Air flow rate: for all the different types of experiments, one consistent flow rate was used, and the choice of this flow rate was very important. If the flow rate chosen was too slow or too fast, then the rate of mass transfer would be dependent upon the flow rate rather than upon the mass transfer characteristics of the system. An intermediate flow rate was therefore chosen that allowed the mass transfer characteristics of the system to be investigated. The flow rate of 18 ± 2 mL/s was the same as was used by the author in a previous study [13]. One of two Cole Parmer flow meters were used to set the flow rate. One flow meter was equipped with a medium flow tube, tube number N034-39 and a glass float. The other flow meter used a high flow tube, tube number N044-40 together with a glass float. Both meters were constructed such that the flow of air through them was metered at the top of the tube. All experiments were performed under vacuum. Figure 4.2 is a diagram of the flow meters, showing their orientation in the experiments.

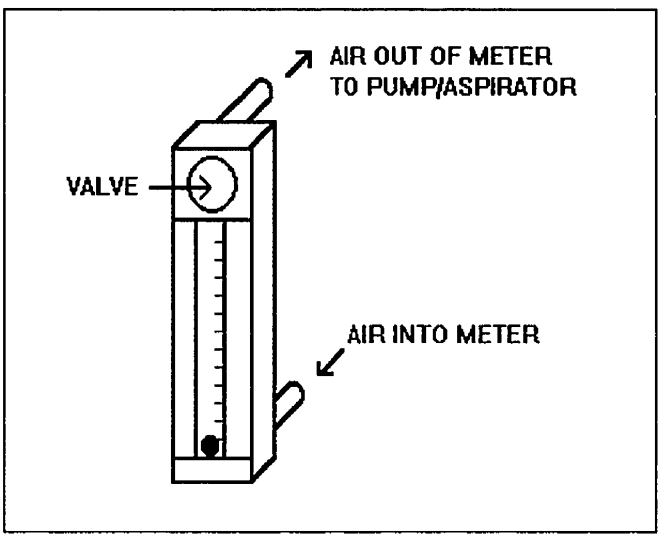

Figure 4.2: Diagram showing the direction of the flow of air through the flow meters

Plastic tubing: the plastic tubing used in all the experiments was clear plastic tubing with an inside diameter of 1/4 ".

Experiments were performed on the rate of evaporation of water in order to determine the gas phase mass transfer coefficient of water, and hence determine via empirical correlations, the gas phase mass transfer coefficient of iodine.

In these experiments, a stream of air at the flow rate specified above was passed through the system. The stream of air impinged upon 100 mL of water held in the reaction vessel. The initial volume of water was measured using a 100 mL measuring cylinder. Using a Cole Parmer humidity probe and a Barnant humidity probe, the relative humidity of the incoming and exiting air streams were measured. Two vessels were used to hold the humidity probes. Each vessel was stoppered with a rubber bung, through which two holes had been bored: one to allow air to enter the vessel and one to hold the humidity probe upright in the vessel. Air was removed from the humidity probe vessel by an outlet on the side of the vessel. A diagram of the apparatus used in these experiments is shown in figure 4.3.

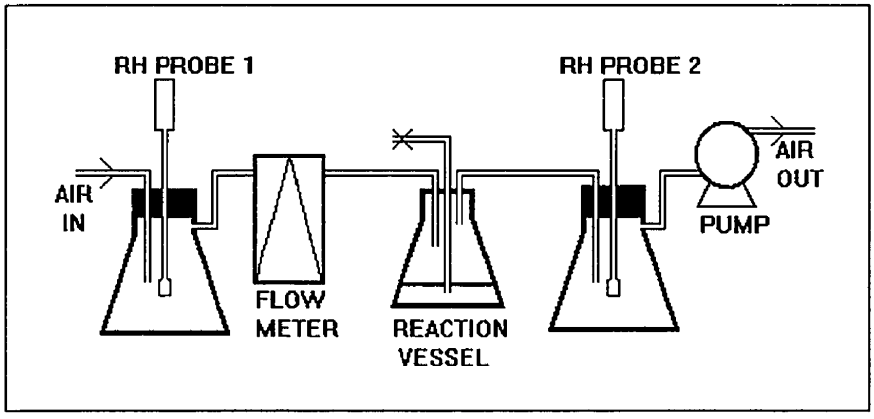

Figure 4.3: apparatus used for the experiments on the evaporation of water

At the beginning and end of each experiment, the temperature of the water was measured using a FISHER thermometer with a temperature range of -10 °C to 260 °C. The temperature of the water was taken as the average of these two temperatures. The 100 mL measuring cylinder used to measure the initial volume of water was dried with a paper towel and used at

experiments were performed using the above procedure, each experiment being run for between 3 and 8 hours.

4.2 ABSORPTION OF IODINE INTO SODIUM THIOSULPHATE SOLUTION

These experiments were performed for two main reasons. The first purpose was to observe the effect that reaction with sodium thiosulphate has on the rate of absorption of iodine gas, and the second purpose was to obtain a value for the gas phase mass transfer coefficient of iodine from the experiments on the higher concentrations of thiosulphate ion solutions. The value of k_g that was obtained from these experiments was compared to the value obtained from the experiments described in section 4.1. The concentrations of sodium thiosulphate solutions used in the experiments were 1×10^{-4} M, 2×10^{-4} M, 5×10^{-4} M, 1×10^{-3} M, 2×10^{-3} M, 5×10^{-3} M, 1×10^{-2} M, 5×10^{-2} M and 1×10^{-1} M. At least two runs were performed for each concentration.

4.2.1 INITIAL PREPARATION

Firstly, a constant source of iodine gas was prepared by dissolving 11.76 g of potassium iodide and 0.77 g of molecular iodine in deionized water in a 250 mL volumetric flask. The flask was filled up to the mark with deionized water. The iodine molecules reacted with the iodide ions to form triiodide ions such that the initial concentrations in the solution were: 6×10^{-5} M free molecular iodine, 0.012 M triiodide ions and 0.28 M iodide ions. To this iodine gas source, 67 μCi of I-131 tracer, in the form of iodide ions, was added. Using a 100 mL measuring cylinder, 100 mL of this gas source was then measured out and poured into the iodine gas source vessel. This vessel was then covered and all openings sealed with stopcocks until ready for an actual experiment. A lubricant was used to ensure that all the seals were secure.

The mass of sodium thiosulphate needed to make a specific solution of sodium thiosulphate was determined and weighed out on an OHAUS mass balance. The sodium thiosulphate solution was then prepared by dissolving the mass of solid sodium thiosulphate

to the mark with deionized water.

Charcoal traps were prepared by cutting 6 cm lengths of plastic tubing and plugging one end with glass wool. Using a spatula, charcoal was then poured into the other end of the tubing, such that the charcoal was loosely packed, and the length of the charcoal packing was approximately 4 cm. The other end of the tubing was then plugged with glass wool. For each experiment, at least four charcoal traps were prepared in advance.

4.2.2 EXPERIMENTAL PROCEDURE

100 mL of sodium thiosulphate solution was measured out using a 100 mL measuring cylinder, and poured into the reaction vessel. The iodine gas source vessel and the reaction vessel were then connected using a 5 cm long piece of Teflon tubing. The connection was securely sealed using Teflon tape. Using Cole Parmer quick disconnect fittings, one end of a charcoal trap was connected to the outlet of the reaction vessel and the other end was connected to the bottom fitting of the flow meter. The top fitting of the flow meter was connected to the aspirator. The aspirator was then turned on. The valve on the flow meter was adjusted such that the middle of the glass float in the medium flow tube aligned with the 20 marking on the tube. This flow reading was equivalent to a flow rate of 17.1 ± 1 mL/s. If the high flow tube was used, the valve was adjusted such that the middle of the float aligned with the 10 marking on the tube. This flow reading was equivalent to a flow rate of 18.6 ± 1 mL/s. Air was allowed to flow through the system for the entire experiment, with occasional interruptions for sample removal and charcoal trap changeover.

4.2.3 SAMPLE REMOVAL

Samples were removed at intervals of 20 to 30 minutes. For each sample removal, the stopcock between the iodine gas source vessel and the reaction vessel was closed and the stopcock closing off the sample removal tube was opened. A 21G1½ needle was attached to a syringe, and the needle was inserted into one end of a length of thin plastic dialysis tubing. The other end of the tubing was inserted into the now open sample removal tube. Approximately 1.5 mL of solution was removed from the reaction vessel via the sample

then removed from the reaction vessel, the stopcock at the top of the sample removal tube was closed and the stopcock between the iodine gas source and the reaction vessel was reopened. The solution in the syringe was transferred to a 3 mL scintillation vial. Using an Eppendorf 1 mL micropipette, 1 mL of solution was removed from the scintillation vial and placed in a new 3 mL scintillation vial labelled with the number of the sample. The vial was then placed in a rack for counting in an LKB gamma counter. Using this procedure, 5 to 6 samples were collected for each experiment.

4.2.4 CHARCOAL TRAP CHANGEOVER

At intervals of 25 minutes, the charcoal traps were changed, a total of 4 to 6 traps being used in each experiment. Before changing each trap, the stopcock between the iodine gas source vessel and the reaction vessel was closed. Using the quick disconnect fittings, the charcoal trap was quickly removed and replaced by a new charcoal trap. The stopcock was then reopened. The old charcoal trap was freed from all fittings and placed in a test tube, with the end of the charcoal trap that was nearest to the reaction vessel at the bottom, rounded end of the test tube. A piece of parafilm was then used to seal the mouth of the test tube, and the test tube was placed in a rack, rounded end facing down, to await counting in an LKB gamma counter. A diagram of the experimental set-up used in these experiments is shown in figure 4.4.

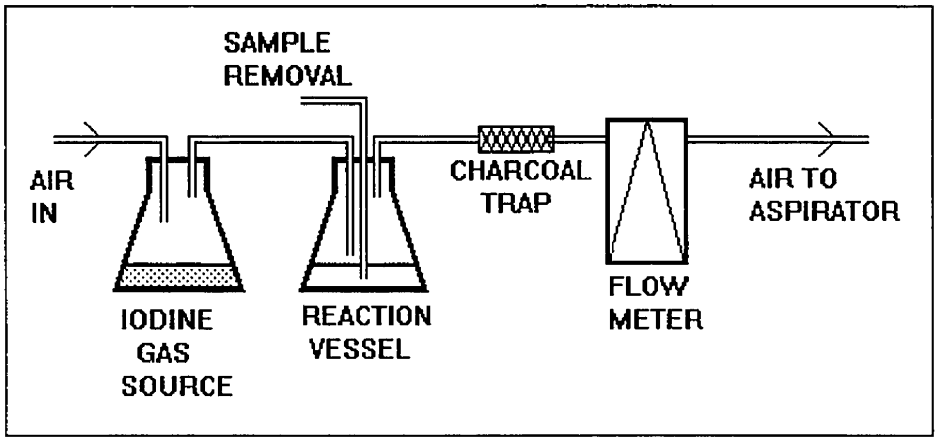

Figure 4.4: apparatus used for the experiments on the absorption of iodine into sodium thiosulphate

by placing two charcoal traps in series, downstream of the reaction vessel. It was found that less than 2 % of iodine leaving the reaction vessel reached the second charcoal trap. Therefore, only one charcoal trap was used in subsequent experiments.

Each experiment was run for a duration of 100 to 180 minutes. At the end of each experiment, the aspirator was turned off, all stopcocks attached to the iodine gas source vessel were closed and appropriate procedures were followed to dispose of all radioactive waste.

4.3 THE EVAPORATION OF IODINE FROM SOLUTIONS CONTAINING IODINE, IODIDE IONS AND TRIIODIDE IONS

These experiments were performed to observe the effect that the presence of iodide ions has on the mass transfer of iodine. A Varian Cary 3 UV-Vis spectrophotometer was used to analyse the samples in these experiments for iodine content. The total iodide concentration in the solutions used were 1×10^{-4} M, 1×10^{-3} M, 2.5×10^{-3} M, 5×10^{-3} M, 1×10^{-2} M, 2.5×10^{-2} M, 5×10^{-2} M, 1×10^{-1} M, 2×10^{-1} M and 5×10^{-1} M. For each of these concentrations, more than one experimental run was performed.

4.3.1 SOLUTION PREPARATION

All solutions prepared and used in these experiments were categorized by the concentration of iodide ions in them. These solutions of molecular iodine, iodide ions and triiodide ions were prepared by weighing out the amount of potassium iodide required to make a solution of specific iodide ion concentration. This potassium iodide was then dissolved in deionized water in a 100 mL, 250 mL or 500 mL volumetric flask, together with a small amount of molecular iodine. Enough deionized water was then added to fill the volumetric flask up to the mark. The amount of molecular iodine added was determined by requiring that the concentration of triiodide ions in the final solution be such that its absorbance at 350 nm was less than 2.0.

Using a 100 mL measuring cylinder, 100 mL of the prepared iodine, iodide ion and triiodide ion solution was poured into the reaction vessel. The vessel was then closed off, the inlet tube being left open to the surrounding air, and the outlet tube being connected to the flow meter with a charcoal trap between the reaction vessel and the flow meter. The purpose of this charcoal trap was to keep the flow meter free from contamination by iodine gas, which is corrosive. The flow meter was connected to the aspirator, and the aspirator was turned on. Using the valve on the flow meter the flow was adjusted as described in section 4.2.2. The sample removal method was the same as that described in section 4.2.3. Once the samples were removed, they were transferred to a cuvette and placed in the sample compartment of the Cary 3 UV spectrophotometer, which had been previously zeroed with water at a wavelength of 350 nm. The effect of using water to zero the spectrophotometer rather than a solution of the appropriate iodide ion concentration was investigated. It was found that iodide ions have negligible absorbance at 350 nm, and therefore did not have to be taken into account when zeroing the machine. For each experiment, 4 to 6 samples were taken, sample removal intervals varying from 15 minutes for low iodide ion concentrations to 4 hours for high iodide ion concentrations. Experiments on 0.2 M and 0.5 M iodide solutions were repeated with a charcoal trap attached to the apparatus upstream of the flow meter. Figure 4.5 shows a diagram of the apparatus.

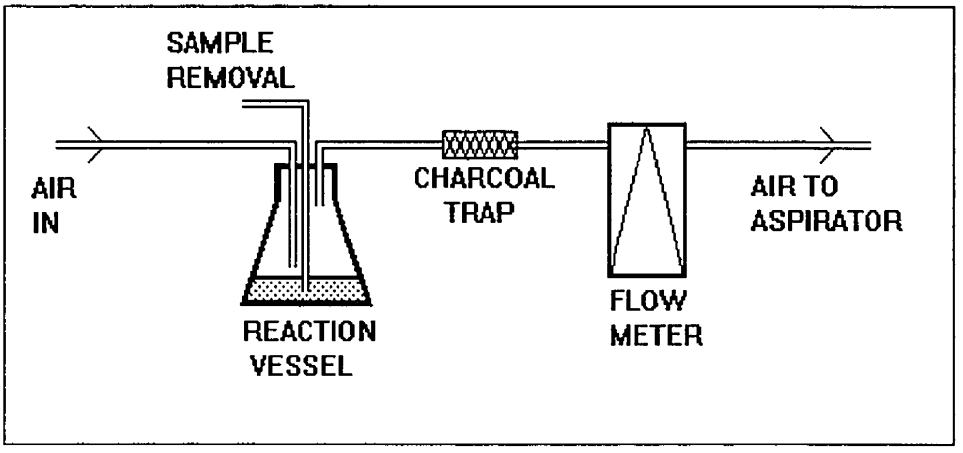

Figure 4.5: apparatus used for experiments on the evaporation of I_2 from triiodide solutions

IODINE

These experiments were performed in order to determine a value for the liquid phase mass transfer coefficient of iodine in the absence of chemical reaction. The procedure was the same as in section 4.3.2, but instead of a solution containing iodine, iodide ions and triiodide ions in the reaction vessel, the reaction vessel contained a saturated solution of molecular iodine only. The saturated solution of molecular iodine was prepared by placing about 5 g of iodine crystals in 500 mL of deionized water and allowing the iodine to dissolve over two weeks or more. The method of sample removal was also the same as in section 4.3.2. The concentration of iodine in the samples was measured at a wavelength of 460 nm using the UV-Vis spectrophotometer.

4.4 ABSORPTION OF IODINE INTO IODIDE ION SOLUTIONS

These experiments were performed to observe the effect that the direction of mass transfer has on the mass transfer coefficients. For the experiments on evaporation, overall mass transfer occurred from the liquid to the gas phase, whereas in these experiments overall mass transferred occurred from the gas to the liquid phase. The concentrations of iodide solutions used were, 1×10^{-3} M, 1×10^{-2} M, 1×10^{-1} M, 5×10^{-1} M and 1 M. At least two experimental runs were performed for each concentration.

4.4.1 INITIAL PREPARATION

Solutions for the iodine gas source were prepared by the same method described in section 4.2.1. In some of these experiments, however, samples were periodically removed from the iodine gas source vessel and analysed in the Cary 3 UV spectrophotometer. Therefore, in these cases, the total iodine content of the iodine gas source was kept low to allow for analysis in the spectrophotometer.

A humidifier was placed upstream of the apparatus so that the incoming air was pre-humidified. This was to compensate for any water that might have evaporated due to convection. The humidifier was simple in design. It consisted of a flask filled with

flask by an outlet tube at the top of the humidifier.

For each experiment, one charcoal trap was prepared using the same method as described in section 4.2.1. This charcoal trap was placed before the humidifier to ensure that the air entering the system was free of all iodine.

Instead of using charcoal traps to remove all the iodine leaving the system, as was done in the experiments on the absorption of iodine into sodium thiosulphate, solutions of high iodide ion concentration were used as traps. Each iodide trap contained 500 mL of 0.1 M potassium or sodium iodide inside a bubbler. Iodine leaving the reaction vessel was bubbled through the first iodide trap and reacted with the iodide ions in the trap to form involatile triiodide ions. Any iodine that escaped the first bubbler was trapped in the second iodide bubbler.

Potassium iodide solutions were prepared, 100 mL at a time, using deionized water in a 100 mL volumetric flask. These solutions were then poured into the reaction vessel for the experiment. The solutions were prepared less than one hour before the start of each experiment to ensure that as little of the iodide ions as possible were oxidized to molecular iodine.

4.4.2 EXPERIMENTAL PROCEDURE

The charcoal trap was attached to the inlet on the humidifier by wiping the outside of the humidifier inlet tube with a drop of stopcock grease, and then gently easing the charcoal trap onto the inlet tube. Again using stopcock grease, the outlet to the humidifier was connected to the bottom fitting of the flow meter using plastic tubing. A length of plastic tubing was fitted onto the top fitting of the flow meter, to await connection to the iodine gas source.

The prepared potassium iodide was poured directly from the 100 mL volumetric flask into the reaction vessel. The iodine gas source vessel and the reaction vessel were then both raised to a height of approximately 10 cm off the bench top using two retort stands, and connected using a 5 cm long piece of Teflon tubing. The connection was securely sealed using Teflon tape. Using Teflon tubing, the outlet to the reaction vessel was then attached to

the second iodide trap, again using Teflon tubing. The outlet from the second iodide trap was connected to a length of plastic tubing, the end of which was fitted with one half of a quick disconnect fitting. The other half of the quick disconnect fitting was fitted onto a length of plastic tubing, and this plastic tubing was then attached to the pump, which was set to draw air through the system.

The connections between the humidifier and the flow meter and between the second iodide trap and the pump were made, and the pump was turned on. The valve on the flow meter was adjusted as described in section 4.2.2. Air was allowed to flow through the system for the entire experiment, with occasional interruptions to allow for sample removal. Samples were removed from the reaction vessel and the iodine gas source vessel using the procedure described in section 4.2.3, and were analysed using the procedure described in section 4.3.3. If the absorbance of any sample exceeded 2.0, then the sample was diluted with the appropriate iodide ion solution and re-analysed in the Cary 3 UV spectrophotometer. The intervals between sample removals ranged from 10 minutes to 2 hours. A diagram of the experimental set-up is shown in figure 4.6.

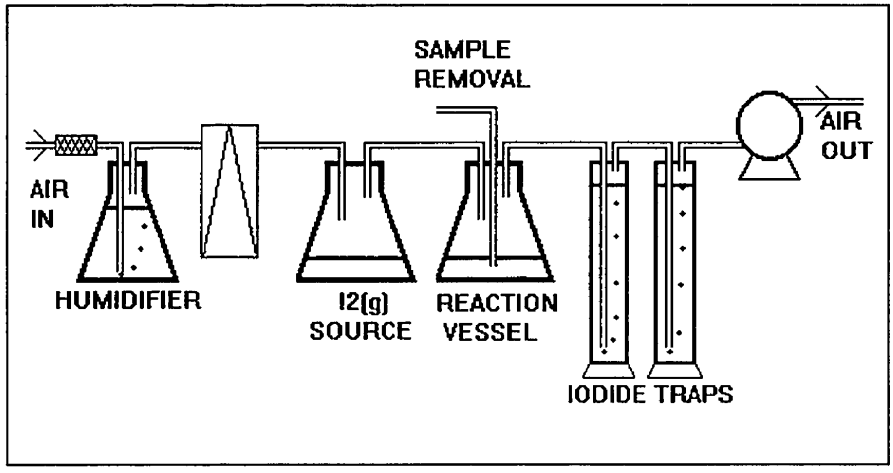

Figure 4.6: apparatus used for the experiments on the absorption of I_2 into iodide solutions

sample from each of the iodine gas source vessel, the reaction vessel, the first iodide trap and the second iodide trap were removed and analysed in the UV spectrophotometer.

4.4.3 ABSORPTION OF IODINE INTO WATER

Using water in the reaction vessel instead of potassium iodide solutions, the procedure outlined above was followed. In this experiment, the concentration of iodine in the water was too low to be detected at a wavelength of 460 nm. Therefore, the iodine in each sample was converted to triiodide ions by adding 500 μL of each sample to a cuvette containing 500 μL of a 0.1 M iodide solution. The concentration of triiodide solution was then measured in the spectrophotometer at a wavelength of 350 nm.

These experiments were performed to compare evaporation and absorption in the absence of chemical reaction.

In this chapter, details of the FACSIMILE models constructed to simulate the interfacial transfer of iodine are presented. Seven models were created; the first two involved the transfer of iodine in the absence of chemical reaction, and the other five involved the transfer of iodine in the presence of various chemical reactions. The seven models were:

(i) the absorption of iodine into water

(ii) the absorption of iodine into thiosulphate solutions

(iii) the absorption of iodine into iodide solutions

(iv) the absorption of iodine into hydroxide solutions

(v) the evaporation of iodine from an aqueous solution of molecular iodine

(vi) the evaporation of iodine from solutions containing iodine, iodide ions and triiodide ions

(vii) the evaporation of iodine from solution in the presence of radiolytic reactions

All seven models were constructed by modifying one basic model. The parameters and conditions used in the basic model were the same as those used in the experimental part of the project. The models are listed in appendix D.

5.1 THE BASIC MODEL

The reactions considered in this study are all aqueous reactions, and hence enhancement of mass transfer due to these reactions occurs in the liquid phase. Therefore, in the basic model, focus was placed on the liquid phase.

For the diffusion of a species C through a column of water, the equivalent form of equation 2-1 is equation 5-1,

$$\frac{\partial[C]}{\partial t} = D_C \frac{\partial^2[C]}{\partial x^2} \qquad 5\text{-}1$$

where [C] is the aqueous concentration of species C, D_C is the diffusion coefficient of C in water and x is the direction of diffusion. If the column is divided into a number of smaller

equation 5-2 [14].

$$\frac{d[C]_i}{dt} \approx \frac{D_C}{s^2}([C]_{i-1} - 2[C]_i + [C]_{i+1}) \qquad 5\text{-}2$$

In equation 5-2, subscript i denotes the ith zone, subscript i-1 denotes the zone above zone i and subscript i+1 denotes the zone below zone i. Equation 5-2 describes a set of ordinary differential equations that is easier to work with than equation 5-1. The TRANSPORT routine of FACSIMILE was used to set up equation 5-2 for the model.

The liquid phase film was divided into a number of zones of height s, the total number of zones being denoted by #NZONE in the model. Using TRANSPORT, the transfer of species between the liquid phase zones was modelled. The thickness of the liquid phase film, δ_l, and hence the value of s, was determined by using the stagnant film theory. Rearranging equation 2-11 yielded equation 5-3 for δ_l.

$$\delta_l = \frac{D_{I_2,H_2O}}{k_l} \qquad 5\text{-}3$$

The height of each zone, s, was calculated using equation 5-4.

$$s = \frac{\delta_l}{\#NZONE - 1} \qquad 5\text{-}4$$

$D_{I2,H2O}$ was determined to be 1.2 x 10^{-5} cm/s by averaging the values of $D_{I2,H2O}$ calculated from the Othmer and Thakar, Wilke and Chang, and Hayduk and Minhas diffusivity equations [4, 18, 19], and the value of k_l was the value obtained from experiment. The only equations that had to be defined for TRANSPORT were those involving the boundary conditions. Transfer between the gas phase and the first zone in the liquid phase film was modelled by using the value of k_g determined from the experiment described in section 4.2 for high thiosulphate concentration. Transfer between the last zone and the bulk liquid was modelled by assuming rapid transfer between the two layers. Bulk liquid concentrations were therefore equal to the concentrations in the last zone of the liquid phase film.

In the experiments, a flow of air was passed through the system at a flow rate of 18 mL/s. In the models, this flow of air was simulated by including an appropriate form of equation 5-5 in the TRANSPORT routine.

$$\frac{d[C]_{gas}}{dt} = KVENT([C]_{gasin} - [C]_{gas})$$

In this equation, $[C]_{gas}$ is the gaseous concentration of C in contact with the interface, $[C]_{gasin}$ is the concentration of C in the gas phase entering the system, and KVENT is equal to the flow rate of air divided by the volume of gas in the system. Figure 5.1 is a diagram showing how the liquid phase film was divided into zones.

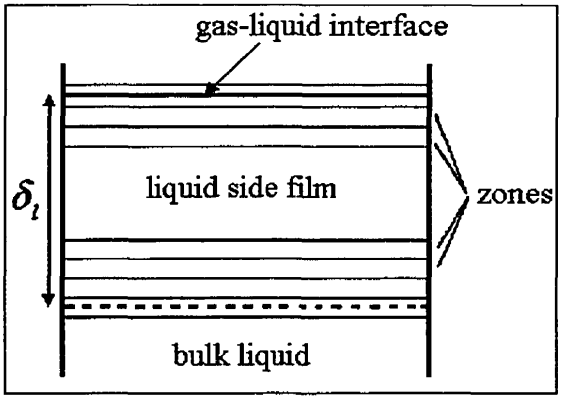

Figure 5.1: division of the liquid phase film into zones

Three output files were created for each model. The first output file showed the bulk concentrations of iodine at specified times, the second output file showed the rates of the reactions at specified times, and the third output file showed the concentrations in each zone at any time. The output data was imported into Microsoft Excel version 5.0 as delimited files and analysed using the tools available in Excel.

5.2 MODELLING OF ABSORPTION

Absorption of iodine into solution was modelled by defining the initial aqueous iodine concentration to be zero and $[I_2]_{gasin}$ to be greater than zero. Four absorption models were created; one to simulate the absorption of iodine into water and three to simulate the absorption of iodine into solution in the presence of various chemical reactions. The

(iii) hydroxide ions.

5.2.1 ABSORPTION OF IODINE INTO WATER

No initial concentrations were specified, the default value being zero, and only one TRANSPORT routine for the diffusion of iodine was included in the model. The TRANSPORT routine is given below.

```
  TRANSPORT <#nzone> I2 fI2 fI2;
* inlet condition at gas/liquid interface;
% Kgas*A*(I2gas*80 - I2<0>)/(80*s*A) : = I2<0>;
% Kgas*A*(I2<0> - I2gas*80)/(Vgas*80) : = I2gas;
% Kvent*(I2gasin - I2gas)  : = I2gas;
* outlet condition at film/bulk interface;
% fI2*1e06*(I2<#1> - I2bulk)/(Vliq) : = I2bulk;
% fI2*1e06*(I2bulk - I2<#1>)/(s*A) : = I2<#1>;
**;
```

The value of $[I_2]_{gasin}$ used in the model was 5×10^{-8} M. This value was an approximation of the gas phase concentrations in the experiments described in sections 4.2 and 4.4. The program was compiled for time intervals of 100 seconds for a total time of one hour.

5.2.2 ABSORPTION OF IODINE GAS INTO THIOSULPHATE SOLUTIONS

The reactions that occur when iodine reacts with thiosulphate ions is given in equations 5-6 to 5-10 [15].

$$I_2 + S_2O_3^{2-} \leftrightarrow I_2S_2O_3^{2-} \qquad 5\text{-}6$$

$$I_3^- + S_2O_3^{2-} \leftrightarrow I_2S_2O_3^{2-} + I^- \qquad 5\text{-}7$$

$$I_2S_2O_3^{2-} \leftrightarrow IS_2O_3^- + I^- \qquad 5\text{-}8$$

$$IS_2O_3^- + S_2O_3^{2-} \rightarrow I^- + S_4O_6^{2-} \qquad 5\text{-}9$$

$$I_2 + I^- \leftrightarrow I_3^- \qquad 5\text{-}10$$

The forward, k_f, and reverse, k_b, rate constants for the reactions at 25°C are as follows [15, 16]: for reaction 5-6, $k_f = 7.8 \times 10^9$ $M^{-1}s^{-1}$ and $k_b = 2.5 \times 10^2$ s^{-1}, for reaction 5-7, $k_f = 4.2 \times 10^8$ $M^{-1}s^{-1}$ and $k_b = 9.5 \times 10^3 M^{-1}s^{-1}$, for reaction 5-8, $k_f / k_b = 0.245$, for reaction 5-9, $k = 1.29 \times 10^6$ $M^{-1}s^{-1}$, and for reaction 5-10, $k_f = 5.6 \times 10^9$ $M^{-1}s^{-1}$ and $k_b = 7.5 \times 10^6$ s^{-1}.

concentrations in the zones and the bulk layer. The initial concentrations of all other species were set at the default value of zero. The concentration of iodine gas entering the system was the same as that in the model in section 5.2.1. Seven TRANSPORT routines were created, one each for I_2, I^-, I_3^-, $S_2O_3^{2-}$, $I_2S_2O_3^{2-}$, $IS_2O_3^-$ and $S_4O_6^{2-}$. The TRANSPORT routines for the ions did not include a boundary condition for the gas/first zone interface because ions are essentially involatile. The program was compiled for a range of initial thiosulphate concentrations, and using the output files, the effect of thiosulphate concentration on the absorption of iodine into solution was studied. The effect of the size of the rate constants on the output was also studied by recompiling the program with different values of the rate constants.

5.2.3 THE ABSORPTION OF IODINE GAS INTO IODIDE SOLUTIONS

The initial concentrations defined in this model were those of iodide ions in the bulk and the zones. Iodine reacts with iodide ions by reaction 5-11.

$$I_2 + I^- \leftrightarrow I_3^- \qquad 5\text{-}11$$

The forward and reverse rate constants for the reaction are given in section 5.2.2. For this model, three TRANSPORT routines were needed to describe the diffusion of each of the species present in solution: iodine molecules, iodide ions and triiodide ions. The TRANSPORT routine for iodine incorporated transfer between the gas phase and the first zone, but the TRANSPORT routines for iodide and triiodide ions did not.

The model was run for the same time and time intervals as the model in section 5.2.1. The effect of concentration on the mass transfer of iodine was studied by compiling the program for a range of initial iodide concentrations. By changing the values of the forward and reverse rate constants, the effect of these constants on the output data was also investigated.

5.2.4 ABSORPTION OF IODINE GAS INTO HYDROXIDE SOLUTIONS

Iodine reacts with hydroxide ions by reactions 5-12 to 5-14.

$$I_2 + OH^- \leftrightarrow I_2OH^- \qquad 5\text{-}12$$

$$I^- + I_2 \leftrightarrow I_3^- \qquad 5\text{-}14$$

For reaction 5-12, $k_f = 8 \times 10^8\ M^{-1}s^{-1}$ and $k_b = 5 \times 10^4\ s^{-1}$ and for reaction 5-13, $k_f = 1.4 \times 10^6\ s^{-1}$ and $k_b = 4 \times 10^8\ M^{-1}s^{-1}$. TRANSPORT routines were set up as for the previous absorption models. By changing the appropriate parameters in the model, the effect of concentration and inlet iodine gas concentration on the absorption of iodine gas into hydroxide solutions were studied.

5.3 MODELLING OF EVAPORATION

Evaporation was modelled by defining $[I_2]_{gasin}$ to be zero and the initial aqueous iodine concentration to be greater than zero. Three evaporation models were created; one for the evaporation of iodine from a solution of aqueous iodine, one for the evaporation of iodine from solutions containing iodine, iodide ions and triiodide ions, and one for the evaporation of iodine from solution in the presence of radiolytic reactions. Models for the evaporation of iodine in the presence of reaction with thiosulphate and hydroxide ions were not constructed because of the almost irreversible, instantaneous nature of these reactions.

5.3.1 EVAPORATION OF IODINE FROM AQUEOUS IODINE

The initial concentrations defined in this model were those of iodine in the zones and the bulk layer. The initial iodine concentration was set at 1.1×10^{-3} M, which is the concentration of a saturated solution of iodine. Only one TRANSPORT routine was needed, and that was used to model the diffusion of I_2 through the system. The TRANSPORT routine used is given below.

```
TRANSPORT <#nzone> I2 fI2 fI2;
* inlet condition at gas/liquid interface;
% Kgas*A*(I2<0> - I2gas*80)/(80*Vgas) : = I2gas;
% Kgas*A*(I2gas*80 - I2<0>)/(s*A*80) : = I2<0>;
% Kvent*(0 - I2gas) : = I2gas;
% 2*Kvent*Vgas*I2gas : = TRAP;
* outlet condition at film/bulk interface;
```

```
% fI2*1e06*(I2bulk - I2<#1>)/(s*A) : = I2<#1>;
**;
```

The model was run using one hour as the total time, with data recordings at time intervals of 100 seconds.

5.3.2 EVAPORATION OF IODINE FROM SOLUTIONS CONTAINING IODINE, IODIDE IONS AND TRIIODIDE IONS

The model for the evaporation of iodine from solutions containing iodine, iodide ions and triiodide ions was the same as the model for the absorption of iodine into iodide solutions. The initial concentration of iodide ions was defined in this model as well as that of iodine, in both the bulk layer and the zones. The initial concentration of triiodide ions was calculated from the FACSIMILE form of reaction 5-11 describing the kinetics of the reaction.

The model was run for the same time and time intervals as the model in section 5.3.1. The effect of concentration on the mass transfer of iodine was studied by compiling the program for a range of initial iodide concentrations.

5.3.3 EVAPORATION OF IODINE IN THE PRESENCE OF RADIOLYTIC REACTIONS

Radiolytic reactions are reactions that occur as a result of the presence of a radiation field. The radiolytic reactions considered in this model are those that occur when an aqueous iodide solution is exposed to a radiation field. The complete set of radiolytic reactions included in the model contains 63 reaction equations, and is given in appendix D. Unlike the two previous models, an initial aqueous iodine concentration was not defined in the model. The only initial concentration specified was an initial iodide concentration of 1×10^{-4} M. A TRANSPORT routine was created for each species in the model. The program was compiled, and by changing the radiation dose rate input to the model, the effect of dose rate on the mass transfer of iodine was investigated.

In this chapter, the experimental results of this study are presented. The first experiments that were performed were those to determine the liquid and gas phase mass transfer coefficients in the absence of chemical reaction. Having obtained these coefficients, experiments were then performed to determine the overall mass transfer coefficient of iodine for three systems: (1) absorption of iodine gas into solutions containing thiosulphate ions, (2) evaporation of iodine from solutions containing triiodide ions and (3) absorption of iodine into solutions containing iodide ions. Each of the above systems were examined using a range of solution concentrations.

Using the empirical values of the liquid and gas phase mass transfer coefficients together with the FACSIMILE program, models were constructed to simulate the mass transfer of iodine, first in the absence of chemical reaction and then in the presence of chemical reaction. The output files from the programs were manipulated to yield overall mass transfer coefficients for different conditions and reactions. These coefficients were then compared to the experimental results obtained from systems under the same conditions. This was to verify that the FACSIMILE models constructed to simulate the interfacial transfer of iodine in the presence of chemical reaction correctly imitate the real system. The effect of concentration of solution and reaction rate constants on the overall mass transfer coefficient were considered with respect to both the experimental and modelling data. Once the models were validated, a new model was constructed to simulate the mass transfer of iodine in the presence of a radiation field and all the accompanying radiolytic reactions.

6.1 MASS TRANSFER WITHOUT CHEMICAL REACTION

6.1.1 EXPERIMENTAL RESULTS

THE GAS PHASE MASS TRANSFER COEFFICIENT OF IODINE

The experiment outlined in section 4.1 was performed seven times. Based on the rate of evaporation of water, a gas phase mass transfer coefficient of water was obtained from

first method, the rate of evaporation was based on the total change in the volume of water during the experiment. In the second method, the evaporation rate was based on the difference in the relative humidity of the inlet and outlet air streams. Generally, the volumes of water evaporated over periods of 5 to 11 hours ranged from 4 mL to 8 mL. The difference in the percent relative humidity between the inlet and outlet air streams varied from 45% to 78%. The temperature of the water was approximately constant for the duration of each experiment, but varied between 21°C and 24°C from day to day. The results of these experiments are given in table 6.1.

Table 6.1: experimental values of the gas phase mass transfer coefficient of water

run #	**$k_{g,H2O}$ (cm/s) (based on change in volume of water)**	**$k_{g,H2O}$ (cm/s) (based on change in %RH of air stream)**
1	0.38	0.32
2	0.24	0.24
3	0.27	0.27
4	0.28	0.28
5	0.26	0.35
6	0.28	0.35
7	0.32	0.35

Using the values in table 6.1, the average gas phase mass transfer coefficient based on the change in volume of water was calculated to be 0.29 cm/s. The standard deviation between these values was 0.05. The average gas phase mass transfer coefficient based on the difference in the %RH between the inlet and outlet air streams was 0.31 cm/s. The standard deviation between these values was 0.04. These two mass transfer coefficients are in very good agreement, and so were averaged to obtain a value of 0.30 ± 0.05 cm/s for the gas phase mass transfer coefficient of water. The gas phase mass transfer coefficient of iodine is related to the gas phase mass transfer coefficient of water by equation 6-1.

$$\frac{k_{g,H_2O}}{D^n_{air,H_2O}} = \frac{k_{g,I_2}}{D^n_{air,I_2}} \qquad 6\text{-}1$$

Using the Fuller, Schettler and Giddings equation [4], the diffusivity of iodine in air was calculated to be 0.085 cm^2/s, and the diffusivity of water in air was calculated to be 0.23 cm^2/s. The magnitude of n in equation 6-1 is 1 if the film theory is used and ½ if the penetration theory is used. Generally n is taken to be ⅔, a value between ½ and 1. Using a value of ⅔ for n yielded an average gas phase mass transfer coefficient of iodine of 0.16 ± 0.03 cm/s. This average was calculated using all the data values in table 6-1.

The calculation to determine the gas phase mass transfer coefficient of water required the partial pressure of the ambient water vapour. This partial pressure was not measured directly during the performance of the experiments, but the percent relative humidity in the inlet and outlet air streams were determined. The inlet air stream entered the system at a height of 1 cm above the surface of the water, and the outlet air stream exited the system from the top of the flask, as shown in figure 6.1a. It was initially assumed that the bulk gas phase could be approximated by the gas phase 1 cm above the surface of the water. Therefore, the ambient partial pressure of the water vapour in the system was assumed to be the partial pressure of the water vapour in the inlet air stream, as calculated from the percent relative humidity of the inlet stream. The validity of this assumption was tested by reversing the apparatus such that the inlet air stream entered the system from the top of the flask, and the outlet stream exited the system from a position 1 cm above the surface of the water, as shown in figure 6.1b.

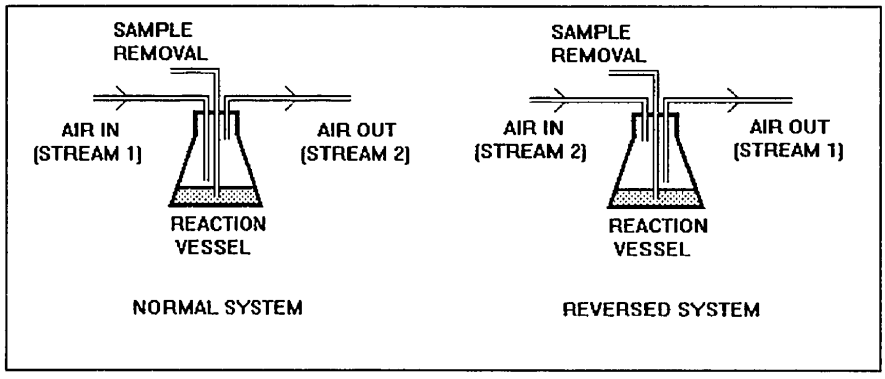

Figure 6.1: configuration of the reaction vessel in the (a) normal and (b) reversed experiments

analysing the data from the experiment, the ambient partial pressure of the water vapour in the system was assumed to be the partial pressure of the water vapour in the outlet air stream, rather than in the inlet air stream. The gas phase mass transfer coefficient of water from the reversed experiment was calculated to be 0.22 ± 0.03 cm/s, as compared to 0.16 ± 0.03 cm/s from the previous experiments. It was postulated that the actual partial pressure of the water vapour above the surface of the water was a linear function of both the inlet and outlet water vapour partial pressures, such that

$$p_{bulk} = \alpha p_1 + \beta p_2 \qquad 6\text{-}2$$

where α and β are constants, and p1 and p2 are the partial pressures of the water vapour in air streams 1 and 2, as shown in figures 6.1a and 6.1b. The experimental data was re-analysed using equation 6-2 to describe the ambient partial pressure of the water vapour. Two equations for k_g were obtained from the experimental data, one each for the normal system and the reversed system. Solving these equations by trial and error produced values of 0.9 and 0.1 for α and β respectively. Therefore, water vapour in the bulk air above the surface of the water was made up of approximately 90% air stream 1 and 10% air stream 2. This supports the assumption that the partial pressure of the water vapour above the surface of the water could be approximated by the partial pressure of the water vapour in the inlet air stream for the normal systems. It should be noted that the value of K_{OL} may not have been solely dependent upon the amount of water vapour in the bulk air. As will be discussed later in section 6.3, another factor that might have contributed to the difference between the K_{OL}'s for the two systems is the effect of the impingement of the air onto the interface for the normal system.

ERROR IN THE MASS TRANSFER COEFFICIENTS

In determining each of the above mass transfer coefficients, two or more experimental runs were performed. The mass transfer coefficients found from these runs were then averaged and the standard deviation between the results calculated. An error associated with the performance of each individual experiment was also determined using the propagation of

uncertainties, air flow rate fluctuations and relative humidity variations.

However, for these gas phase mass transfer coefficients, the standard deviation in the results was greater than that estimated based on the propagation of known errors. Hence, the mass transfer coefficient quoted is the average of a number of data points, and the error associated with this coefficient is the standard deviation amongst the data points. A detailed table of the standard deviations and performance errors for all the experiments is presented in appendix C.

THE LIQUID PHASE MASS TRANSFER COEFFICIENT OF IODINE

Using the experimental procedure given in section 4.3.3, eight similar experiments were performed in order to determine the overall mass transfer coefficient of iodine for evaporation in the absence of chemical reaction. A value of the liquid phase mass transfer coefficient was obtained for each experiment from the slope of a plot of ln[abs] against time, where abs = constant*$[I_2]$. Figure 6.2 shows one such plot. The initial aqueous iodine concentration was 2.2 x 10^{-4} M, and the concentration dropped to 1.2 x 10^{-4} M after 120 minutes. Table 6.2 summarizes the values of K_{OL} and k_l obtained from all eight experiments. Using the results in table 6.2, an average empirical value for the liquid phase mass transfer coefficient of iodine of 2.0 x 10^{-4} cm/s was obtained. The standard deviation associated with this mean is 5 x 10^{-5}.

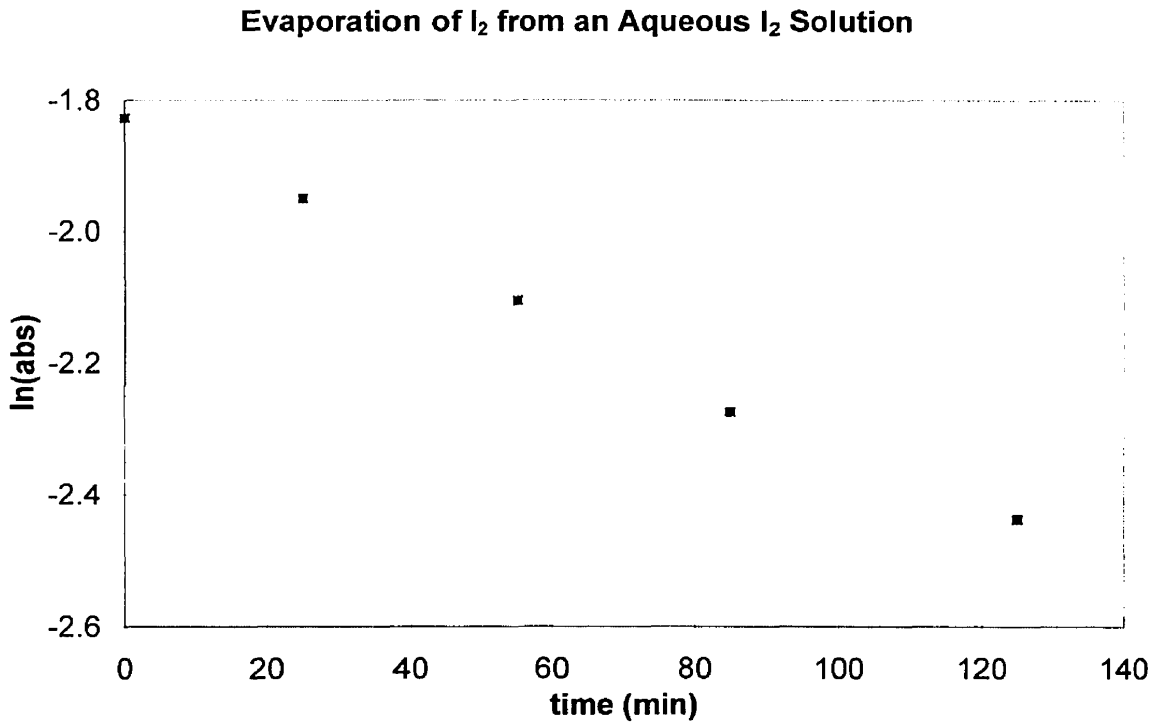

Figure 6.2: plot of the natural log of the absorbance against time for the evaporation of I_2 from an aqueous iodine solution

Table 6.2: values of k_l based on the evaporation of iodine from aqueous iodine

run #	K_{OL} (cm/s)	k_l (cm/s)
1	0.00019	0.00020
2	0.00012	0.00012
3	0.00025	0.00026
4	0.00022	0.00023
5	0.00018	0.00019
6	0.00024	0.00025
7	0.00018	0.00019
8	0.00010	0.00010

performed to determine the overall mass transfer coefficient of iodine for absorption into water in the absence of chemical reaction. For each experiment, the overall mass transfer coefficient was calculated from the slope of a plot of $\ln(H[I_2]_{gasin} - [I_2]_{aq})$ against time. Figure 6.3 shows the plot obtained from one of the experiments. The iodine gas concentration in the inlet air was 2×10^{-7} M.

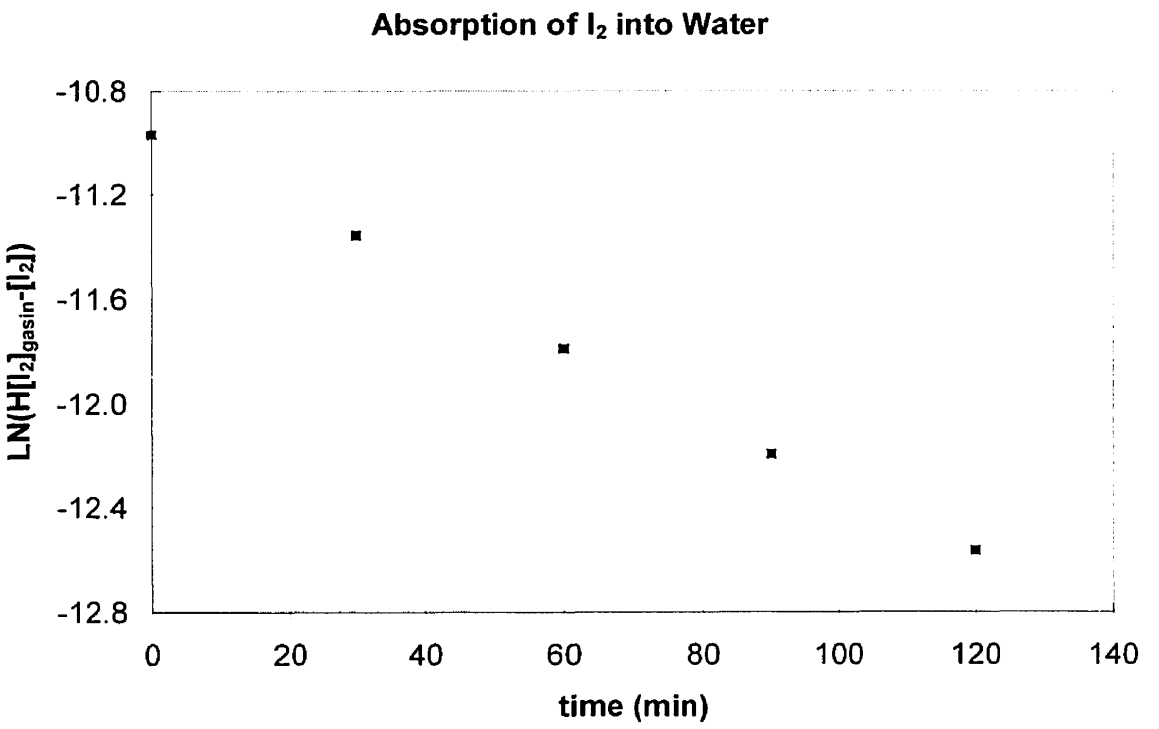

Figure 6.3: plot of $\ln(H[I_{2gasin}]-[I_2])$ against time for the absorption of I_2 into water.

Table 6.3: values of k_l based on the absorption of iodine into water

run #	K_{OL} (cm/s)	k_l (cm/s)
1	0.00052	0.00059
2	0.00073	0.00087
3	0.00059	0.00068
4	0.00018	0.00019
5	0.00020	0.00021

transfer coefficient of 5.1×10^{-4} cm/s. The standard deviation amongst the data was 3×10^{-4}. It was expected that the liquid phase mass transfer coefficients for absorption and evaporation would be equal. While these numbers are in agreement within experimental error, there is a 57% difference between them. The value obtained based on the evaporation of iodine from an aqueous solution of iodine was taken to be the more reliable result because the standard deviation for this result was less.

The iodine concentration in the evaporation experiments was more than a factor of 5 greater than the concentration in the absorption experiments. The aqueous iodine concentrations in the evaporation experiments ranged from 6.5×10^{-4} M to 1×10^{-4} M, while in the experiments on the absorption of iodine into water, the maximum aqueous iodine concentration observed was 1.5×10^{-5} M.

Comparing the magnitude of the gas phase mass transfer coefficient to that of the liquid phase mass transfer coefficient in the absence of chemical reaction, it is evident that the gas phase mass transfer coefficient is a factor of 2000 larger than the liquid phase mass transfer coefficient. Thus, in the absence of chemical reaction, the mass transfer of I_2 is limited by transfer on the liquid side.

6.1.2 MODELLING

Two simple models were constructed to mimic the mass transfer of iodine between the gas phase and water in the absence of chemical reaction; the first model simulated the evaporation of iodine from an aqueous solution containing molecular iodine, and the second model simulated the absorption of iodine gas into water. Details of the models are given in sections 5.2.1 and 5.3.1. The empirical value for the gas phase mass transfer coefficient was input into the models to simulate mass transfer in the gas phase. Transfer in the liquid phase was based on the thickness of the liquid phase film, as calculated using the film theory together with the empirical value of the liquid phase mass transfer coefficient. The diffusivity of iodine used in the model was the average of the diffusivities calculated using the equations given by Othmer and Thakar, Wilke and Chang, and Hayduk and Minhas [4,

equations was less than 5%.

Output files containing the concentrations of iodine in the liquid and gas phases at specific time intervals were created. The output files from the models were imported into Microsoft Excel version 5.0 and the output data was analysed. From the output data, the overall mass transfer coefficient was calculated. The rate of mass transfer of iodine in the gas phase is given by equation 6-3.

$$V_g \frac{d}{dt} C_g = FC_{g,in} + K_{OL}A(HC_g - C_l) - FC_{g,out} \approx 0 \qquad 6\text{-}3$$

The output files contained all the information needed to calculate K_{OL}. By rearranging equation 6-3, an equation for K_{OL} was obtained.

$$K_{OL} = \frac{F(C_{g,in} - C_{g,out})}{A(C_l - HC_g)} \qquad 6\text{-}4$$

Figure 6.4 is a plot of K_{OL} against time for the evaporation of I_2 from an I_2(aq) solution.

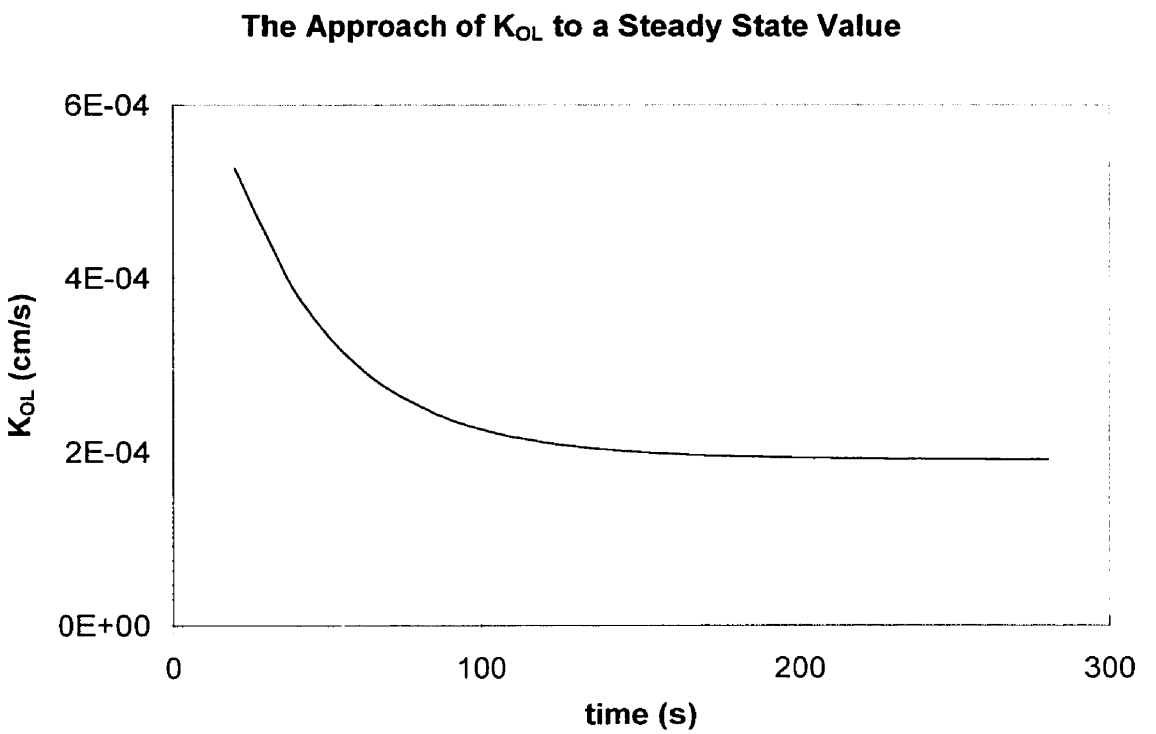

Figure 6.4 : approach of the overall mass transfer coefficient to a steady state value

initial decrease in K_{OL} . This decrease was a result of the initial conditions input to the model. The initial concentration of I_2 in the liquid side film was equated to the bulk I_2 concentration. At the interface, however, $[I_2]_{aq}$ would be less than the bulk concentration. Therefore, there was an initial period during which iodine was depleted from the liquid side film. This resulted in an apparent initial decrease in K_{OL}, as calculated from equation 6-4.

The steady state value of K_{OL} was compared to the overall mass transfer coefficient expected, based on the gas and liquid phase mass transfer coefficients input into the model. This was done to verify that the models correctly mimic the real system. Table 6.4 below summarizes the results from the models.

Table 6.4 : modelling results for the mass transfer of iodine without chemical reaction

model	**K_{OL} (cm/s)**
expected value	1.91×10^{-4}
absorption model	1.90×10^{-4}
evaporation model	1.89×10^{-4}

It has been proven that, for no chemical reaction, the model adequately mimics the real system. Therefore, the method of dividing the liquid phase film into a number of thinner zones is suitable for modelling the mass transfer of iodine in the aqueous phase. Also the assumptions made in the model have been justified and can be used in future models involving chemical reaction. These assumptions were :

- the thickness of the liquid phase film can be estimated by using equation 2-11 and the empirical value obtained for the liquid phase mass transfer coefficient. The thickness of the liquid phase film was estimated to be 0.06 cm.
- diffusion in the bulk aqueous phase occurs so rapidly that the mass transfer coefficient can be arbitrarily increased by a large amount

The effect of the number of zones in the liquid phase film on the mass transfer coefficient was investigated by varying the number of zones used in the model from 2 to 20. The result

shows the dependence of the overall mass transfer coefficient on the number of zones in the liquid phase film for the evaporation model.

Table 6.5 : dependence of the overall mass transfer coefficient on the number of zones in the liquid phase film

# zones in Liquid Phase Film	K_{OL} (cm/s) (evaporation model)
2	1.867×10^{-4}
4	1.886×10^{-4}
6	1.889×10^{-4}
8	1.891×10^{-4}
10	1.892×10^{-4}
20	1.894×10^{-4}

As the number of zones in the liquid phase film was increased, the overall mass transfer coefficient also increased and, in fact, approached the value expected based on the gas and liquid phase mass transfer coefficients input into the model. This demonstrates that not only is the method of dividing the liquid phase film into a number of thinner zones an adequate way of simulating the mass transfer of iodine between the gas and liquid phases, but also, the greater the number of zones in the liquid phase film, the more closely the model simulates the real system. Figure 6.5 is a graphical representation of how the number of zones in the film affects the concentration of iodine in the film of the evaporation model. During evaporation, the aqueous iodine concentration is lowest at the gas/liquid interface and highest in the bulk solution. As the number of zones increases, the model output approaches the result expected based on theoretical predictions. That is, in the film the aqueous concentration of iodine varies linearly with the distance from the gas/liquid interface.

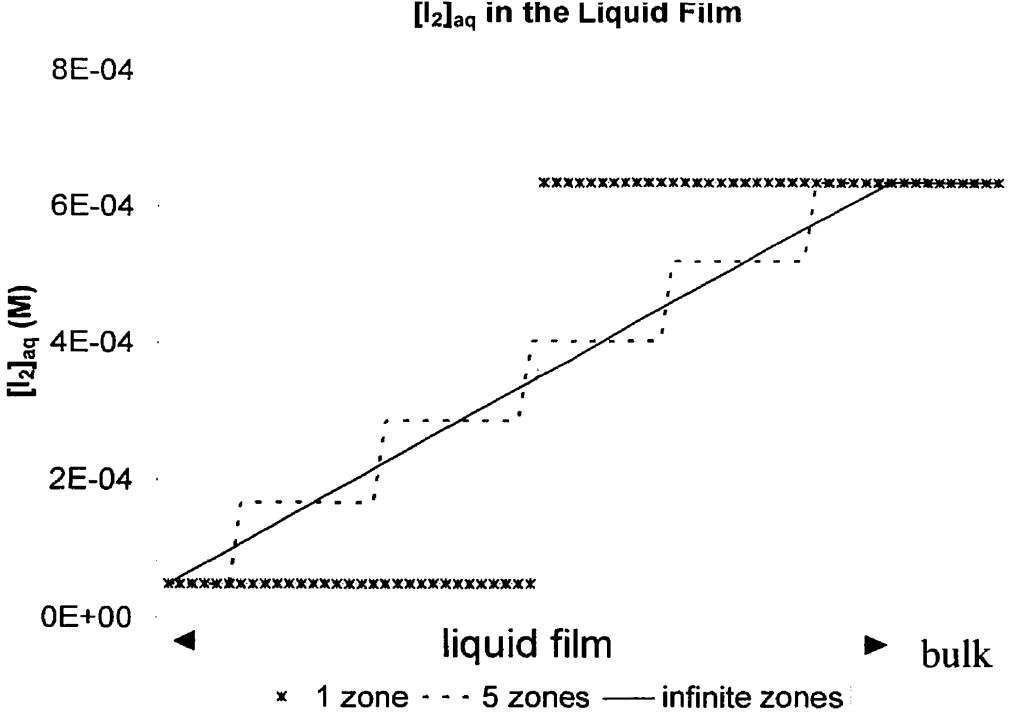

Figure 6.5: the effect of increasing the number of zones in the film

6.2 MASS TRANSFER ACCOMPANIED BY REACTION WITH THIOSULPHATE IONS

6.2.1 EXPERIMENTAL RESULTS

Using the experimental procedure given in section 4.2, experiments were performed on the absorption of iodine into solutions of sodium thiosulphate ranging in concentration from 1 x 10^{-4} M to 0.1 M.

Three experiments were done on the absorption of iodine gas into 0.1M sodium thiosulphate. Figure 6.6 shows the plot of activity against time that was made from the results of one of these experiments. The rate of absorption of iodine gas into the 0.1M sodium thiosulphate solution equaled the rate of increase of activity in the solution. This rate, equal to the slope of the plot shown in figure 6.6, was calculated to be 3.2 cpm/mL·min using the linear regression tool in Microsoft Excel version 5.0. By performing an activity

were determined to be 0.4 cpm/mL and 0.1 cpm/mL respectively. Using these results, the overall mass transfer coefficient for the absorption of iodine gas into 0.1M sodium thiosulphate was calculated to be 0.0044 cm/s.

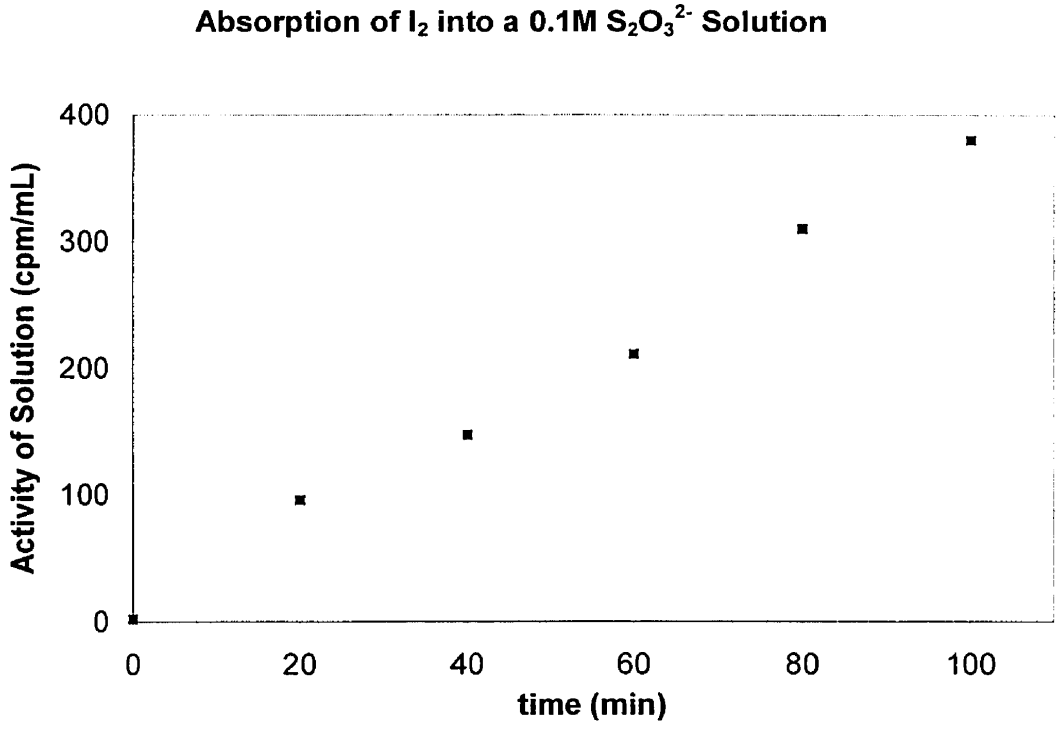

Figure 6.6: rate of absorption of I_2 gas into a 0.1M sodium thiosulphate solution

Table 6.6 below shows the overall mass transfer coefficients obtained from the three experiments performed on the absorption of iodine gas into 0.1M sodium thiosulphate. The experiments were reproducible, with a standard deviation between the data points of 8%.

Table 6.6: K_{OL} values for the absorption of iodine into 0.1M sodium thiosulphate

run #	K_{OL} (cm/s)
1	0.0043
2	0.0046
3	0.0039

overall mass transfer coefficient, with a standard deviation of 8% between the values.

Using the above procedure, average values of the overall mass transfer coefficients were obtained from replicate experiments on a range of thiosulphate concentrations. These average overall mass transfer coefficients are summarized in table 6.7. The error associated with each average is the standard deviation between the results from the replicate experiments used to calculate that average.

Table 6.7: K_{OL} values for the absorption of iodine into sodium thiosulphate solutions

$[S_2O_3^{2-}]$ (M)	K_{OL} (cm/s)	% error
1×10^{-4}	9×10^{-4}	32
2×10^{-4}	23×10^{-4}	3
5×10^{-4}	21×10^{-4}	1
1×10^{-3}	42×10^{-4}	2
2×10^{-3}	43×10^{-4}	3
5×10^{-3}	43×10^{-4}	1
1×10^{-2}	44×10^{-4}	2
5×10^{-2}	42×10^{-4}	4
1×10^{-1}	44×10^{-4}	3

These average mass transfer coefficients demonstrate that the reaction between iodine and sodium thiosulphate has a significant impact on the mass transfer of iodine. As the concentration of the sodium thiosulphate solution increased from 10^{-4} M to 10^{-3} M, the overall mass transfer coefficient also increased. For concentrations of thiosulphate ions above 1×10^{-3} M, the overall mass transfer coefficient was a constant, limiting value. This shows that, for concentrations of sodium thiosulphate of 1×10^{-3} M or greater, the absorption of iodine into sodium thiosulphate solution is only limited by the transfer of iodine through the gas side film, with no resistance due to transfer through the liquid side layer. For the absorption of iodine gas into sodium thiosulphate solutions of concentrations less than 1×10^{-3}

liquid side films.

By averaging the average overall mass transfer coefficients for experiments involving thiosulphate solutions of concentrations 10^{-3} M and greater, a mean value for the limiting value was obtained. This mean value was 0.0045 cm/s with a standard deviation of 0.0008. Using equation 2-9 with H =80, and assuming a large value of k_l, the gas phase mass transfer coefficient of iodine was estimated from this constant value to be 0.36 ± 0.06 cm/s. Comparing this value of the gas phase mass transfer coefficient to that of 0.16 cm/s obtained in sec 6.1.1 above shows a factor of two difference between the two values. This unexpected difference is due to the effect of impingement on the interface, and will be discussed in section 6.3.2.

The concentration of iodine gas in the bulk gas phase was determined by using the same assumptions as in the experiments to determine the gas phase mass transfer coefficient of water. That is, the concentration of iodine in the bulk gas phase was assumed to be approximately equal to the concentration of iodine gas at the inlet, located at a height of 1 cm above the surface of the solution. The inlet and outlet iodine gas concentrations were calculated by performing a balance on the total activity in the system.

THE ENHANCEMENT FACTOR

Enhancement factors for the absorption of iodine into sodium thiosulphate ranged from 3 to 450. A summary of the enhancement factors is given in table 6.8.

$[S_2O_3^{2-}]$ (M)	Liquid phase mass transfer coefficient (cm/s)	Enhancement factor
0	0.5×10^{-3}	1
1×10^{-4}	1.1×10^{-3}	2 ± 65%
2×10^{-4}	4.7×10^{-3}	9 ± 60%
5×10^{-4}	3.9×10^{-3}	8 ± 60%
1×10^{-3}	6.3×10^{-2}	126 ± 60%
2×10^{-3}	9.7×10^{-2}	194 ± 60%
5×10^{-3}	9.7×10^{-2}	194 ± 60%
1×10^{-2}	2.0×10^{-1}	400 ± 60%
5×10^{-2}	6.3×10^{-2}	126 ± 60%
1×10^{-1}	2.0×10^{-1}	400 ± 60%

The values of k_l were calculated from the difference between two large numbers. Therefore, the uncertainties in k_l, and hence φ, were large. Within these uncertainties however, it is evident that for thiosulphate concentrations greater than 1×10^{-3} M, the enhancement factors were greater than 100.

6.2.2 MODELLING RESULTS

The absorption of iodine gas into thiosulphate ion solutions was modelled using the FACSIMILE program together with reactions 6-5 to 6-9. Figure 6.7 depicts the relationship between the overall mass transfer coefficient and the concentration of thiosulphate ions in the absorbing solution, as predicted by the model. The model results are compared to the experimentally determined mass transfer coefficients.

$$I_2 + I^- \leftrightarrow I_3^- \qquad 6\text{-}5$$

$$I_2 + S_2O_3^{2-} \leftrightarrow I_2S_2O_3^{2-} \qquad 6\text{-}6$$

$$I_3^- + S_2O_3^{2-} \leftrightarrow I_2S_2O_3^{2-} + I^- \qquad 6\text{-}7$$

$$I_2S_2O_3^{2-} \leftrightarrow IS_2O_3^- + I^- \qquad 6\text{-}8$$

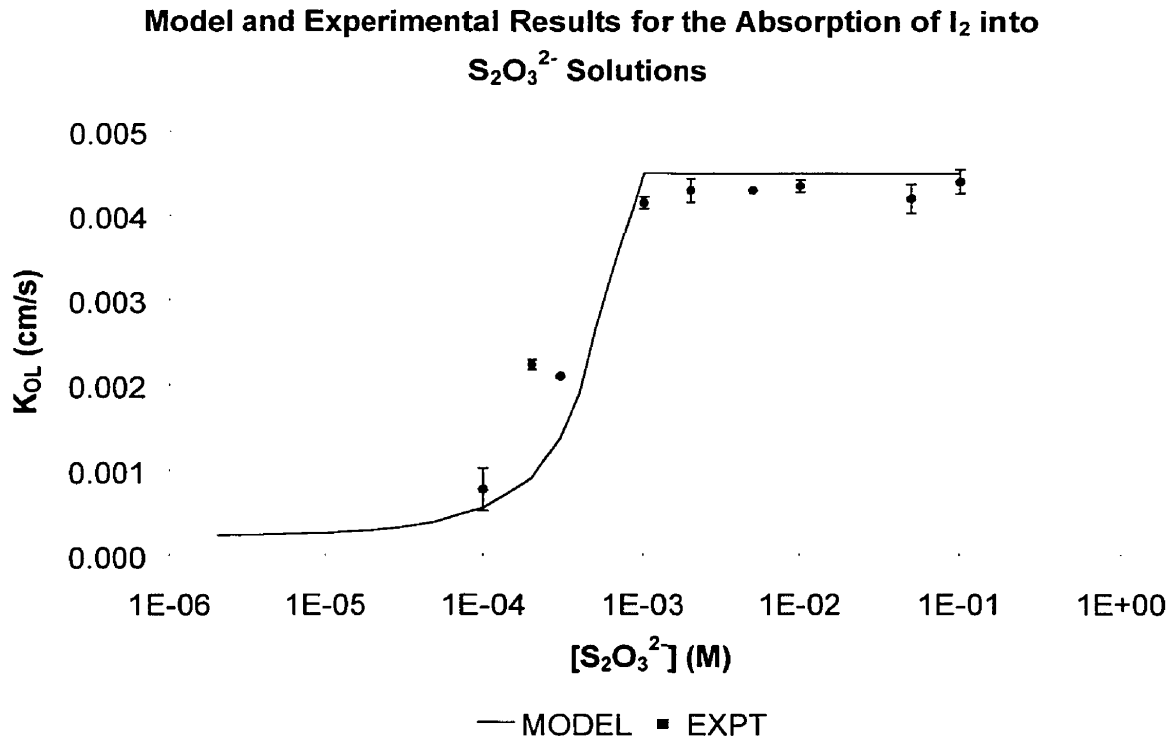

Figure 6.7: comparison of experimental and modelling results for the absorption of I_2 into $S_2O_3^{2-}$ solutions

In figure 6.7, the concentration at which K_{OL} started to increase was dependent upon the value of $[I_2]_{gasin}$. In the experiments, the initial $[I_2]_{gasin}$ produced by the iodine gas source was estimated to have been 1×10^{-6} M. It was not expected that this value would change significantly over the course of the experiments for two reasons. Firstly, the initial iodide concentration in the gas source was 0.3 M, which was high enough to ensure that almost all of the iodine in the solution was in the form of involatile triiodide ions. The concentration of I_2 in the solution, and hence the rate of evaporation of I_2, were therefore very small. Secondly, enough iodine crystals were initially added to the iodine gas source such that significant depletion of iodine from the source would only occur after all the experiments

arbitrarily chosen because although the initial $[I_2]_{gasin}$ was known, the final $[I_2]_{gasin}$ produced by the gas source was not determined. The model and the experimental results agree well, suggesting that the value of $[I_2]_{gasin}$ chosen was in the right range. For both the model and experiments, the trend was the same. As the concentration of thiosulphate ions was increased, the overall mass transfer coefficient also increased, until a limiting value of the mass transfer coefficient was reached. Beyond this point, increasing the concentration of thiosulphate ions had no effect on the overall mass transfer coefficient.

The dependence of the values of K_{OL} on $[I_2]_{gasin}$ is demonstrated in figure 6.8. For the lower $[I_2]_{gasin}$, the enhancement of the absorption of I_2 started at a lower thiosulphate concentration.

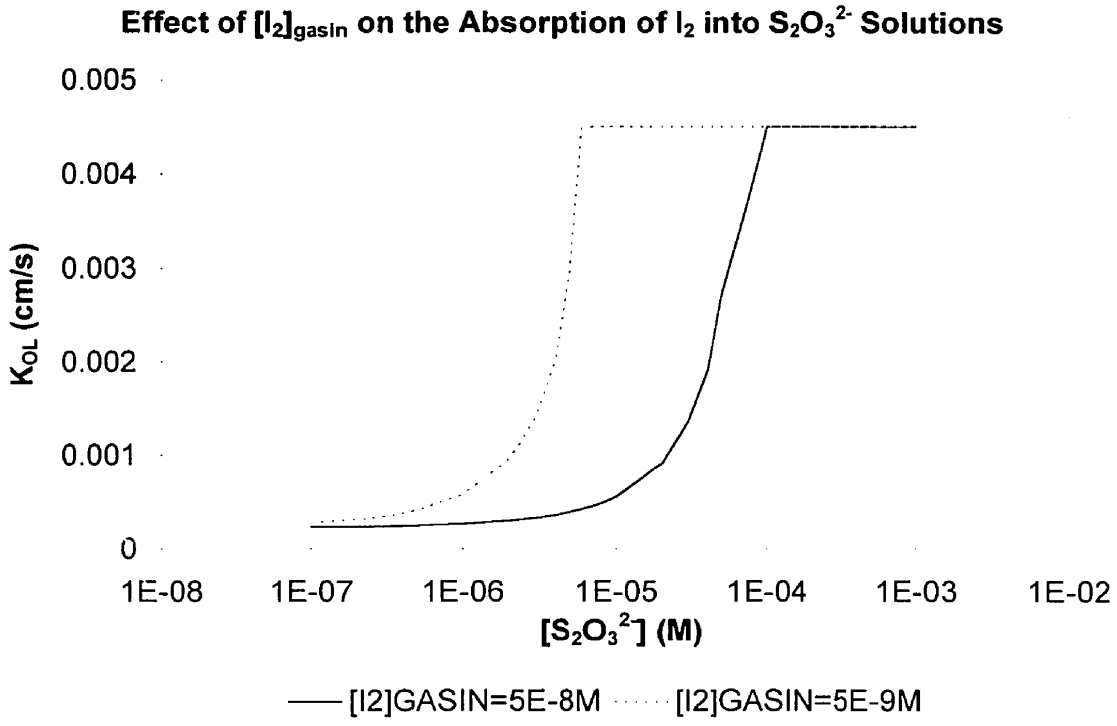

Figure 6.8: dependence of K_{OL} on $[I_2]_{gasin}$ for the absorption of I_2 into thiosulphate solutions

transfer coefficient was investigated by increasing the forward rate constants of the reactions, one at a time, and observing the effect on the model output. The initial thiosulphate concentration input into the model was 5×10^{-5} M. This concentration was chosen because for this concentration, the mass transfer of iodine is limited by both the gas and the liquid side films. Table 6.9 summarizes the results of the changes to the model.

Table 6.9: effect of increasing the forward rate constants of reactions 6-5 to 6-9 by a factor of 10^3 on the overall mass transfer coefficient.

Reaction that was changed	**K_{OL} (cm/s)**
no change	0.00031
$k_{f,rxn6\text{-}5}$ increased by 10^3	0.00135
$k_{f,rxn6\text{-}6}$ increased by 10^3	0.00031
$k_{f,rxn6\text{-}7}$ increased by 10^3	0.00031
$k_{f,rxn6\text{-}8}$ increased by 10^3	0.00031
$k_{f,rxn6\text{-}9}$ increased by 10^3	0.00031

The only change that had any effect on the overall mass transfer coefficient was the increase in $k_{f,rxn6\text{-}5}$, and hence K_{eq}, of reaction 6-5 by a factor of 1000.

Combining reactions 6-6, 6-7, 6-8 and 6-9, the overall reaction between iodine and thiosulphate ions can be represented by reaction 6-10, which is practically irreversible.

$$I_2 + 2\ S_2O_3^{2-} \rightarrow 2\ I^- + S_4O_6^{2-} \qquad 6\text{-}10$$

This reaction is a second order reaction, with I_2 and $S_2O_3^{2-}$ having similar diffusivities in water. Therefore, using equation 2-19, an equation for φ_{max} for this reaction can be written.

$$\varphi_{max} = 1 + \frac{[S_2O_3^{2-}]_{initial}}{2[I_2]_{interface}} \qquad 6\text{-}11$$

At the interface equilibrium concentrations are present, and therefore $[I_2]_{interface} = H[I_2]_{gas}$. Equation 6-11 then becomes

$$\varphi_{max} = 1 + \frac{2[S_2O_3^{2-}]_{initial}}{2H[I_2]_{gas}} \qquad 6\text{-}12$$

For constant $[S_2O_3^{2-}]$, it can be seen from equation 6-12 that as $[I_2]_{gas}$ increases, φ_{max} decreases. This results in a decrease in K_{OL} , as was observed in figure 6.8.

CONCENTRATION GRADIENTS IN THE FILM

The concentration gradients of iodine in the liquid phase and gas phase films are an important aspect of mass transfer because they indicate the magnitudes of the driving forces of mass transfer in the different phases. The concentration gradients of iodine in the liquid phase film after one hour were compared for the models of the absorption of iodine gas into water, 10^{-6}M and 10^{-5}M thiosulphate solution. The liquid phase film in each model was divided into 20 zones. As expected, the iodine concentration gradient increased as the concentration of thiosulphate ions increased.

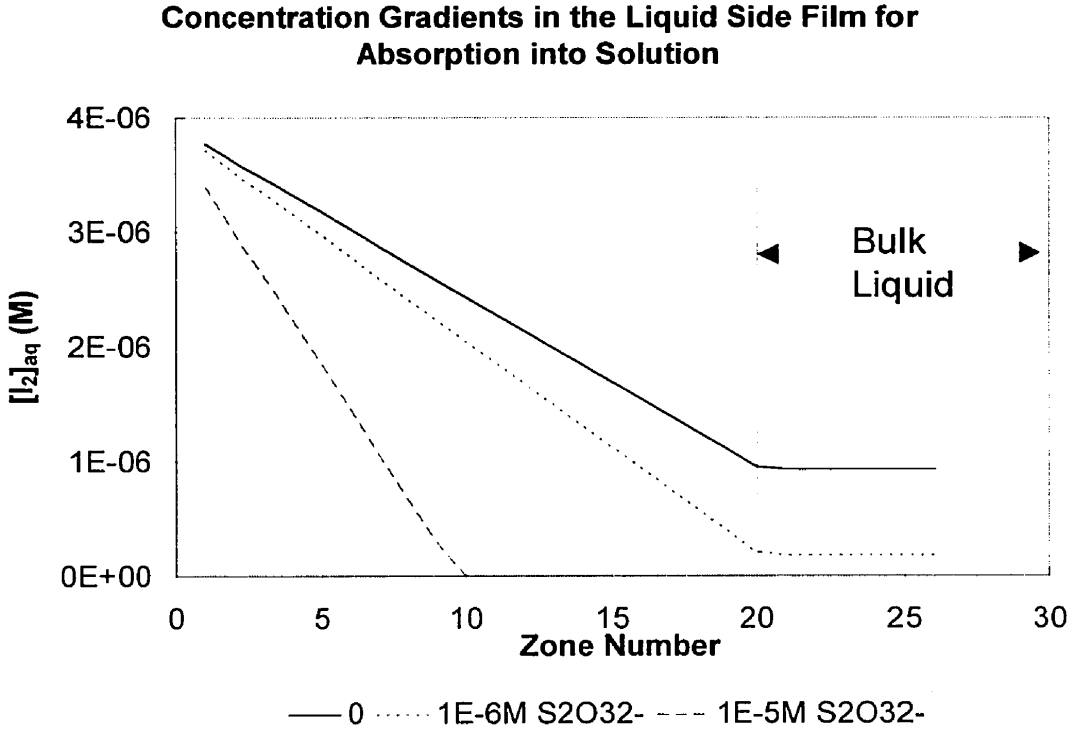

Figure 6.9: I_2 concentration gradients in the liquid phase film after one hour for the absorption of iodine gas into 0 M, 1 x10^{-6} M and 1 x 10^{-5} M $S_2O_3^{2-}$ solutions

thiosulphate solution was greater than that for absorption into water, the effective thickness of the liquid phase film was not decreased, and hence the mass transfer of iodine into the liquid phase was not enhanced. For absorption into 1 x 10^{-5} M thiosulphate solution, the concentration of iodine in the liquid phase dropped to almost zero by zone 10. Therefore, the thickness of the liquid phase film was effectively reduced by a factor of two, and the mass transfer of iodine was enhanced. For thiosulphate concentrations in which the thickness of the liquid phase film was reduced to essentially zero, the mass transfer of iodine was dependent only on the thickness of the gas phase film. This thickness was unaffected by the thiosulphate ions because reaction only occurs in the liquid phase, and so at this stage, the mass transfer of iodine was gas phase limited.

6.3 MASS TRANSFER ACCOMPANIED BY REACTION WITH IODIDE IONS

The effect that reaction with iodide ions has on the mass transfer of iodine was investigated for two different systems: (1) the evaporation of iodine from solutions containing iodine molecules, iodide ions and triiodide ions and (2) the absorption of iodine gas into iodide ion solutions.

6.3.1 EVAPORATION

Using the experimental procedure outlined in section 4.3, experiments were performed on the evaporation of iodine from triiodide solutions containing iodide ions in concentrations ranging from 1 x 10^{-4} M to 0.5 M.

The experiment was repeated five times for the evaporation of iodine from triiodide solutions containing 0.05 M iodide ions. To determine the overall mass transfer coefficient of iodine from these experiments, graphs of $\ln[I_2]_{aq}$ against time were plotted. The slopes of these plots, which were directly proportional to the overall mass transfer coefficients, were determined by using the linear regression tool of Microsoft Excel version 5.0. Figure 6.10 shows the plot of $\ln\{[I_2]_{aq}\}$ against time for one of the experiments. The overall mass

plot.

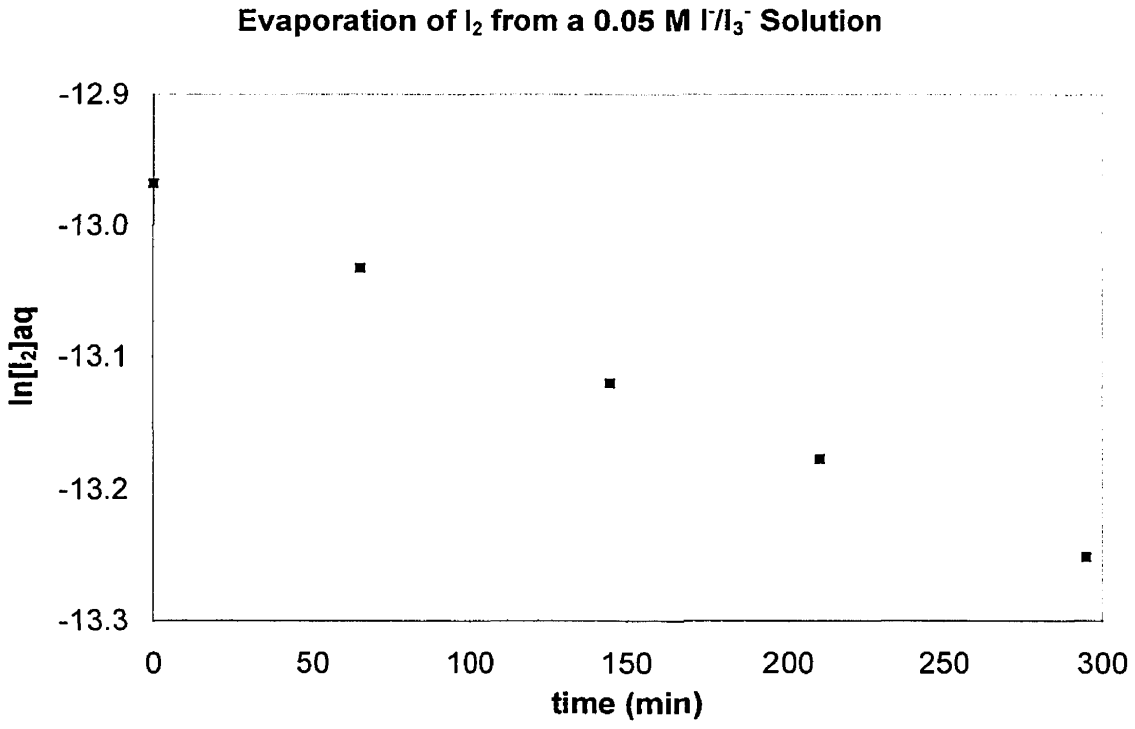

Figure 6.10: rate of change of ln[I2] for the evaporation of I_2 from a 0.05 M I^-/I_3^- Solution

The overall mass transfer coefficients obtained from the two experiments on the evaporation of iodine from 0.05 M iodide/triiodide solutions are summarized in table 6.10. These results were averaged to yield an average overall mass transfer coefficient of 0.0016 cm/s for the evaporation of iodine from 0.05M I-.

Table 6.10: K_{OL} from the experiments on the evaporation of I_2 from a 0.05 M I^-/I_3^- solution

run #	K_{OL} (cm/s)
1	0.0019
2	0.0020

ion concentration. For each iodide ion concentration, the overall mass transfer coefficients were averaged. The mean mass transfer coefficients obtained are summarized in table 6.11. The errors in the overall mass transfer coefficients are the standard deviations between the results of replicate experiments.

Table 6.11: K_{OL} values for the evaporation of iodine from I^-/I_3^- solutions

$[I^-]$ (M)	K_{OL} (cm/s)	% error
0	0.00019	29
1×10^{-4}	0.00018	17
1×10^{-3}	0.00042	7
2.5×10^{-3}	0.00054	13
5×10^{-3}	0.00077	8
1×10^{-2}	0.0010	17
2.5×10^{-2}	0.0013	6
5×10^{-2}	0.0020	4
1×10^{-1}	0.0023	11
2×10^{-1}	0.0026	16
5×10^{-1}	0.0024	5

The trend between the overall mass transfer coefficient and the concentration of the solution was the same as for the absorption of iodine gas into sodium thiosulphate solution. For iodide ion concentrations of 1×10^{-4} M and lower, the overall mass transfer coefficient was constant. As the iodide ion concentration was increased past 1×10^{-4} M, the overall mass transfer coefficient increased dramatically with iodide ion concentration. As the iodide ion concentration was increased past 0.1 M, the increase in the overall mass transfer coefficient diminished, and in fact, the overall mass transfer coefficient approached a limiting value.

The assumption that the concentration of iodine gas in the bulk gas phase could be approximated by the concentration of iodine gas in the inlet stream was again used in calculating the overall mass transfer coefficients for the evaporation of iodine from solutions

in the inlet air, which was taken from the laboratory environment, was assumed to be zero. It was found that for the evaporation of iodine from triiodide solutions with iodide concentrations greater than 0.1M, the rate of decrease of iodine in the system was a factor of 10 smaller than expected based on the trends observed so far. It was speculated that if the concentration of iodine gas entering the system was not zero as assumed, then the rate of mass transfer would be smaller, as was observed. Therefore, these experiments were repeated, but with a charcoal trap placed before the inlet air stream. This was to ensure that the inlet stream was free of any iodine gas that might be in the laboratory surroundings. Table 6.12 shows the values obtained for the mass transfer coefficient for the experiments performed with and with out charcoal traps.

Table 6.12: comparison of K_{OL} values for triiodide evaporation experiments with and without charcoal traps

$[I^-]$ (M)	K_{OL} (cm/s)	
	with charcoal	without charcoal
0.2	0.0026	0.0015
0.5	0.0024	0.0005

Adding charcoal traps to the experimental apparatus dramatically increased the rate of volatilization of iodine from the triiodide solution. This suggested that the iodine gas concentration in the ambient air was not zero, and raised questions with regards to the overall mass transfer coefficients previously calculated from the experiments involving low iodide ion concentrations. Therefore the experiments performed on the evaporation of iodine from triiodide solutions with low iodine ion concentration were re-performed with the new experimental set-up to observe if there would be any difference in the overall mass transfer coefficients. The overall mass transfer coefficients were experimentally similar whether the inlet air stream was passed through a charcoal trap before entering the system or not. It was therefore concluded that the concentration of iodine gas in the laboratory surroundings was sufficiently low that it had no effect on the evaporation of iodine from triiodide solutions

evaporation of iodine from triiodide solutions containing high iodide concentrations. Based on the experimental results, the concentration of iodide ions at which the iodine gas in the laboratory surroundings started to have an impact on the rate of iodine mass transfer was 0.1M.

MODELLING

Iodine reacts with iodide ions by reaction 6-13 to form triiodide ions. The forward rate constant of this reaction is 5.6×10^9 $M^{-1}s^{-1}$ and the reverse rate constant is 7.5×10^6 s^{-1}. The equilibrium constant of the reaction is 747 M^{-1}.

$$I_2 + I^- \leftrightarrow I_3^- \qquad 6\text{-}13$$

Using the model created to simulate the evaporation of iodine from solutions containing iodide ions, triiodide ions and iodine molecules, a graph depicting the dependence of the overall mass transfer coefficient on the iodide ion concentration of the solution was obtained. The modelling results agree well with the experimental results for the lower iodide concentrations, as shown in figure 6.11. For the higher iodide concentrations however, the experimental results deviate from the modelling results. The value of k_g input to the model was the value determined from the experiments on the absorption of I_2 into high thiosulphate concentration solutions. It is at high reactant concentration, when mass transfer is gas-side limited, that any inaccuracy in k_g will be reflected in the limiting value of K_{OL}. As was mentioned in section 6.2.1, the values of k_g determined from the absorption of I_2 into thiosulphate solution and from the evaporation of water differed by more than a factor of 2. This difference, which is essentially a difference between evaporation and absorption, is the reason for the deviation between the experimental and modelling results at high $[I^-]$. The difference between absorption and evaporation is discussed in section 6.3.2.

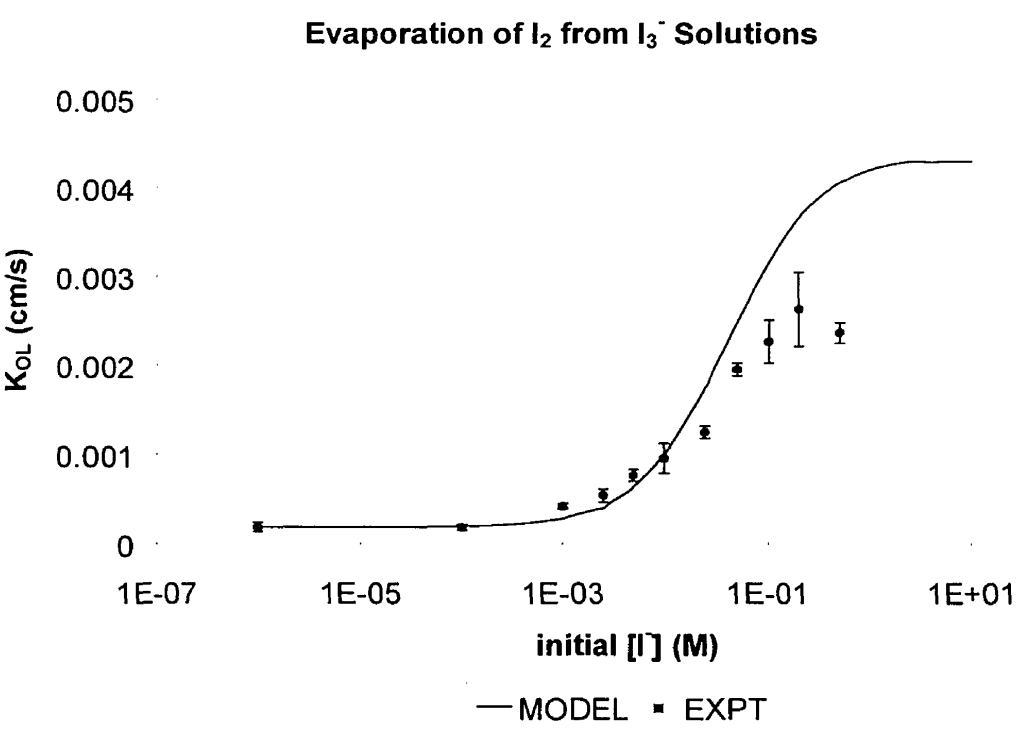

Figure 6.11: dependence of K_{OL} on I^- concentration for the evaporation of I_2 from I_3^-solutions

6.3.2 ABSORPTION

Experiments on the absorption of iodine gas into solutions of iodide ions were performed using the procedure given in section 4.4. Iodide ion concentrations ranged from 10^{-6} M to 0.5 M. Graphs of $\ln\{H[I_2]_{gasin} - [I_2]_{aq}\}$ were plotted and from the slopes, the overall mass transfer coefficients were calculated. The slopes were determined by using linear regression from Microsoft excel 5.0. Three identical experiments were performed on the absorption of iodine into a 0.5 M iodide solution. Figure 6.12 shows the plot of $\ln\{H[I_2]_{gasin} - [I_2]_{aq}\}$ against time for one of these experiments.

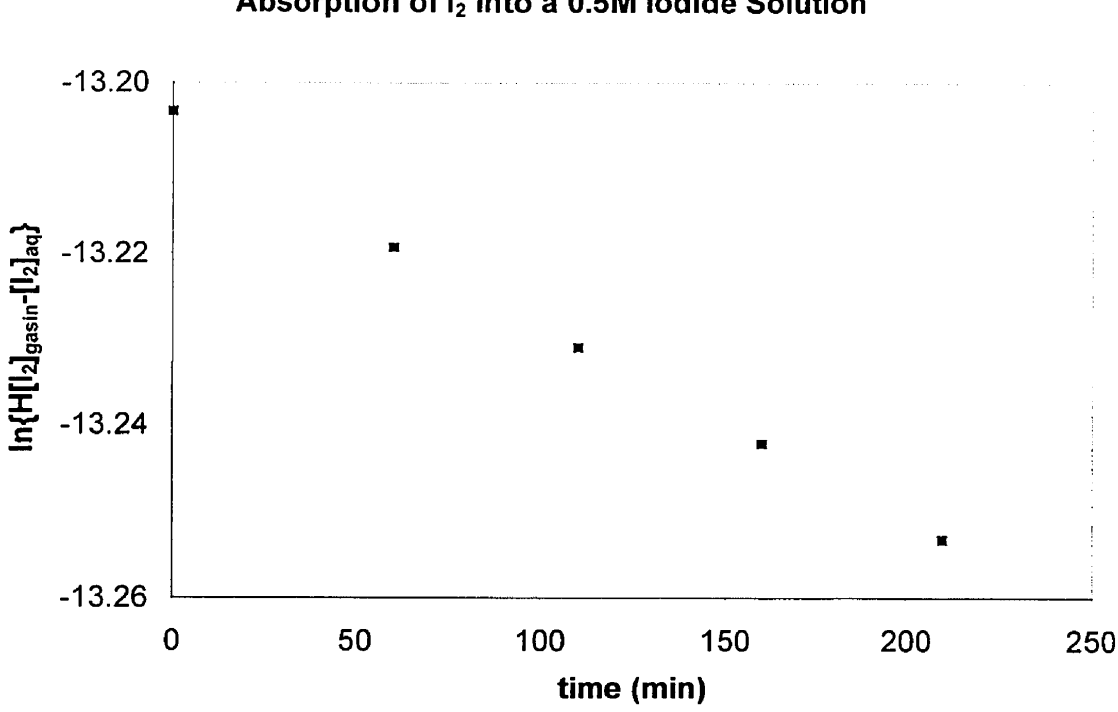

Figure 6.12: plot of $\ln\{H[I_2]_{gasin}-[I_2]_{aq}\}$ against time for the absorption of I_2 into a 0.5 M iodide ion solution

Table 6.13 summarizes the overall mass transfer coefficients obtained from the three experiments. These values were averaged to obtain an average value of 0.0037 cm/s for the absorption of iodine into 0.5 M I-.

Table 6.13: K_{OL} values from the experiments on absorption of iodine into 0.5 M I^-

run #	K_{OL} (cm/s)
1	0.0034
2	0.0038
3	0.0039

Two or more experiments were performed for the absorption of iodine into iodide ions solutions. The overall mass transfer coefficients obtained for each iodide ion concentration

In general, the overall mass transfer coefficients follow the same trend as those produced by the absorption of iodine gas into sodium thiosulphate solutions and the evaporation of iodine from triiodide ion solutions. However, the experiments to determine these overall mass transfer coefficients were less reproducible than all previous experiments, with percent standard deviations in the coefficients ranging from 70 % to 6 %.

Table 6.14: K_{OL} values for the absorption of iodine into iodide solutions

$[I^-]$ (M)	K_{OL} (cm/s)	% error
0	0.0004	55
1×10^{-3}	0.0005	70
1×10^{-2}	0.0020	20
1×10^{-1}	0.0028	4
5×10^{-1}	0.0037	7
1×10^{0}	0.0036	5

THE EFFECT OF REVERSING THE FLASK ON THE MASS TRANSFER COEFFICIENT

The assumption that the iodine gas concentration in the bulk gas phase could be approximated by the inlet concentration if the inlet stream entered at a height of 1 cm above the solution surface was tested with the experimental apparatus used for these absorption experiments. Using the experimental procedure outlined in section 4.4, an experiment was performed on the absorption of iodine gas into a 0.1M iodide solution. Assuming that the bulk iodine gas concentration was equal to the inlet iodine gas concentration the overall mass transfer coefficient was calculated to be 0.0037 cm/s. The experiment was then performed again, but this time with the absorption flask reversed such that iodine gas entered the system from the top of the flask and exited from a height of 1 cm above the surface of the iodide solution. Assuming that the bulk iodine gas concentration was equal to the iodine gas concentration leaving the system, the overall mass transfer coefficient of iodine was

concentrations at the inlet and outlet to the system were determined by performing a mass balance on the system. The above procedure was repeated for the following four experiments: (1) evaporation of water, (2) absorption of iodine gas into 0.1M sodium thiosulphate, (3) evaporation of iodine from 0.005 M and 0.5 M iodide/triiodide ion solutions and (4) absorption of iodine into 0.1M iodide solution. Table 6.15 summarizes the results obtained. The normal system is shown in figure 6.1a and the reversed system is shown in figure 6.1b.

Table 6.15: comparison of K_{OL} values for the normal and reversed systems

experiment	**K_{OL} (cm/s)**	
	normal system	**reversed system**
evaporation of water	0.16*	0.22*
evaporation from 0.005M I^-	0.00077	0.00056
evaporation from 0.5M I^-	0.0024	0.0018
absorption into 0.1M $S_2O_3^{2-}$	0.0044	0.0033
absorption into 0.5M I^-	0.0037	0.0022

* these values are gas phase mass transfer coefficients. All other values are overall mass transfer coefficients.

Using the last three rows in table 6.15, gas phase mass transfer coefficients were calculated for the normal system by assuming that for thiosulphate and iodide solutions of concentration 0.1 M and greater, the absorption of iodine into solution was limited by transfer through the gas side. Equation 6-14 was used to calculate k_g. The calculated values of k_g are summarized in table 6.16.

$$k_g = HK_{OL} \qquad 6\text{-}14$$

experiment	gas phase mass transfer coefficient (cm/s)	
	normal system	**reversed system**
evaporation of water	0.16	0.22
evaporation from 0.5M I^-	0.19	0.14
absorption into 0.1M $S_2O_3^{2-}$	0.35	0.26
absorption into 0.5M I^-	0.30	0.17

Except for the experiment on the evaporation of water, the mass transfer coefficient is smaller for the reversed system than for the normal system. The difference between the two systems is the pattern of air flow. In the normal system, air is impinged on the interface and disturbs the gas side film. In the reversed system, air is drawn through the system without disturbing the gas side film to any great extent. Therefore, in the last three cases in table 6.16, impingement had a significant effect on mass transfer, increasing the gas phase mass transfer coefficient by a factor of approximately 1.5.

ABSORPTION VERSUS EVAPORATION

The results presented in table 6.16 for the normal system are again summarized in table 6.17, but this time evaporation and absorption experiments are compared.

Table 6.17: comparison of k_g values for evaporation and absorption experiments

experiment		**k_g (cm/s)**
evaporation	of water	0.16
	from 0.5 M I^-	0.19
absorption	into 0.1 M $S_2O_3^{2-}$	0.35
	into 0.5 M I^-	0.30

The gas phase mass transfer coefficients determined from the experiments on evaporation are approximately a factor of two smaller than the coefficients determined from the absorption experiments. However, the models for the mass transfer of iodine predict that the mass transfer coefficients are independent of the direction of mass transfer. The models are based upon well established theories that have been empirically proven to be correct. It is therefore

experimental conditions. It has already been shown that the impingement of air on the interface had a significant effect on the mass transfer of iodine. This effect of impingement was not incorporated into the models. If the force of impingement was strong enough, it could explain why the mass transfer coefficients were not equal for absorption and evaporation. Figure 6.13 illustrates how impingement may have resulted in an increase in the rate of absorption and/or a decrease in the rate of evaporation of iodine.

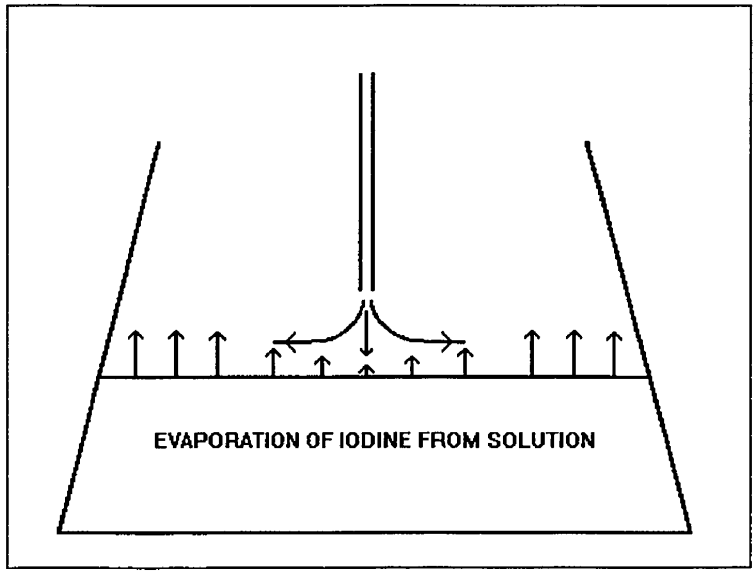

Figure 6.13: diagram showing how impingement might affect interfacial mass transfer.

In both the evaporation and absorption experiments, the direction of air flow is down onto the interface. As shown in figure 6.13, the impinging air stream might hamper evaporation by providing an extra resistive force to upward transfer. Specifically, I_2 evaporating from the surface would have to diffuse in a countercurrent flow of impinging air. Similarly, the impinging air might also promote absorption by decreasing the resistive force to downward transfer.

MODELLING

Using the model for the absorption of iodine into iodide ion solutions, a graph showing the dependence of the overall mass transfer coefficient on the iodide ion

follow the same trend, as shown in figure 6.14.

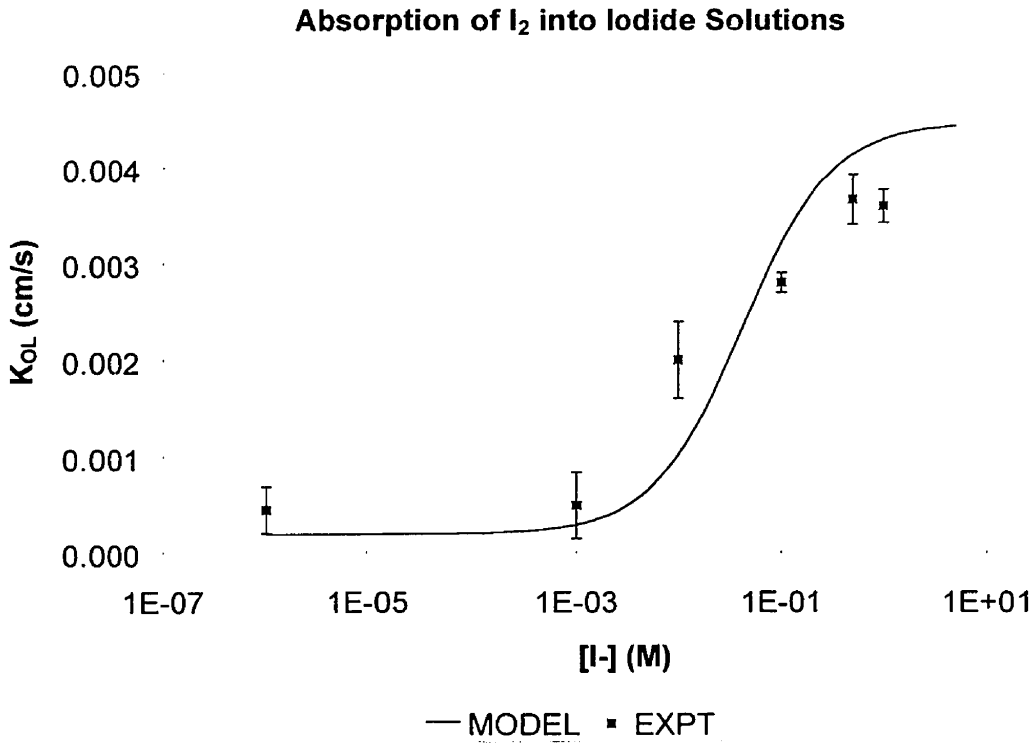

Figure 6.14: dependence of K_{OL} on I^- concentration for the absorption of I_2 into I^- ion solutions

SENSITIVITY OF THE MODEL TO CHANGES IN THE RATE AND EQUILIBRIUM CONSTANTS

The effect of changing the forward and/or reverse rate constant for the reaction between iodine and iodide ions was investigated using the model for the absorption of iodine gas into iodide solutions.

$$I_2 + I^- \leftrightarrow I_3^- \qquad 6\text{-}15$$

constant, K_{eq}, is 747 M^{-1} . The value of k_b was decreased by a factor of ten and input into the model. Figure 6.15 shows how this change in $k_{b,rxn6\text{-}15}$ affected the model output.

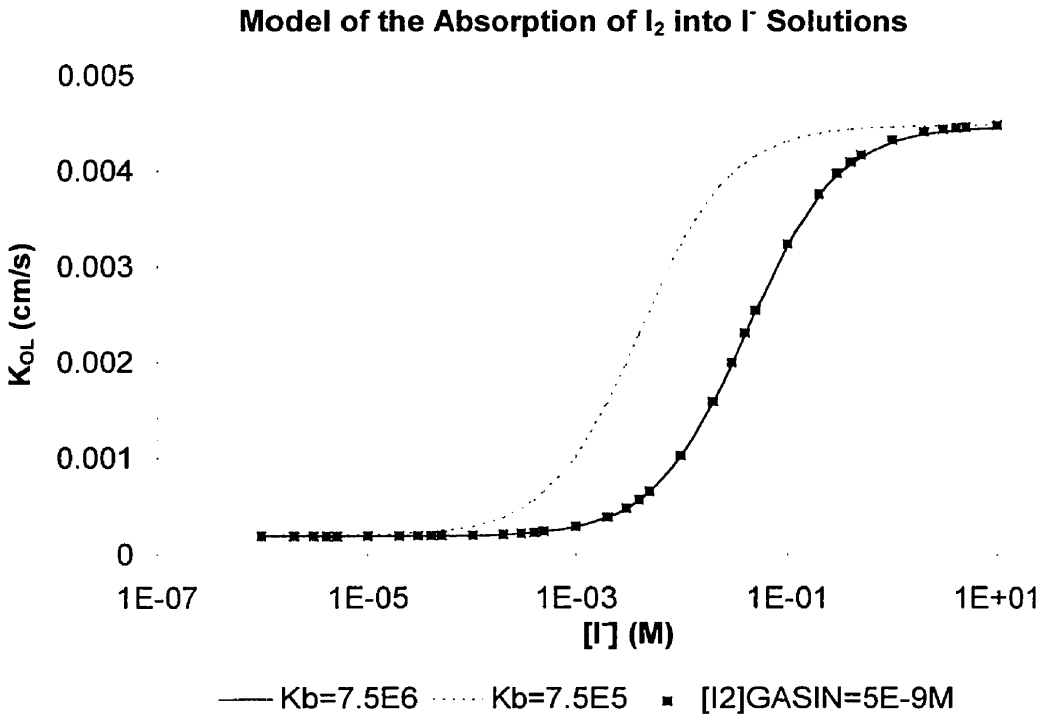

Figure 6.15: effect of changes in k_b and $[I_2]_{gasin}$ on the model output for the absorption of I_2 into iodide solutions

The effects of other changes in the forward and reverse rate constants were investigated for the absorption of iodine into a 0.01 M iodide solution. The results of the investigation are summarized in table 6.18.

k_f ($M^{-1}s^{-1}$)	k_b (s^{-1})	K_{eq}	K_{OL} (cm/s)
5.6×10^8	7.5×10^6	74.7	0.00029
5.6×10^9	7.5×10^7	74.7	0.00029
5.6×10^8	7.5×10^5	747	0.0010
5.6×10^9	7.5×10^6	747	0.0010
5.6×10^{10}	7.5×10^7	747	0.0010
5.6×10^9	7.5×10^5	7467	0.0032
5.6×10^{10}	7.5×10^6	7467	0.0032

It is evident that changes in $k_{f,rxn6\text{-}15}$ and $k_{b,rxn6\text{-}15}$ did not affect K_{OL}, as long as K_{eq} was kept constant. In the model for the absorption of I_2 into thiosulphate solutions, it was observed that the value of $[I_2]_{gasin}$ was an important factor. This was not the case for the model for the absorption of I_2 into iodide solutions. As shown in figure 6.15, the curve for $[I_2]_{gasin} = 5 \times 10^{-9}$ M lies on top of the curve for $[I_2]_{gasin} = 5 \times 10^{-8}$ M, both curves having a $k_{b,rxn6\text{-}15} = 7.5 \times 10^6$ s^{-1}.

The forward reaction of 6-15 is a second-order reaction between iodine and iodide ions. If the reaction can be assumed to be pseudo-first order, then the pseudo first order forward rate constant would be $k_{f,rxn6\text{-}15}[I^-]$, and the equilibrium constant would be $K_{eq}[I^-]$. For a range of iodide concentrations, values of φ_{max} could then be estimated from equation 2-18, and compared to values of φ from the model. Table 6.19 presents the results of such a comparison.

determined from the iodide absorption model.

[I-] (M)	φ_{max} (equation 2-18)	φ (model for absorption of I_2 into I^- solutions)
1 x 10-4	1.075	1.055
1 x 10-3	1.75	1.56
1 x 10-2	8.5	6.7
1 x 10-1	76	56

The values of φ are comparable in size, and therefore, φ is dependent on the value of K_{eq} for the reaction between iodine and iodide ions. This explains why changes in K_{eq} affected the values of K_{OL} for the model of the absorption of I_2 into iodide solutions.

6.4 MASS TRANSFER ACCOMPANIED BY REACTION WITH HYDROXIDE IONS

MODELLING RESULTS

The reactions that occur between iodine and hydroxide ions are given below.

$$I_2 + OH^- \leftrightarrow I_2OH^- \qquad 6\text{-}16$$

$$I_2OH^- \leftrightarrow I^- + HOI \qquad 6\text{-}17$$

$$I_2 + I^- \leftrightarrow I_3^- \qquad 6\text{-}18$$

The overall mass transfer coefficients calculated from the model of the absorption of iodine gas into solutions of varying hydroxide concentrations, and hence pH, show the same trend as for all the other models. As the hydroxide concentration was changed from low to high, the overall mass transfer coefficient was initially constant for low hydroxide concentration, then increased with increasing hydroxide concentration, and finally leveled off again for high hydroxide concentration.

As noted in sections 6.2.2 and 6.3.2, both $[I_2]_{gasin}$ and K_{eq} have the potential to influence K_{OL}. Consider the following reaction:

$$A + \beta B \rightarrow C$$

Case (i) $$\varphi_{max,1} = 1 + \frac{[B]_{initial}}{\beta[A]_{interface}} = 1 + \frac{[B]_{initial}}{\beta H[A]_{gas}} \quad 6\text{-}19$$

Case (ii) $$\varphi_{max,2} = 1 + K_{eq}'[B]_{eq}^{\beta} = 1 + \frac{[C]_{eq}}{[A]_{eq}} \quad 6\text{-}20$$

If [C]/[A] is large compared to $[B]_{initial} / [A]_{interface}$, then the value of $[I_2]_{gasin}$ will determine how K_{OL} changes with the concentration of the reactant. If the opposite is true then K_{eq} will be the important factor. The reaction between I_2 and $S_2O_3^{2-}$ ions is very rapid and almost irreversible, hence $[A]_{eq}$ is very small. Therefore $[C]_{eq}/[A]_{eq}$ is large and case (i) prevails. The reaction between I_2 and I^- ions has a finite K_{eq}, and so case (ii) prevails. Both these reactions have already been discussed in sections 6.2.2 and 6.3.2. The effect of the reaction between I_2 and OH^- on the mass transfer enhancement of I_2 is now considered with respect to $[I_2]_{gasin}$ and the rate constant of reaction.

The effect of the inlet iodine gas concentration and the rate constant of the reaction on the overall mass transfer coefficient was investigated for the absorption of I_2 into hydroxide solutions. The model was run for three different conditions:

(i) $[I_2]_{gasin} = 5 \times 10^{-8}$ M and $k_{f,rxn6\text{-}16} = 8.0 \times 10^8$ $M^{-1}s^{-1}$

(ii) $[I_2]_{gasin} = 5 \times 10^{-9}$ M and $k_{f,rxn6\text{-}16} = 8.0 \times 10^8$ $M^{-1}s^{-1}$

(iii) $[I_2]_{gasin} = 5 \times 10^{-8}$ M and $k_{f,rxn6\text{-}16} = 8.0 \times 10^9$ $M^{-1}s^{-1}$

The results are depicted in figure 6.16. Unlike the thiosulphate and iodide cases, the OH- model output was dependent upon the values of both $[I_2]_{gasin}$ and K_{eq}.

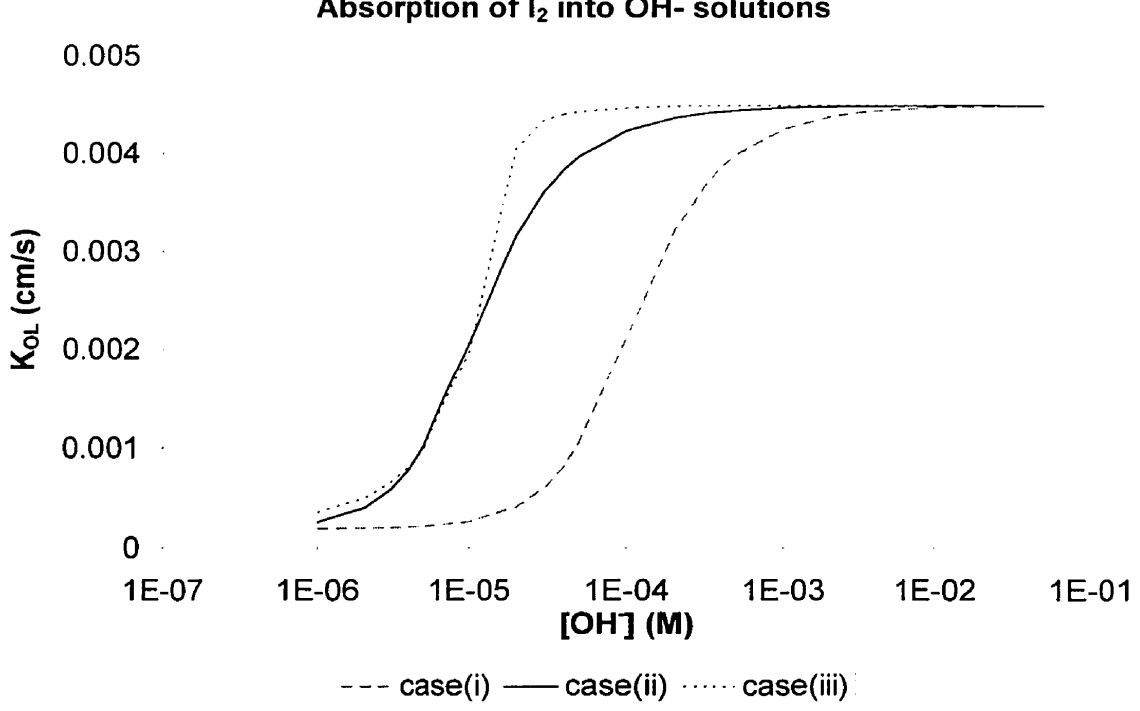

Figure 6.16: effect of $[I_2]_{gasin}$ and rate constant on the absorption of iodine into hydroxide solutions.

In figure 6.17, the models for the absorption of I_2 into thiosulphate, iodide and hydroxide solutions are compared. As expected , the hydroxide model lies between the thiosulphate and iodide models.

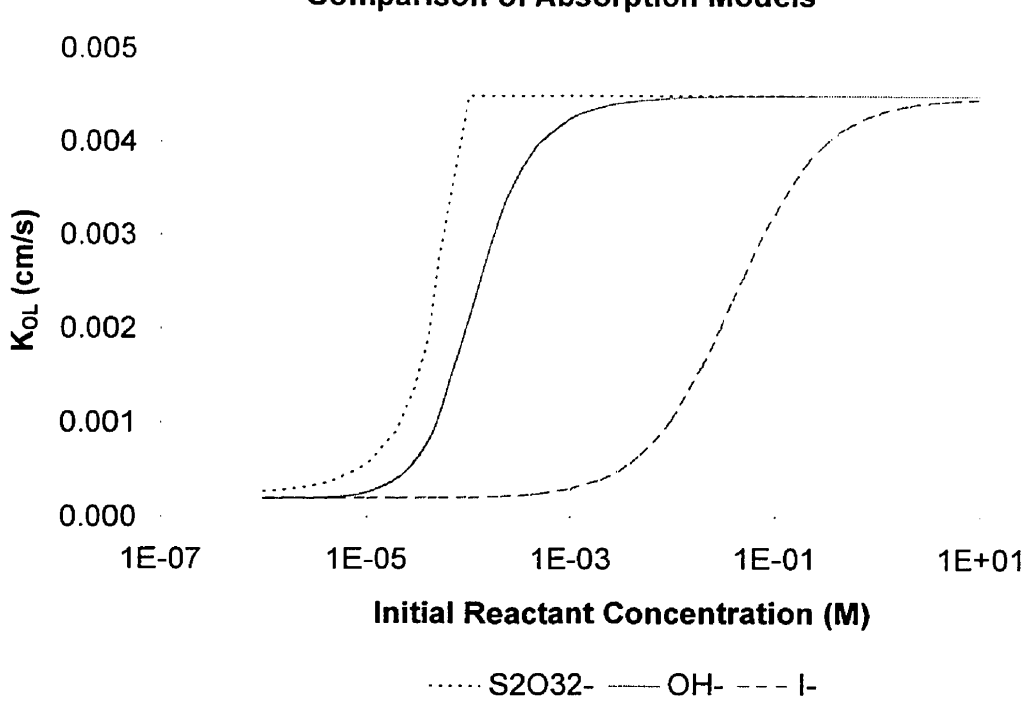

Figure 6.17: dependence of K_{OL} on the reactant concentration for the absorption models.

6.5 MODEL OF THE MASS TRANSFER OF IODINE IN THE PRESENCE OF A RADIATION FIELD

When an aqueous iodide solution is irradiated, the I^- ions are oxidized to I_2 molecules, which are then volatilized. Enhancement of the volatilization of I_2 under these conditions was studied using the model for the evaporation of iodine from solution. The model was adjusted to incorporate the radiolytic reactions that I_2 undergoes in the presence of a radiation field. These reactions are listed in appendix E.7.

In the model, the only initial concentration specified was 10^{-5} M I^-. The overall mass transfer coefficient of I_2 was calculated from the model output using the same method as for all previous models.

Atomic I is an intermediate species in the oxidation of I^- to I_2. I is believed to be very volatile, although this is still subject to debate. Two variations of the model were compiled;

6.18 compares the results from the two compilations.

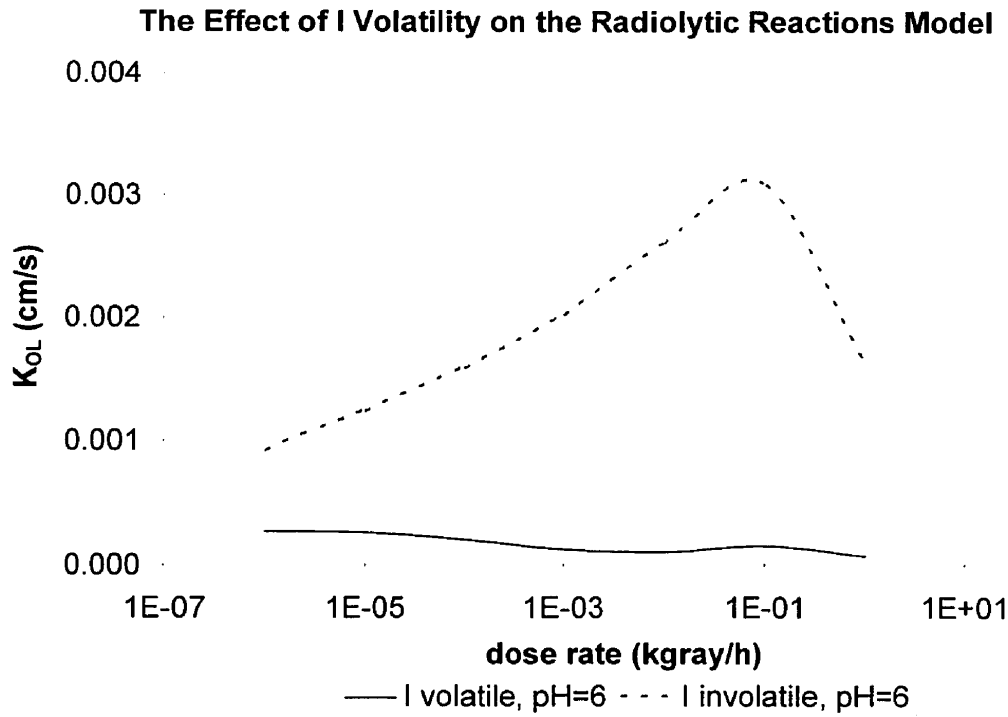

Figure 6.18: dependence of K_{OL} on the volatility of atomic I

In figure 6.18 it can be seen that for the same dose rate, enhancement of the interfacial transfer of iodine was greater for the model in which I was assumed to be involatile. In this model, the atomic I, being involatile, accumulated in the liquid side film. It then reacted to produce more I_2 than would otherwise have been produced in the liquid side film, increasing the enhancement of the interfacial transfer of iodine. Some of the important reactions involving I are given below.

$$I + I \rightarrow I_2 \qquad 6\text{-}21$$

$$I + e^- \rightarrow I^- \qquad 6\text{-}22$$

$$I + I^- \leftrightarrow I_2^- \qquad 6\text{-}23$$

$$I_2^- + OH \rightarrow I_2 + OH^- \qquad 6\text{-}24$$

The effect of the pH of the solution on the model output was also investigated. The pH's input to the model were 6, 7, 8, and 9. The results are shown in figure 6.19.

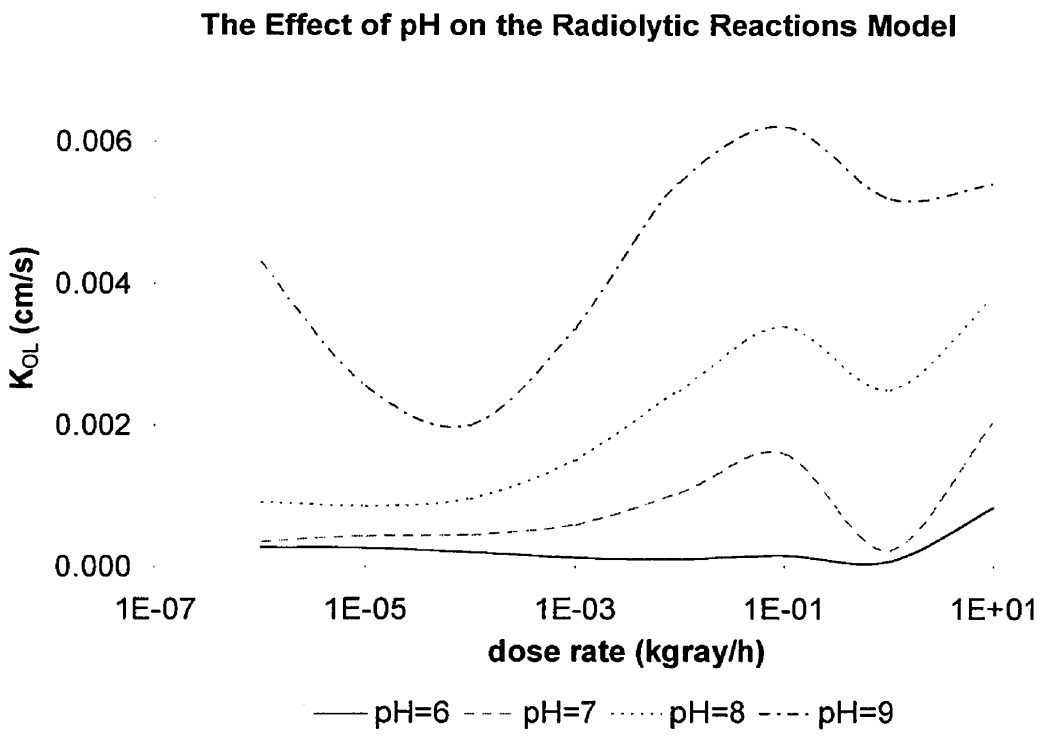

Figure 6.19: effect of pH on the evaporation of I_2 from an irradiated iodide solution

The pH of the solution had a dramatic effect on the model output. At any pH, K_{OL} fluctuates greatly with dose rate. Reactions that produce I_2 in the liquid side film promote the evaporation of I_2, and reactions that consume I_2 hinder evaporation. At dose rates where K_{OL} is large, the effect of the radiation field is to produce species that react to form I_2. The opposite is true for dose rates where K_{OL} is small.

7. CONCLUSIONS

In the absence of chemical reaction, the interfacial transfer of iodine is limited by transfer through the liquid side of the interface.

Enhancement of the interfacial transfer of iodine by chemical reaction is dependent upon the concentration of the reactants, enhancement being larger for higher concentrations. For reaction with thiosulphate ions, infinite enhancement of the transfer of iodine through the liquid phase is possible. At this stage, transfer is limited by the gas side. For the reaction between iodine and iodide ions, enhancement becomes significant at iodide concentrations of 10^{-3} M, and increases as the iodide concentration increases. For iodide concentrations greater than 0.1 M, enhancement is at a maximum, and the mass transfer of iodine is limited by the gas side.

The reaction between iodine and thiosulphate ions is so rapid that enhancement of the mass transfer of iodine does not depend on the kinetics of the reaction, but rather on the concentration of iodine in the gas phase. The enhancement is greater for low I_2(g) concentrations than for high I_2 (g) concentrations.

The method of modelling interfacial transfer by dividing the liquid phase film into a number of smaller zones can be applied to more complicated systems in which many simultaneous reactions occur.

When an iodide solution is exposed to a radiation field, molecular iodine is produced. Interfacial transfer of this molecular iodine is enhanced by the radiolytic reactions that accompany irradiation. Because of the hazardous nature of iodine, the conditions under which this enhancement occurs must be known. The method of modelling interfacial transfer by dividing the liquid phase film into a number of smaller zones was used for this purpose. It was found that enhancement is a function of the dose rate of the radiation field and the pH of the solution. As the dose rate and pH increase, the enhancement also increases. Further study on the effect of the radiolytic reactions on enhancement of the interfacial transfer of iodine is needed to better assess the conditions under which this enhancement may create a high risk situation.

8. REFERENCES

1. Bird, R. B., Stewart, W. E., and Lightfoot, E. N., "Transport Phenomena", John Wiley & Sons (1960).
2. Danckwerts, P. V., "Gas-Liquid reactions", McGraw-Hill (1970).
3. Sherwood, T. K., Pigford, R. L., and Wilke, C. R., "Mass Transfer", McGraw-Hill (1975).
4. Perry, R. H., and Green, D. W., "Perry's Chemical Engineers' Handbook", 6th ed., McGraw-Hill (1984).
5. Brian, P. L. T., Vivian, J. E., and Habib, A. G., "The Effect of Hydrolysis Reaction Upon the Rate of Absorption of Chlorine into Water", A.I.Ch.E. Journal, 8, p.205-210 (1962).
6. Takahashi, T., Hatanaka, M., and Konaka, R., "Absorption of Chlorine into Still Liquid in a Simple Stop-Cock Type Absorber", The Canadian Journal of Chemical Engineering, 45, p.145-149 (1967).
7. Marshall Hix, R., and Lynn. S., "Reactive Absorption of H_2S by a Solution of SO_2 in Poly(glycol ether): Effect of a Volatile Dissolved Reactant on Mass-Transfer Enhancement", Ind. Eng. Chem. Res., 30, p.930-939 (1991).
8. Johnson, A. I., Hamielec, A. E., and Houghton, W. T., "An Experimental Study of Mass Transfer with Chemical Reaction from Single Gas Bubbles", The Canadian Journal of Chemical Engineering, 45, p.140-144 (1967).
9. Whitmore, A., and Corsi, R. L., "Measurement of Gas-Liquid Mass Transfer Coefficients for Volatile Organic Compounds in Sewers", Environmental Progress, 13, p.114-123 (1994).
10. Trabold, T. A., and Obot, N. T., "Evaporation of Water With Single and Multiple Impinging Air Jets", Journal of Heat Transfer, 113, p.696-704 (1991).
11. Polissar, M. J., "The Rates of Evaporation of Chlorine, Bromine, and Iodine from Aqueous Solutions", Journal of Chemical Education, 12, p.89-92 (1935).
12. Taylor, R. F., "Absorption of iodine vapour by aqueous solutions", Chemical Engineering Science, 10, p.68-79 (1959).

Undergraduate Thesis, University of Toronto, Toronto (1995)

14. "FACSIMILE v3.0 USER GUIDE", AEA Technology, Oxfordshire, U.K. (1994)
15. Scheper, W. M., and Margerum, D. W., "Non-Metal Redox Kinetics of Iodine and Triiodide with Thiosulfate via $I_2S_2O_3^{2-}$ and $IS_2O_3^-$ Intermediates", Inorganic Chemistry, 31, p.5466-5473 (1992).
16. Ruasse, M., Aubard, J., Galland, B., and Adenier, A., "Kinetic Study of the Fast Halogen-Trihalide Ion Equilibria in Protic Media by the Raman-Laser Temperature-Jump Technique. A Non-Diffusion-Controlled Ion-Molecule Reaction", J. Phys. Chem., 90, p.4382-4388 (1986).
17. "1st Year Physics Laboratory Manual", unpublished, University of Toronto (1991).
18. Reid, R. C., and Sherwood, T. K., "The Properties of Gases and Liquids", 2nd ed., McGraw-Hill (1966).
19. Reid, R. C., Prausnitz, J. M., and Poling, B. E., "The Properties of Gases and Liquids", 4th ed., McGraw-Hill (1987).
20. Moran, M. J., and Shapiro, H., N., "Fundamentals of Engineering Thermodynamics", 2nd ed., John Wiley & Sons (1992).

CHEMICALS USED

INSTRUMENTS

Mass balance:	All solids were weighed out using an OHAUS mass balance, model number TS120S. The sensitivity of the balance was 0.001 g
Gamma counter:	The activity of samples was measured in a 1282 Compu Gamma counter.
Relative humidity probes:	Two relative humidity and temperature probes were used in the experiments. One was a Barnant probe, model number 637-0050 and the other was a Cole-Parmer probe, model number 37000-50. The sensitivity of both probes was 0.1 %, and the accuracy was ± 2 %.
Flow meters:	Two Cole-Parmer flow meters were used. One was equipped with a medium flow tube and the other was equipped with a high flow tube. The model number of the medium flow tube was N034-39. This flow meter was capable of measuring flow rates of air between 357 mL/min and 9229 mL/min. The high flow tube used was model N044-40 and was capable of measuring air flow rates between 1115 mL/min and 23121 mL/min.
Spectrophotometer:	The absorbance of all liquid samples was measured using a Varian Cary 3 UV-Vis Spectrophotometer with a wavelength range of 200 nm to 900 nm. The sensitivity of the instrument was 0.001.
Thermometer:	All temperature readings were recorded with a FISHER thermometer. The thermometer had a temperature range of -10°C to 260°C, and a sensitivity of 1°C.

CHEMICALS AND SUPPLIES

Needles and Syringes:	The needles and syringes used were manufactured by Becton Dickinson and Co. The needles were 21G1½ needles and the syringes were 3cc LuerLok syringes.
Plastic tubing:	The plastic tubing used in all the experiments was clear plastic tubing with an inside diameter of ¼".
Sodium thiosulphate:	The sodium thiosulphate used was manufactured by Caledon and had a minimum assay of 99.5 %.
Sodium iodide:	The sodium iodide used was manufactured by BDH Chemicals and had a minimum assay of 99.5 %.
Potassium iodide:	The potassium iodide used was manufactured by BDH Chemicals and had a minimum assay of 99.8 %.
Sodium chloride:	The sodium chloride used was manufactured by BDH Chemicals and had a minimum assay of 99.9 %.
Iodine crystals:	The iodine crystals used were manufactured by either BDH Chemicals or Mallinckrodt.

ACCURACY OF THE MASS BALANCE

Using a 500 μL Cole-Parmer micropipette, 500 μL samples of water were weighed out. The reading on the balance was compared to the expected mass of water based on the density of water at the room temperature. It was found that the balance was accurate to 0.002g.

ACCURACY OF THE RELATIVE HUMIDITY PROBES

The accuracy of the relative humidity probes was determined by placing each probe above a saturated solution of sodium chloride in a closed system. The relative humidity in such a system is 75.3 %. The Barnant probe was accurate to 5 %, and the Cole-Parmer probe was accurate to 25 %.

CALIBRATION OF THE UV-VIS SPECTROPHOTOMETER

A calibration curve of absorbance against concentration was constructed for aqueous triiodide ions at a wavelength of 350 nm using the Cary 3 UV-Vis spectrophotometer. Data for the calibration curve was obtained by measuring the absorbance of solutions of known triiodide concentration.

The triiodide solution for the calibration was prepared by weighing out known amounts of potassium iodide and iodine crystals and dissolving them in deionized water in a 100 mL volumetric flask. Another solution of potassium iodide of the same iodide concentration as the triiodide solution was prepared. Using this second solution as a diluent, a number of solutions of the same iodide concentration as the first, but different triiodide concentrations, were prepared for the calibration. Figure B.1 shows the calibration curve for triiodide solutions at a wavelength of 350 nm. Using the regression tool of Microsoft Excel version 5.0, the extinction coefficient of triiodide solutions at 350 nm was determined to be 26800.

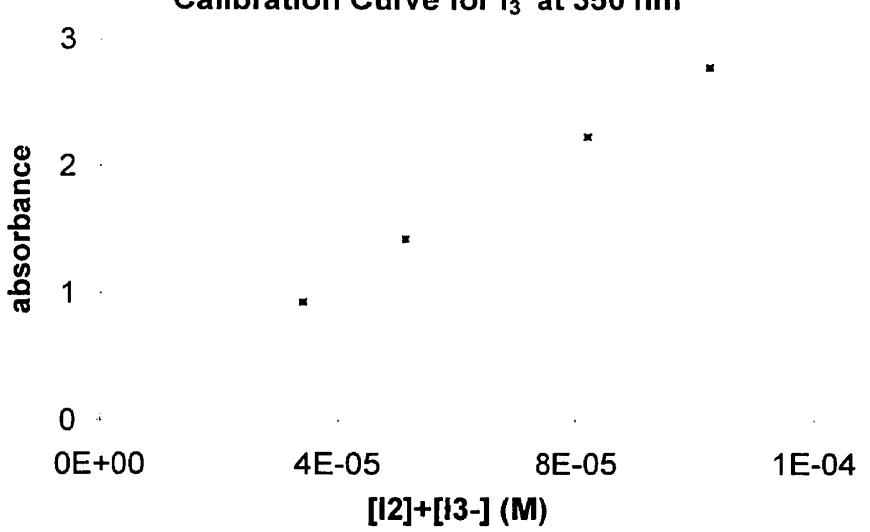

Figure B.1: calibration curve for triiodide solutions at a wavelength of 350 nm

C.1 EXPERIMENTS ON THE EVAPORATION OF WATER

run	duration of run (min)	T of water (K)	%RH in	%RH out	Vol. of water evaporated (mL)
A	344	294	27.0	81.0	4.4
B	645	297	22.8	63.0	6.5
C	460	296	6.8	65.6	6.0
D	550	294	1.7	66.0	7.0
E	455	295	4.2	81.4	5.5
F	605	295	10.7	83.4	7.5
G	445	296	25.0	85.5	5.5

C.2 EXPERIMENTS ON THE ABSORPTION OF IODINE GAS INTO WATER

run A

time (min)	[I2] (M)
0	0
30	5.5×10^{-6}
60	9.6×10^{-6}
90	1.2×10^{-5}
120	1.4×10^{-5}

run B

time (min)	[I2] (M)
0	0
47	9.0×10^{-6}
65	1.1×10^{-5}
95	1.2×10^{-5}
125	1.4×10^{-5}

run C

time (min)	[I2] (M)
0	0
45	7.9×10^{-6}
85	1.1×10^{-5}
120	1.3×10^{-5}
160	1.5×10^{-5}

run D

time (min)	[I2] (M)
0	0
30	2.2×10^{-6}
55	4.3×10^{-6}
80	4.4×10^{-6}
110	6.0×10^{-6}

run E

time (min)	[I2] (M)
0	0
30	1.6×10^{-6}
74	3.5×10^{-6}
125	5.0×10^{-6}
140	7.3×10^{-6}

C.3 EXPERIMENTS ON THE EVAPORATION OF IODINE FROM AQUEOUS IODINE

absorbances were measured at a wavelength of 460 nm

run A

time (min)	Abs
0	0.161
25	0.142
55	0.122
85	0.103
125	0.087

run B

time (min)	Abs
0	0.342
30	0.311
60	0.293
100	0.261
160	0.21

run C

time (min)	Abs
0	0.478
30	0.391
60	0.327
90	0.269
120	0.221

time (min)	Abs
0	0.476
35	0.39
85	0.282
115	0.25
160	0.191

time (min)	Abs
0	0.299
26	0.276
50	0.237
85	0.203

time (min)	Abs
0	0.309
30	0.254
60	0.21
90	0.177
135	0.134

run G

time (min)	Abs
15	0.32
35	0.288
55	0.266
75	0.244
95	0.223

run H

time (min)	Abs
5	0.427
31	0.386
82	0.341
115	0.315
143	0.295

C.4 EXPERIMENTS ON THE ABSORPTION OF IODINE INTO SODIUM THIOSULPHATE

C.4.1 ABSORPTION INTO 1 x 10^{-4} M THIOSULPHATE SOLUTIONS

run A

aqueous samples		charcoal samples	
time (min)	activity (cpm)	time (min)	activity (cpm)
0	18	25	42219
20	112	25	34074
40	140	25	34994
60	157	25	31814
80	193		
100	220		

run B

aqueous samples		charcoal samples	
time (min)	activity (cpm)	time (min)	activity (cpm)
0	5	25	15820
20	155	25	62228
40	190	25	24940
60	222	25	30300
80	251		
100	277		

run C

aqueous samples		charcoal samples	
time (min)	activity (cpm)	time (min)	activity (cpm)
0	2	25	7529
20	27	25	8713
40	51	25	8615
60	58	25	9526
80	82		
100	98		

run D

aqueous samples		charcoal samples	
time (min)	activity (cpm)	time (min)	activity (cpm)
0	9	25	16389
20	71	25	17099
40	105	25	18182
60	137	25	19753
80	161		
100	173		

aqueous samples		charcoal samples	
time (min)	activity (cpm)	time (min)	activity (cpm)
0	8	25	17357
20	43	25	18321
40	90	25	18347
60	104	25	20176
80	122		
100	140		

aqueous samples		charcoal samples	
time (min)	activity (cpm)	time (min)	activity (cpm)
0	9	25	3670
30	29	25	3773
60	36	25	4274
90	52	25	4314
120	52	25	4586
150	74	25	4537

C.4.2 ABSORPTION INTO 2 x 10^{-4} M THIOSULPHATE SOLUTIONS

run A

aqueous samples		charcoal samples	
time (min)	activity (cpm)	time (min)	activity (cpm)
0	4	25	3436
20	31	25	3764
40	56	25	4273
60	83	25	4739
80	100		
100	121		

run B

aqueous samples		charcoal samples	
time (min)	activity (cpm)	time (min)	activity (cpm)
0	0	25	2155
30	52	25	2713
60	99	25	3397
90	127	25	3850
120	150	25	4913
150	170	25	5479

C.4.3 ABSORPTION INTO 5 x 10^{-4} M THIOSULPHATE SOLUTIONS

run A

aqueous samples		charcoal samples	
time (min)	activity (cpm)	time (min)	activity (cpm)
0	26	25	15789
20	205	25	19508
40	291	25	22356
60	434	25	25394
80	516		
100	574		

run B

aqueous samples		charcoal samples	
time (min)	activity (cpm)	time (min)	activity (cpm)
0	15	25	11974
20	174	25	16641
40	229	25	18643
60	309	25	20040
80	384		
100	497		

C.4.4 ABSORPTION INTO 1 x 10^{-3} M THIOSULPHATE SOLUTIONS

run A

aqueous samples		charcoal samples	
time (min)	activity (cpm)	time (min)	activity (cpm)
0	0	25	2899
20	75	25	3451
40	146	25	4024
60	234	25	4235
80	326		
100	353		

run B

aqueous samples		charcoal samples	
time (min)	activity (cpm)	time (min)	activity (cpm)
0	8	25	2783
20	93	25	2828
40	153	25	2770
60	245	25	2520
80	314		
100	369		

run A

aqueous samples		charcoal samples	
time (min)	activity (cpm)	time (min)	activity (cpm)
0	7	25	2402
20	64	25	2287
40	137	25	2115
60	192	25	2211
80	268		
100	328		

run B

aqueous samples		charcoal samples	
time (min)	activity (cpm)	time (min)	activity (cpm)
0	0	25	2096
20	75	25	2191
40	133	25	2199
60	188	25	2251
80	282		
100	313		

C.4.6 ABSORPTION INTO 5 x 10^{-3} M THIOSULPHATE SOLUTIONS

run A

aqueous samples		charcoal samples	
time (min)	activity (cpm)	time (min)	activity (cpm)
0	14	25	6153
20	145	25	6739
40	344	25	5492
60	557	25	5811
80	669		
100	872		

run B

aqueous samples		charcoal samples	
time (min)	activity (cpm)	time (min)	activity (cpm)
0	4	25	5875
20	150	25	6155
40	345	25	5428
60	570	25	6100
80	662		
100	847		

C.4.7 ABSORPTION INTO 1 x 10^{-2} M THIOSULPHATE SOLUTIONS

run A

aqueous samples		charcoal samples	
time (min)	activity (cpm)	time (min)	activity (cpm)
0	2	25	3093
20	125	25	3661
40	191	25	3655
60	329	25	3702
80	421		
100	565		

run B

aqueous samples		charcoal samples	
time (min)	activity (cpm)	time (min)	activity (cpm)
0	0	25	2895
20	122	25	2971
40	194	25	3002
60	299	25	2912
100	524		

C.4.8 ABSORPTION INTO 5 x 10^{-2} M THIOSULPHATE SOLUTIONS

run A

aqueous samples		charcoal samples	
time (min)	activity (cpm)	time (min)	activity (cpm)
0	0	25	4599
20	106	25	4360
60	374	25	4230
80	499	25	4250
100	627		

run B

aqueous samples		charcoal samples	
time (min)	activity (cpm)	time (min)	activity (cpm)
0	4	25	3685
20	105	25	3806
40	241	25	3302
80	435	25	3346
100	784		

aqueous samples		charcoal samples	
time (min)	activity (cpm)	time (min)	activity (cpm)
0	9	25	1374
20	128	25	2066
40	159	25	2150
60	229	25	2367
80	263		
100	352		

C.4.9 ABSORPTION INTO 1 x 10^{-1} M THIOSULPHATE SOLUTIONS

run A

aqueous samples		charcoal samples	
time (min)	activity (cpm)	time (min)	activity (cpm)
0	4	25	1881
20	128	25	2191
40	176	25	2386
60	253	25	2352
80	345		
100	430		

run B

aqueous samples		charcoal samples	
time (min)	activity (cpm)	time (min)	activity (cpm)
0	2	25	1469
20	96	25	1699
40	147	25	1842
60	211	25	1717
80	310		
100	380		

run C

aqueous samples		charcoal samples	
time (min)	activity (cpm)	time (min)	activity (cpm)
0	0	50	3548
30	41	50	3658
60	84	50	3778
90	99		
120	122		
150	148		

C.5 EXPERIMENTS ON THE EVAPORATION OF IODINE FROM TRIIODIDE SOLUTIONS

C.5.1 INITIAL IODIDE CONCENTRATION = 1 x 10^{-4} M

run A

time (min)	$[I_2]$ (M)
0	6.37 x 10^{-6}
25	5.62 x 10^{-6}
50	4.82 x 10^{-6}
110	3.87 x 10^{-6}
170	2.59 x 10^{-6}

run B

time (min)	$[I_2]$ (M)
0	9.54 x 10^{-6}
35	7.87 x 10^{-6}
85	6.35 x 10^{-6}
120	5.55 x 10^{-6}
157	4.79 x 10^{-6}

run C

time (min)	$[I_2]$ (M)
0	2.21 x 10^{-5}
30	1.97 x 10^{-5}
60	1.75 x 10^{-5}
90	1.58 x 10^{-5}
145	1.30 x 10^{-5}

time (min)	$[I_2]$ (M)
0	2.70×10^{-5}
30	2.27×10^{-5}
72	1.92×10^{-5}
135	1.57×10^{-5}
220	1.16×10^{-5}

time (min)	$[I_2]$ (M)
0	2.15×10^{-5}
30	1.86×10^{-5}
60	1.59×10^{-5}
95	140×10^{-5}
135	1.11×10^{-5}

time (min)	$[I_2]$ (M)
0	3.47×10^{-5}
23	3.15×10^{-5}
61	2.30×10^{-5}
105	1.24×10^{-5}
135	1.02×10^{-5}
171	5.80×10^{-6}

C.5.2 INITIAL IODIDE CONCENTRATION = 1×10^{-3} M

run A

time (min)	$[I_2]$ (M)
0	6.43×10^{-6}
15	5.87×10^{-6}
65	4.37×10^{-6}
95	3.66×10^{-6}
125	3.12×10^{-6}

run B

time (min)	$[I_2]$ (M)
0	7.40×10^{-6}
15	6.55×10^{-6}
30	6.08×10^{-6}
50	5.30×10^{-6}
70	4.79×10^{-6}

run C

time (min)	$[I_2]$ (M)
0	7.82×10^{-6}
20	6.82×10^{-6}
40	6.11×10^{-6}
70	5.00×10^{-6}
100	4.54×10^{-6}

C.5.3 INITIAL IODIDE CONCENTRATION = 2.5×10^{-3} M

run A

time (min)	$[I_2]$ (M)
0	8.40×10^{-6}
20	7.52×10^{-6}
60	6.74×10^{-6}
100	6.00×10^{-6}
140	5.01×10^{-6}

run B

time (min)	$[I_2]$ (M)
0	7.44×10^{-6}
20	6.88×10^{-6}
40	6.40×10^{-6}
70	5.27×10^{-6}
100	4.71×10^{-6}

run C

time (min)	$[I_2]$ (M)
0	8.03×10^{-6}
20	6.88×10^{-6}
40	6.20×10^{-6}
70	5.33×10^{-6}
100	4.71×10^{-6}

run D

time (min)	$[I_2]$ (M)
0	7.62×10^{-6}
20	6.78×10^{-6}
53	5.83×10^{-6}
85	4.95×10^{-6}
115	4.44×10^{-6}

run E

time (min)	$[I_2]$ (M)
0	7.35×10^{-6}
20	6.74×10^{-6}
45	6.02×10^{-6}
85	4.99×10^{-6}
135	4.02×10^{-6}

run F

time (min)	$[I_2]$ (M)
0	2.23×10^{-5}
35	1.87×10^{-5}
65	1.62×10^{-5}
95	1.47×10^{-5}
135	1.27×10^{-5}

run G

time (min)	$[I_2]$ (M)
0	2.19×10^{-5}
25	1.97×10^{-5}
55	1.69×10^{-5}
80	1.51×10^{-5}
110	1.32×10^{-5}

run A

time (min)	$[I_2]$ (M)
0	1.13×10^{-5}
60	9.20×10^{-6}
95	7.98×10^{-6}
125	7.45×10^{-6}
170	6.45×10^{-6}

run B

time (min)	$[I_2]$ (M)
0	2.92×10^{-5}
60	2.41×10^{-5}
95	2.13×10^{-5}
125	1.88×10^{-5}
155	1.65×10^{-5}

run C

time (min)	$[I_2]$ (M)
0	2.77×10^{-5}
20	2.61×10^{-5}
50	2.36×10^{-5}
80	2.07×10^{-5}
110	1.86×10^{-5}

run D

time (min)	$[I_2]$ (M)
0	8.80×10^{-6}
20	8.15×10^{-6}
40	7.54×10^{-6}
65	6.65×10^{-6}
95	6.06×10^{-6}

run E

time (min)	$[I_2]$ (M)
20	5.95×10^{-6}
40	5.51×10^{-6}
70	4.90×10^{-6}
105	4.23×10^{-6}
135	3.81×10^{-6}

C.5.5 INITIAL IODIDE CONCENTRATION = 1×10^{-2} M

run A

time (min)	$[I_2]$ (M)
0	3.84×10^{-6}
60	3.30×10^{-6}
122	2.86×10^{-6}
200	2.35×10^{-6}

run B

time (min)	$[I_2]$ (M)
0	3.66×10^{-6}
60	3.14×10^{-6}
120	2.59×10^{-6}
183	2.30×10^{-6}
245	1.91×10^{-6}

run C

time (min)	$[I_2]$ (M)
0	5.28×10^{-6}
52	3.63×10^{-6}
83	2.96×10^{-6}
113	2.47×10^{-6}

run D

time (min)	$[I_2]$ (M)
0	5.28×10^{-6}
55	3.69×10^{-6}
87	3.07×10^{-6}
117	2.59×10^{-6}

C.5.6 INITIAL IODIDE CONCENTRATION = 2.5×10^{-2} M

run A

time (min)	$[I_2]$ (M)
0	4.47×10^{-6}
60	4.25×10^{-6}
120	3.78×10^{-6}
180	3.53×10^{-6}
240	3.21×10^{-6}

run B

time (min)	$[I_2]$ (M)
0	4.44×10^{-6}
60	4.21×10^{-6}
120	3.82×10^{-6}
180	3.58×10^{-6}
245	3.25×10^{-6}

C.5.7 INITIAL IODIDE CONCENTRATION = 5 x 10^{-1} M

run A

time (min)	$[I_2]$ (M)
0	2.33 x 10^{-6}
65	2.19 x 10^{-6}
145	2.01 x 10^{-6}
210	1.89 x 10^{-6}
295	1.76 x 10^{-6}

run B

time (min)	$[I_2]$ (M)
0	2.27 x 10^{-6}
65	2.08 x 10^{-6}
135	1.90 x 10^{-6}
265	1.78 x 10^{-6}
325	1.61 x 10^{-6}
355	1.51 x 10^{-6}

C.5.8 INITIAL IODIDE CONCENTRATION = 1 x 10^{-1} M

run A

time (min)	$[I_2]$ (M)
60	1.41 x 10^{-6}
135	1.34 x 10^{-6}
210	1.29 x 10^{-6}
340	1.22 x 10^{-6}

run B

time (min)	$[I_2]$ (M)
0	1.33 x 10^{-6}
120	1.26 x 10^{-6}
240	1.16 x 10^{-6}
360	1.10 x 10^{-6}
480	1.03 x 10^{-6}

run C

time (min)	$[I_2]$ (M)
0	7.38 x 10^{-7}
120	6.70 x 10^{-7}
240	5.94 x 10^{-7}
363	5.29 x 10^{-7}
500	4.67 x 10^{-7}

run D

time (min)	$[I_2]$ (M)
0	4.37 x 10^{-7}
122	4.01 x 10^{-7}
230	3.61 x 10^{-7}
365	3.26 x 10^{-7}
485	3.12 x 10^{-7}

run E

time (min)	$[I_2]$ (M)
0	6.00 x 10^{-7}
97	5.58 x 10^{-7}
175	5.24 x 10^{-7}
259	4.95 x 10^{-7}
360	4.55 x 10^{-7}

run F

time (min)	$[I_2]$ (M)
0	5.66 x 10^{-7}
147	4.93 x 10^{-7}
291	4.51 x 10^{-7}
422	3.82 x 10^{-7}
575	3.57 x 10^{-7}

C.5.9 INITIAL IODIDE CONCENTRATION = 2 x 10^{-1} M

run A
no charcoal upstream of air flow

time (min)	$[I_2]$ (M)
0	6.89 x 10^{-7}
180	6.69 x 10^{-7}
360	6.42 x 10^{-7}
570	6.15 x 10^{-7}

run B
charcoal trap upstream of air flow

time (min)	$[I_2]$ (M)
0	2.59 x 10^{-7}
155	2.34 x 10^{-7}
300	2.16 x 10^{-7}
440	2.01 x 10^{-7}
605	1.88 x 10^{-7}

run C
charcoal trap upstream of air flow

time (min)	$[I_2]$ (M)
0	4.34 x 10^{-7}
303	3.81 x 10^{-7}
445	3.59 x 10^{-7}
605	3.42 x 10^{-7}

run A
no charcoal upstream of air flow

time (min)	$[I_2]$ (M)
0	3.15×10^{-7}
280	3.08×10^{-7}
580	3.07×10^{-7}
1430	2.96×10^{-7}
1840	2.90×10^{-7}

run B
no charcoal upstream of air flow

time (min)	$[I_2]$ (M)
0	3.25×10^{-7}
530	3.20×10^{-7}
1430	3.15×10^{-7}
2070	3.11×10^{-7}

run C
charcoal trap upstream of air flow

time (min)	$[I_2]$ (M)
0	1.18×10^{-7}
150	1.14×10^{-7}
323	1.10×10^{-7}
505	1.07×10^{-7}
692	1.06×10^{-7}

run D
charcoal trap upstream of air flow

time (min)	$[I_2]$ (M)
175	1.01×10^{-7}
351	9.80×10^{-7}
533	9.58×10^{-7}

C.6 EXPERIMENTS ON THE ABSORPTION OF IODINE INTO POTASSIUM IODIDE

C.6.1 ABSORPTION INTO 1×10^{-3} M IODIDE SOLUTIONS

run A
$[I_2]_{gasin} = 4.4 \times 10^{-8}$ M

time (min)	$[I_2]$ (M)
0	0
122	2.63×10^{-6}
239	3.59×10^{-6}
357	3.94×10^{-6}
479	3.98×10^{-6}

run B
$[I_2]_{gasin} = 1.0 \times 10^{-7}$ M

time (min)	$[I_2]$ (M)
0	0
40	1.62×10^{-6}
75	2.72×10^{-6}
100	3.04×10^{-6}
135	3.66×10^{-6}

run C
$[I_2]_{gasin} = 1.4 \times 10^{-7}$ M

time (min)	$[I_2]$ (M)
0	0
10	5.77×10^{-7}
20	1.30×10^{-6}
30	2.16×10^{-6}
45	3.51×10^{-6}

run D
$[I_2]_{gasin} = 1.5 \times 10^{-7}$ M

time (min)	$[I_2]$ (M)
0	0
20	1.18×10^{-6}
40	2.30×10^{-6}
60	3.20×10^{-6}
80	4.27×10^{-6}

run A

$[I_2]_{gasin}$ = 1.8×10^{-8} M

time (min)	$[I_2]$ (M)
0	0
120	8.82×10^{-7}
265	1.44×10^{-6}
390	1.63×10^{-6}
495	1.69×10^{-6}

run B

$[I_2]_{gasin}$ = 2.2×10^{-8} M

time (min)	$[I_2]$ (M)
0	0
120	8.69×10^{-7}
250	1.39×10^{-6}
395	1.56×10^{-6}

run C

$[I_2]_{gasin}$ = 1.3×10^{-7} M

time (min)	$[I_2]$ (M)
0	0
30	1.14×10^{-6}
62	2.08×10^{-6}
91	2.90×10^{-6}
120	3.85×10^{-6}

run D

$[I_2]_{gasin}$ = 1.8×10^{-8} M

time (min)	$[I_2]$ (M)
0	0
60	2.05×10^{-7}
120	3.37×10^{-7}
180	4.61×10^{-7}
210	5.06×10^{-7}
240	5.65×10^{-7}

run E

$[I_2]_{gasin}$ = 1.5×10^{-7} M

time (min)	$[I_2]$ (M)
0	0
30	2.57×10^{-6}
50	3.87×10^{-6}
70	4.97×10^{-6}
90	6.15×10^{-6}

run F

$[I_2]_{gasin}$ = 1.3×10^{-7} M

time (min)	$[I_2]$ (M)
0	0
20	1.60×10^{-6}
40	2.40×10^{-6}
60	3.17×10^{-6}
80	3.90×10^{-6}
100	4.81×10^{-6}

C.6.3 ABSORPTION INTO 1×10^{-1} M IODIDE SOLUTIONS

run A

$[I_2]_{gasin}$ = 1.8×10^{-8} M

time (min)	$[I_2]$ (M)
0	0
90	2.20×10^{-7}
135	3.05×10^{-7}
180	4.09×10^{-7}
225	5.12×10^{-7}
270	6.31×10^{-7}

run B

$[I_2]_{gasin}$ = 1.8×10^{-8} M

time (min)	$[I_2]$ (M)
0	0
90	1.71×10^{-7}
155	3.14×10^{-7}
200	3.96×10^{-7}
230	4.73×10^{-7}
260	5.45×10^{-7}

run C

$[I_2]_{gasin}$ = 1.8×10^{-8} M

time (min)	$[I_2]$ (M)
0	0
75	4.78×10^{-8}
125	9.02×10^{-8}
185	1.12×10^{-7}
245	1.40×10^{-7}
305	1.60×10^{-7}

C.6.4 ABSORPTION INTO 5×10^{-1} M IODIDE SOLUTIONS

run A

$[I_2]_{gasin}$ = 2.3×10^{-8} M

time (min)	$[I_2]$ (M)
0	0
60	2.91×10^{-8}
110	5.02×10^{-8}
160	7.02×10^{-8}
210	8.98×10^{-8}

run B

$[I_2]_{gasin}$ = 3.0×10^{-8} M

time (min)	$[I_2]$ (M)
0	0
60	3.20×10^{-8}
110	6.29×10^{-8}
170	9.91×10^{-8}
230	1.38×10^{-7}

run C

$[I_2]_{gasin}$ = 2.7×10^{-8} M

time (min)	$[I_2]$ (M)
0	0
95	4.43×10^{-8}
155	8.07×10^{-8}
221	1.32×10^{-7}
290	1.55×10^{-7}

run A

$[I_2]_{gasin}$ = 4.9×10^{-9} M

time (min)	$[I_2]$ (M)
0	0
170	9.93×10^{-9}
273	1.56×10^{-8}
360	1.88×10^{-8}
500	2.41×10^{-8}

run B

$[I_2]_{gasin}$ = 2.8×10^{-9} M

time (min)	$[I_2]$ (M)
0	0
120	4.29×10^{-9}
233	7.29×10^{-9}
368	1.01×10^{-8}
485	1.28×10^{-8}

run C

$[I_2]_{gasin}$ = 1.9×10^{-7} M

time (min)	$[I_2]$ (M)
0	0
11	2.32×10^{-8}
17	4.61×10^{-8}
22	5.32×10^{-7}
30	7.35×10^{-7}

C.7 EXPERIMENTS WITH THE REACTION VESSEL IN THE REVERSED POSITION

C.7.1 THE EVAPORATION OF WATER

duration of run (min)	T of water (K)	%RH in	%RH out	Vol. of water evaporated (mL)
450	297	7.4	59.6	4.0

C.7.2 ABSORPTION OF IODINE INTO A 0.1 M THIOSULPHATE SOLUTION

aqueous samples		charcoal samples	
time (min)	activity (cpm)	time (min)	activity (cpm)
0	0	50	8632
30	30	50	8360
60	36	50	8886
90	53		
120	74		
150	83		

C.7.3 EVAPORATION OF IODINE FROM TRIIODIDE SOLUTIONS

initial iodide concentration = 5×10^{-3} M

time (min)	$[I_2]$ (M)
0	5.66×10^{-6}
68	4.40×10^{-6}
121	3.61×10^{-6}
198	3.25×10^{-6}
289	2.49×10^{-6}

initial iodide concentration = 0.5 M

time (min)	$[I_2]$ (M)
0	1.81×10^{-7}
1440	1.84×10^{-7}
2895	1.69×10^{-7}
4305	1.44×10^{-7}
5800	1.16×10^{-7}

$[I_2]_{gasin}$ = 2.7×10^{-8} M

time (min)	$[I_2]$ (M)
0	0
135	2.63×10^{-8}
228	4.37×10^{-8}
301	5.89×10^{-8}
404	8.79×10^{-8}
471	1.06×10^{-7}

The values of the parameters that were assumed to be constant during the performance of all the experiments are given below.

V, average volume of solution = 0.097 ± 0.001 L

A, surface area of solution = 0.42 ± 0.01 dm^2

F, flow rate of air = 0.018 ± 2 L/s

H, iodine air-water partition constant = 80

D.1 CALCULATION OF THE GAS PHASE MASS TRANSFER COEFFICIENT OF WATER USING THE DATA FROM RUN A IN SECTION C.1

The rate of evaporation of water is given by equation D-1.

$$w_c = k_c A(P_{sat} - P_{amb}) \qquad \text{D-1}$$

The parameter k_c is related to the gas phase mass transfer coefficient of water by equation D-2.

$$k_{g,H_2O} = \frac{10^3 k_c RT}{MW_{H_2O}} \qquad \text{D-2}$$

The rate of evaporation was calculated from equation D-3, P_{sat} was obtained from steam tables [20] and P_{amb} was calculated from equation D-4.

$$w_c = \frac{mass\ of\ water\ evaporated}{total\ time\ of\ evaporation} = \frac{volume\ evaporated\ x\ \rho_{H_2O}}{total\ time\ of\ evaporation} \qquad \text{D-3}$$

$$P_{amb} = P_{sat}\left(\frac{\%RH_m}{100\%}\right) \qquad \text{D-4}$$

Using equations D-1, D3 and D-4, the following values were obtained from the data for run A of section C.1

P_{sat} = 2645 Pa

P_{amb} = 714.2 Pa

$w_c/A = 5.08 \times 10^{-5}$ kg/m^2·s

Substituting the above values into equation D-2, the gas phase mass transfer coefficient of water was calculated to be 3.6×10^{-3} cm/s.

D.2 CALCULATION OF K_{OL} FOR THE ABSORPTION OF IODINE INTO WATER USING THE DATA FROM RUN A IN SECTION C.2

Using the data from run A in section C.2, a plot of $\ln\{H[I2]gasin - [I2]_{aq}\}$ against time was constructed, and using the linear regression tool of Microsoft Excel version 5.0, the slope of this plot was determined to be -2.2×10^{-4} s^{-1}. Using equation D-5, K_{OL} was calculated to be 5.2×10^{-4} cm/s.

$$K_{OL} = slope \frac{V}{A} \qquad \text{D-5}$$

D.3 CALCULATION OF K_{OL} FOR THE EVAPORATION OF IODINE FROM AQUEOUS IODINE USING THE DATA FROM RUN A IN SECTION C.3

Using the data from run A in section C.3, a plot of $\ln\{[I2]_{aq}\}$ against time was constructed, and using the linear regression tool of Microsoft Excel version 5.0, the slope of this plot was determined to be -8.3×10^{-5} s^{-1}. Using equation D-5, K_{OL} was calculated to be 1.9×10^{-4} cm/s.

D.4 CALCULATION OF K_{OL} FOR THE ABSORPTION OF IODINE INTO SODIUM THIOSULPHATE USING THE DATA FROM RUN A IN SECTION C.4

Using the linear regression tool in Microsoft Excel version 5.0, the slope of the plots of activity against time were obtained. The value of $[I_2]_{gasin}$ was determined by performing an activity balance on the system. Equation D-6 shows how $[I_2]_{gasin}$ was calculated.

$$[I_2]_{gasin} = \frac{}{F\ x\ time\ of\ experiment} = \frac{}{F\ x\ time\ of\ experiment} \quad \text{D-6}$$

K_{OL} was calculated from equation D-7.

$$K_{OL} = \frac{-slope\ x\ V}{AH[I_2]_{gasin}} \quad \text{D-7}$$

For the data in run A of section C.4, the slope of the plot of activity against time was 1.35 cpm/mL·min and $[I_2]_{gasin}$ was 1.5 cpm/mL. Substituting these values into equation D-7 yielded a value of 4.0×10^{-4} cm/s for K_{OL}.

D.5 CALCULATION OF K_{OL} FOR THE EVAPORATION OF IODINE FROM A TRIIODIDE SOLUTION USING THE DATA FROM RUN A IN SECTION C.5

Using the data from run A in section C.5, a plot of $\ln\{[I2]_{aq}\}$ against time was constructed, and using the linear regression tool of Microsoft Excel version 5.0, the slope of this plot was determined to be $-8.5 \times 10^{-5}\ s^{-1}$. K_{OL} was calculated from equation D-8, in which k_f and k_b were the forward and reverse rate constants of the reaction between iodine and iodide ions. K_{OL} was calculated to be 2.1×10^{-4} cm/s.

$$K_{OL} = -slope\frac{V}{A}\left(1 + \frac{k_f}{k_b}[I^-]_{init}\right) \quad \text{D-8}$$

D.6 CALCULATION OF K_{OL} FOR THE ABSORPTION OF IODINE INTO AN IODIDE ION SOLUTION USING THE DATA FROM RUN A IN SECTION C.6

Using the data from run A in section C.6, a plot of $\ln\{ H[I2]gasin - [I2]_{aq}\}$ against time was constructed, and using the linear regression tool of Microsoft Excel version 5.0, the slope of this plot was determined to be $-2.4 \times 10^{-4}\ s^{-1}$. Using equation D-8, K_{OL} was calculated to be 9.5×10^{-4} cm/s.

D.7 ERROR ANALYSIS

PROPAGATION OF ERRORS METHOD [17]

Using the formulas listed in table D.1, an error associated with each value of K_{OL} was determined.

Table D.1: formulas used for the propagation of errors

OPERATION	PROPAGATED ERROR
Z = X + Y or Z = X - Y	$\Delta Z = \sqrt{(\Delta X)^2 + (\Delta Y)^2}$
Z = XY or Z = X/Y	$\frac{\Delta Z}{Z} = \sqrt{\left(\frac{\Delta X}{X}\right)^2 + \left(\frac{\Delta Y}{Y}\right)^2}$

In table D.1, ΔZ, ΔX and ΔY are the errors associated with Z, X and Y. Table D.2 summarizes these errors for the measurements of the experiments.

Table D.2: errors associated with the parameters of the experiments

parameter	**error**
V = 97 mL	1 mL
A = 42 cm^2	1 cm^2
H = 80	10
F = 18 mL/s	2 mL/s
activity	√(activity)
slope of plots	as determined by linear regression

All other instrument errors are given in appendix B.

E.1 LISTING FOR THE MODEL SIMULATING THE EVAPORATION OF IODINE FROM AQUEOUS IODINE

```
* model of the evaporation of iodine from a solution of molecular iodine;
* the liquid film is divided into #nzone zones;
* the bulk layer is designated as the #nzone+1 zone;

PERMIT + -;
INTEGER #nzone 20;
* I2 is iodine conc., I2bulk is the conc. of iodine in the bulk liquid phase;
VARIABLE  I2bulk 1.1e-03 I2gas ;
VARIABLE <#nzone> I2;

* s is height of a zone (dm);
* BL is thickness of the liquid film (dm);
* dI2 is the diffusion coefficient of iodine in water (dm2/s);
* I2gas is iodine gas conc. (M);
* Vgas is the volume of the gas phase (dm3);
* A is the surface area of solution (dm2);
* flow is the flowrate of air through the system (dm3/s), Kvent = flow/Vgas;
* I20 is the initial concentration of iodine (M);
* Kgas and Kliq are the gas and liquid phase mass transfer coefficients (dm/s);
PARAMETER s  Kliq 2.0E-5 BL dI2 1.2e-07  Kgas 0.036 Kvent;
PARAMETER  A 0.42  Vliq 0.1 Vgas 0.2   I20 1.1e-03 flow 0.0171;

* coefficients of transport;
PARAMETER fI2;

* workspace array for array code;
PARAMETER <200> WORK;

* parameters needed for output;
* I2end (=I2bulk) is the iodine conc. in the last zone, I2n is iodine conc. in nth zone;
PARAMETER I2end;
PARAMETER ZONE 0.0  I2n;

* initialization of variables;
COMPILE INITIAL;
DO 1 FOR #1 = 0 (1) (#NZONE - 1);
I2<#1> = I20;
LABEL 1;
I2<0> = I20;
**;

COMPILE INSTANT;
OPEN 11 "I2evap1.out";
OPEN 13 "I2evap2.out";
OPEN 6 "I2evap.log";

* calculate height, s, of each zone;
BL = dI2/Kliq;
```

```
Kvent = flow/Vgas;
* define transport coefficients;
fl2 = dl2/(s*s);
**;

COMPILE EQUATIONS;
* set index register for last element in arrays;
FOR #1=#nzone - 1;
ARRAY <#nzone> WORK;
ARRAY END;
* add diffusion terms;
TRANSPORT <#nzone> I2 fl2 fI2;
* inlet condition at gas/liquid interface;
% Kgas*A*(I2<0> - I2gas*80)/(80*Vgas) : = I2gas;
% Kgas*A*(I2gas*80 - I2<0>)/(s*A*80)  : = I2<0>;
% Kvent*(0 - I2gas)  : = I2gas;
* outlet condition at film/bulk interface;
% fI2*1e06*(I2<#1> - I2bulk)/(Vliq) : = I2bulk;
% fI2*1e06*(I2bulk - I2<#1>)/(s*A) : = I2<#1>;
**;

PSTREAM 5 11;
time I2end I2bulk I2gas;
**;

PSTREAM 7 13;
zone I2n;
**;

COMPILE TABLE;
* set up tables of results;
FOR #3=#NZONE - 1;
I2end = I2<#3>;
PSTREAM 5;
**;

COMPILE DELTA;
DO 2 FOR #6=0 (1) (#NZONE - 1);
zone = zone + 1;
I2n=I2<#6>;
PSTREAM 7;
LABEL 2;
**;

WHENEVER time = 0.0 + 100.0 * 36% CALL TABLE;
**;

WHENEVER time = 3600 % CALL DELTA;
**;

BEGIN;
STOP;
```

INTO WATER

```
* program to model the absorption of iodine gas into water;
* the liquid film is divided into #nzone zones;
* the bulk layer is designated as the #nzone+1 zone;

PERMIT + -;
INTEGER #nzone 20;
* I2 is iodine conc., I2bulk is the conc. of iodine in the bulk liquid phase;
VARIABLE I2bulk  0.0  I2gas 5E-08 TRAP;
VARIABLE <#nzone> I2;

* s is height of a zone (dm);
* BL is thickness of the liquid film (dm);
* dI2 is the diffusion coefficient of iodine in water (dm2/s);
* I2gasin is the concentration of iodine gas entering the system (M);
* A is the surface area of solution (dm2);
* I20 is the initial concentration of iodine (M);
* Kgas and Kliq are the gas and liquid phase mass transfer coefficients (dm/s);
* flow = flow rate of air (dm3/s), Kvent = flow/Vgas (s-1);
PARAMETER s  Kliq 2.0E-5 BL dI2 1.2e-07  I2gasin 5E-08 flow 0.0171
                A 0.42  I20 0.0 Vliq 0.1 Vgas 0.2 Kgas 0.036 Kvent;

* coefficients of transport;
PARAMETER fI2;

* workspace array for array code;
PARAMETER <200> WORK;

* parameters needed for output;
* I2end is the iodine conc. in the last zone, I2n is the iodine conc. in zone n;
PARAMETER I2end ZONE 0.0  I2n;

* initialization of variables;
COMPILE INITIAL;
DO 1 FOR #1 = 0 (1) (#NZONE - 1);
I2<#1> = I20;
LABEL 1;
I2<0> = I20;
**;

COMPILE INSTANT;
OPEN 11 "I2abs1.out";
OPEN 13 "I2abs3.out";
OPEN 6 "I2abs.log";

* calculate height, s, of each zone;
BL = dI2/Kliq;
s = BL/(FLOAT(#nzone) - 1.0);
Kvent = flow/Vgas;
* define transport coefficients;
fI2 = dI2/(s*s);
**;
```

```
COMPILE EQUATIONS;
* set index register for last element in arrays;
FOR #1=#nzone - 1;
ARRAY <#nzone> WORK;
ARRAY END;
* add diffusion terms;
TRANSPORT <#nzone> I2 fI2 fI2;
* inlet condition at gas/liquid interface;
% Kgas*A*(I2gas*80 - I2<0>)/(80*s*A) : = I2<0>;
% Kgas*A*(I2<0> - I2gas*80)/(Vgas*80) : = I2gas;
% Kvent*(I2gasin - I2gas)  : = I2gas;
* outlet condition at film/bulk interface;
% fI2*1e06*(I2<#1> - I2bulk)/(Vliq) : = I2bulk;
% fI2*1e06*(I2bulk - I2<#1>)/(s*A) : = I2<#1>;
**;

PSTREAM 5 11;
time I2end I2bulk I2gas;
**;

PSTREAM 7 13;
TIME zone I2n;
**;

COMPILE TABLE;
* set up tables of results;
FOR #3=#nzone - 1;
I2end = I2<#3>;
PSTREAM 5;
**;

COMPILE DELTA;
DO 2 FOR #6=0 (1) (#NZONE - 1);
zone = zone + 1;
I2n=I2<#6>;
PSTREAM 7;
LABEL 2;
**;

WHENEVER time = 0.0 + 100.0 * 36 % CALL TABLE;
**;

WHENEVER time = 3600 % CALL DELTA;
**;

BEGIN;
STOP;
```

E.3 LISTING FOR THE MODEL SIMULATING THE ABSORPTION OF IODINE INTO THIOSULPHATE SOLUTIONS

```
* model of the absorption of iodine into solutions of S2O32- ions;
* the liquid film is divided into #nzone zones;
```

```
* allow variable and parameter names to include + and -;
PERMIT + -;
INTEGER #nzone 20;
* species present in solution are: I2, I-, I3-, S2O32-, S4O62-, I2S2O32- and IS2O3-;
* Xbulk is conc of species X in the bulk liquid phase (mol/dm3);
VARIABLE      I2bulk  S2O32-bulk 1E-6 I2S2O32-bulk I-bulk I3-bulk;
VARIABLE      IS2O3-bulk  S4O62-bulk  I2gas 5E-08;
VARIABLE <#nzone> I2  I-  I3-  S2O32-  I2S2O32-  IS2O3-  S4O62-;
* s is height of a zone, BL is thickness of liquid film (dm);
* dX is the diffusion coefficient of species X in water (dm2/s);
* I2gasin is concentration of iodine gas entering the system (mol/dm3);
* BL is the thickness of the liquid phase film (dm);
* A is the surface area of solution (dm2);
* X-0 is the initial concentration of species X (mol/dm3);
* flow is the flow rate of air through the system (dm3/s), Kvent = flow/Vgas (s-1);
* Vgas and Vliq are the volumes of the gas and liquid phases (dm3);
* Kgas and Kliq are the gas and liquid phase mass transfer coefficients (dm/s);
PARAMETER   s  Kliq 2E-5 BL  dI2 1.2e-07  dI- 1.8e-07  dI3- 9.0e-08;
PARAMETER   dS2O32- 1.2E-07  dI2S2O32- 7.7E-08  dIS2O3- 9.2E-08
            dS4O62- 7.6E-08;
PARAMETER   I2gasin 5E-08  flow 0.0186  A 0.42  I-0 0.0  S2O32-0 1E-6;
PARAMETER   kf1 5.6e09  kb1 7.5e06  kf2 7.8E09  kb2 2.5E2  kf3 4.2E08
            kb3 9.5E03 kf4 2.5E02  K4 0.245  kb4  k5 1.29E06 k6 1.29E05
            k7 1.29E05  Kexpt 6.16e08 Vgas 0.2  Kgas 0.036  Kvent  Vliq 0.1;

* declaration of rates of reactions;
PARAMETER   R1 R2 R3 R4 R5 R8;
* coefficients of transport;
PARAMETER   fI2 fI- fI3- fS2O32- fI2S2O32- fIS2O3- fS4O62-;

* workspace array for array code;
PARAMETER <200> WORK;

* parameters needed for output;
* Xend is the conc. of species X in the last zone (mol/dm3);
* Xn is conc. of species X in nth zone;
PARAMETER   I2end  I-end  I3-end  S2O32-end I2S2O32-end
            IS2O3-end S4O62-end;
PARAMETER   ZONE 0.0  I2n I-n I3-n  S2O32-n I2S2O32-n IS2O3-n S4O62-n;

* initialization of variables;
COMPILE INITIAL;
DO I FOR #I = 0 (1) (#NZONE - 1);
I2<#I>          = 0.0;
I-<#I>          = I-0;
I3-<#I>         = 0.0;
S2O32-<#I>      = S2O32-0;
I2S2O32-<#I>    = 0.0;
IS2O3-<#I>      = 0.0;
S4O62-<#I>      = 0.0;
LABEL I;
I-<0>           = I-0;
I3-<0>          = 0.0;
```

```
S2O32-<0>       = S2O32-0;
I2S2O32-<0>     = 0.0;
IS2O3-<0>       = 0.0;
S4O62-<0>       = 0.0;
**;

COMPILE INSTANT;

OPEN 11 "thio1.out";
OPEN 13 "thio3.out";
OPEN 6 "thioA.log";

* calculate height, s, of each zone;
BL = dI2/KIiq;
s = BL/(FLOAT(#nzone) - 1.0);
Kvent = flow/Vgas;
* calculate backward rate constant for equation 4;
kb4 = kf4/K4;
* define transport coefficients;
fI2             = dI2/(s*s);
fI-             = dI-/(s*s);
fI3-            = dI3-/(s*s);
fS2O32-         = dS2O32-/(s*s);
fI2S2O32-       = dI2S2O32-/(s*s);
fIS2O3-         = dIS2O3-/(s*s);
fS4O62-         = dS4O62-/(s*s);
**;

COMPILE EQUATIONS;
* set index register for last element in arrays;
FOR #1 = #nzone - 1;
* reaction equation for each zone;
ARRAY <#nzone> WORK;
R1 % kf1  % kb1 : I2     + I-    = I3-;
R2 % kf2  % kb2 : I2     + S2O32- = I2S2O32-;
R3 % kf3  % kb3 : I3-    + S2O32- = I2S2O32- + I-;
R4 % kf4  % kb4 : I2S2O32-       = IS2O3- + I-;
R5 % k5         : IS2O3-  + S2O32- = I- + S4O62-;
* for experimentally predicted rate constant;
* R8 % Kexpt : I2 + S2O32- + S2O32- = I- + I- + S4O62-;
ARRAY END;
* add diffusion terms;
TRANSPORT <#nzone> I2 fI2 fI2;
* inlet condition;
% Kgas*A*(80*I2gas - I2<0>)/(s*A*80)   : = I2<0>;
% Kgas*A*(I2<0> - 80*I2gas)/(Vgas*80)   : = I2gas;
% Kvent*(I2gasin - I2gas)  : = I2gas;
* outlet condition;
% fI2*1e06*(I2<#1> - I2bulk)/(Vliq) : = I2bulk;
% fI2*1e06*(I2bulk - I2<#1>)/(s*A) : = I2<#1>;
TRANSPORT <#nzone> I- fI- fI-;
* no inlet condition;
* outlet condition;
% fI-*1e06*(I-<#1> - I-bulk)/(Vliq) : = I-bulk;
```

```
TRANSPORT <#nzone> I3- fI3- fI3-;
* no inlet condition;
* outlet condition;
% fI3-*1e06*(I3-<#1> - I3-bulk)/(Vliq) : = I3-bulk;
% fI3-*1e06*(I3-bulk - I3-<#1>)/(s*A) : = I3-<#1>;
TRANSPORT <#nzone> S2O32- fS2O32- fS2O32-;
* no inlet condition;
* outlet condition;
% fS2O32-*1e06*(S2O32-<#1> - S2O32-bulk)/(Vliq) : = S2O32-bulk;
% fS2O32-*1e06*(S2O32-bulk - S2O32-<#1>)/(s*A) : = S2O32-<#1>;
TRANSPORT <#nzone> I2S2O32- fI2S2O32- fI2S2O32-;
* no inlet condition;
* outlet condition;
% fI2S2O32-*1e06*(I2S2O32-<#1> - I2S2O32-bulk)/(Vliq) : = I2S2O32-bulk;
% fI2S2O32-*1e06*(I2S2O32-bulk - I2S2O32-<#1>)/(s*A) : = I2S2O32-<#1>;
TRANSPORT <#nzone> IS2O3- fIS2O3- fIS2O3-;
* no inlet condition;
* outlet condition;
% fIS2O3-*1e06*(IS2O3-<#1> - IS2O3-bulk)/(Vliq) : = IS2O3-bulk;
% fIS2O3-*1e06*(IS2O3-bulk - IS2O3-<#1>)/(s*A) : = IS2O3-<#1>;
TRANSPORT <#nzone> S4O62- fS4O62- fS4O62-;
* no inlet condition;
* outlet condition;
% fS4O62-*1e06*(S4O62-<#1> - S4O62-bulk)/(Vliq) : = S4O62-bulk;
% fS4O62-*1e06*(S4O62-bulk - S4O62-<#1>)/(s*A) : = S4O62-<#1>;
**;

PSTREAM 5 11;
time R8 I2end I-end I3-end S2O32-end I2S2O32-bulk IS2O3-bulk S4O62-bulk I2gas;
**;

PSTREAM 7 13;
zone I2n I-n I3-n S2O32-n I2S2O32-n IS2O3-n S4O62-n;
**;

COMPILE TABLE;
* set up tables of results;
FOR #3=#nzone - 1;
I2end          = I2<#3>;
I-end          = I-<#3>;
I3-end         = I3-<#3>;
S2O32-end      = S2O32-<#3>;
I2S2O32-end    = I2S2O32-<#3>;
IS2O3-end      = IS2O3-<#3>;
S4O62-end      = S4O62-<#3>;
PSTREAM 5;
**;

COMPILE DELTA;
DO 2 FOR #6=0 (1) (#NZONE - 1);
zone = zone + 1;
I2n            = I2<#6>;
I-n            = I-<#6>;
I3-n           = I3-<#6>;
```

```
I2S2O32-n       = I2S2O32-<#6>;
IS2O3-n         = IS2O3-<#6>;
S4O62-n         = S4O62-<#6>;
PSTREAM 7;
LABEL 2;
**;

WHENEVER time = 0.0 + 100.0 * 36 % CALL TABLE;
**;

WHENEVER time =3600 % CALL DELTA;
**;

BEGIN;
STOP;
```

E.4 LISTING FOR THE MODEL SIMULATING THE ABSORPTION OF IODINE INTO IODIDE SOLUTIONS

```
* model of the absorption of iodine into a 0.1M solution of iodide ions;
* the liquid film is divided into #nzone zones;
* the bulk layer is designated as the #nzone+1 zone;

PERMIT + -;
INTEGER #nzone 20;
* Xbulk is the concentration of species X in the bulk liquid phase;
* I2 is iodine conc., I- is iodide conc. and I3- is tri-iodide conc;
VARIABLE      I2bulk 0.0  I-bulk 1e-3 I3-bulk 0.0  I2gas 5E-8;
VARIABLE <#nzone> I2  I-  I3-;

* s is height of a zone (dm);
* BL is thickness of the liquid film (dm);
* dX is the diffusion coefficient of species X in water (dm2/s);
* I2gasin is the concentration of iodine gas entering the system (mol/dm3);
* A is the surface area of solution (dm2);
* I-0 is the initial concentration of iodide ions (mol/dm3);
* flow is the flow rate of air through the system (dm3/s), Kvent = flow/Vgas (s-1);
* Vgas and Vliq are the volumes of the gas and liquid phases (dm3);
* Kgas and Kliq are the gas and liquid phase mass transfer coefficients (dm/s);
* kf (M.s)-1 and kb (s-1)are forward and reverse rate constants;
PARAMETER   s BL 0.01 dI2 1.2e-07 dI- 1.8e-07 dI3- 9.0e-08 I2gasin 5E-8 flow 0.0171
                A 0.42  I-0 1e-3 kb 7.5e6 kf 5.6e9 Vgas 0.2  Kgas 0.036 Kvent Vliq 0.1;

* coefficients of transport;
PARAMETER   fI2 fI- fI3- ;

* workspace array for array code;
PARAMETER <200> WORK;

* parameters needed for output;
* Xend is the conc. of species X in the last zone;
* Xn is the conc. of species X in zone n;
PARAMETER I2end I-end I3-end ZONE 0.0  I2n I-n I3-n;
```

```
* declaration of the rate of the reaction;
PARAMETER R;

* initialization of variables;
COMPILE INITIAL;
DO 1 FOR #1 = 0 (1) (#NZONE - 1);
I2<#1>  = 0.0;
I-<#1>  = I-0;
I3-<#1> = 0.0;
LABEL 1;
I-<0>   = I-0;
I3-<0>  = 0.0;
I2<0>   = 0.0;
**;

COMPILE INSTANT;
OPEN 11 "I-abs1.out";
OPEN 13 "I-abs3.out";
OPEN 6 "I-abs.log";

* calculate height, s, of each zone;
s = BL/(FLOAT(#nzone) - 1.0);
Kvent = flow/Vgas;
* define transport coefficients;
fI2     = dI2/(s*s);
fI-     = dI-/(s*s);
fI3-    = dI3-/(s*s);
**;

COMPILE EQUATIONS;
* set index register for last element in arrays;
FOR #1=#nzone - 1;
* reaction equation for each zone;
ARRAY <#nzone> WORK;
R % kf  % kb : I2 + I- = I3-;
ARRAY END;
* add diffusion terms;
TRANSPORT <#nzone> I2 fI2 fI2;
* inlet condition at gas/liquid interface;
% Kgas*A*(80*I2gas - I2<0>)/(s*A*80) : = I2<0>;
% Kgas*A*(I2<0> - 80*I2gas)/(Vgas*80) : = I2gas;
% Kvent*(I2gasin - I2gas)  : = I2gas;
* outlet condition at film/bulk interface;
% fI2*1e06*(I2<#1> - I2bulk)/(Vliq) : = I2bulk;
% fI2*1e06*(I2bulk - I2<#1>)/(s*A) : = I2<#1>;
TRANSPORT <#nzone> I- fI- fI-;
* no transfer at gas/liquid interface;
* outlet condition at film/bulk interface;
% fI-*1e06*(I-<#1> - I-bulk)/(Vliq) : = I-bulk;
% fI-*1e06*(I-bulk - I-<#1>)/(s*A) : = I-<#1>;
TRANSPORT <#nzone> I3- fI3- fI3-;
* no transfer at gas/liquid interface;
* outlet condition at film/bulk interface;
% fI3-*1e06*(I3-<#1> - I3-bulk)/(Vliq) : = I3-bulk;
```

```
PSTREAM 5 11;
time I2end I-end I3-end I2gas;
**;

PSTREAM 7 13;
zone I2n I-n I3-n;
**;

COMPILE TABLE;
* set up tables of results;
FOR #3=#nzone - 1;
I2end    = I2<#3>;
I-end    = I-<#3>;
I3-end   = I3-<#3>;
PSTREAM 5;
**;

COMPILE DELTA;
DO 2 FOR #6=0 (1) (#NZONE - 1);
zone = zone + 1;
I2n      =I2<#6>;
I-n      =I-<#6>;
I3-n     =I3-<#6>;
PSTREAM 7;
LABEL 2;
**;

WHENEVER time = 0.0 + 100.0 *36 % CALL TABLE;
**;

WHENEVER time =3600 % CALL DELTA;
**;

BEGIN;
STOP;
```

E.5 LISTING FOR THE MODEL SIMULATING THE EVAPORATION OF IODINE FROM TRIIODIDE SOLUTIONS

```
* model of the evaporation of iodine from a solution of tri-iodide ions;
* the liquid film is divided into #nzone zones;
* the bulk layer is designated as the #nzone+1 zone;

PERMIT + - ;
INTEGER #nzone 20;
* Xbulk is the concentration of species X in the bulk liquid phase;
* I2 is iodine conc., I- is iodide conc. and I3- is tri-iodide conc;
VARIABLE      I2bulk 1e-06 I-bulk 1e-3 I3-bulk I2gas TRAP;
VARIABLE      <#nzone> I2  I-  I3-;

* s is height of a zone (dm), BL is thickness of the liquid film (dm);
```

```
* I2gas is the concentration of iodine in the gas phase (M);
* Vgas and Vliq are the volumes of the gas and liquid phases (dm3);
* A is the surface area of solution (dm2);
* flow is the flowrate of air (dm3/s), Kvent = flow/Vgas (s-1);
* X0 is the initial concentration of species X (M);
* kf (M.s)-1 and kb (s-1)are forward and reverse rate constants;
* Kgas and Kliq are the gas and liquid phase mass transfer coefficients (dm/s);
PARAMETER   s BL 0.01 dI2 1.2e-07 dI- 1.8e-07 dI3- 9.0e-08 A 0.42 Vgas 0.2
            I-0 1e-3 I20 1e-06 I3-0 flow 0.0171 kf 5.6e09 kb 7.5e06
            Kgas 0.036 Kvent Vliq 0.1;

* coefficients of transport;
PARAMETER fI2 fI- fI3-;

* workspace array for array code;
PARAMETER <200> WORK;

* parameters needed for output;
* Xend is the conc. of species X in the last zone;
* Xn is the conc. of species X in the nth zone;
PARAMETER I2end I-end I3-end ZONE 0.0 I2n I-n I3-n;

* declaration of the rate of the reaction;
PARAMETER R;

COMPILE INSTANT;
OPEN 11 "I-evap1.out";
OPEN 13 "I-evap3.out";
OPEN 6 "I-evap.log";

* calculate height, s, of each zone;
s = BL/(FLOAT(#nzone) - 1.0);
Kvent = flow/Vgas;
* define transport coefficients;
fI2 = dI2/(s*s);
fI- = dI-/(s*s);
fI3- = dI3-/(s*s);
**;

* initialization of variables;
COMPILE INITIAL;
DO 1 FOR #1 = 0 (1) (#NZONE - 1);
I2<#1>  = I20;
I-<#1>  = I-0;
I3-<#1> = I3-0;
LABEL 1;
I-<0>   = I-0;
I3-<0>  = I3-0;
I2<0>   = I20;
**;


COMPILE EQUATIONS;
* set index register for last element in arrays;
```

```
* reaction equation for each zone;
ARRAY <#nzone> WORK;
R % kf  % kb : I2 + I- = I3-;
ARRAY END;
* add diffusion terms;
TRANSPORT <#nzone> I2 fI2 fI2;
* inlet condition at gas/liquid interface;
% Kgas*A*(I2<0> - 80*I2gas)/(80*Vgas) : = I2gas;
% Kgas*A*(I2gas*80 - I2<0>)/(s*A*80)  : = I2<0>;
% Kvent*(0 - I2gas)  : = I2gas;
* outlet condition at film/bulk interface;
% fI2*1e06*(I2<#1> - I2bulk)/(Vliq) : = I2bulk;
% fI2*1e06*(I2bulk - I2<#1>)/(s*A) : = I2<#1>;
TRANSPORT <#nzone> I- fI- fI-;
* no transfer across the gas/liquid interface;
* outlet condition at film/bulk interface;
% fI-*1e06*(I-<#1> - I-bulk)/(Vliq) : = I-bulk;
% fI-*1e06*(I-bulk - I-<#1>)/(s*A) : = I-<#1>;
TRANSPORT <#nzone> I3- fI3- fI3-;
* no transfer across the gas/liquid interface;
* outlet condition at film/bulk interface;
% fI3-*1e06*(I3-<#1> - I3-bulk)/(Vliq) : = I3-bulk;
% fI3-*1e06*(I3-bulk - I3-<#1>)/(s*A) : = I3-<#1>;
**;

PSTREAM 5 11;
time I2end I-end I3-end I2gas;
**;

PSTREAM 7 13;
zone I2n I-n I3-n;
**;

COMPILE TABLE;
* set up tables of results;
FOR #3=#NZONE - 1;
I2end    = I2<#3>;
I-end    = I-<#3>;
I3-end   = I3-<#3>;
PSTREAM 5;
**;

COMPILE DELTA;
DO 2 FOR #6=0 (1) (#NZONE - 1);
zone = zone + 1;
I2n      =I2<#6>;
I-n      =I-<#6>;
I3-n     =I3-<#6>;
PSTREAM 7;
LABEL 2;
**;

WHENEVER time = 0.0 + 100.0 * 36 % CALL TABLE;
**;
```

```
WHENEVER time = 3600 % CALL DELTA;
**;

BEGIN;
STOP;
```

E.6 LISTING FOR THE MODEL SIMULATING THE ABSORPTION OF IODINE INTO HYDROXIDE SOLUTIONS

```
* model of the absorption of iodine into a solution of hydroxide ions;
* the liquid film is divided into #nzone zones;
* the bulk layer is designated as the #nzone+1 zone;

PERMIT + - ;
INTEGER #nzone 20;
* Xbulk is the concentration of species X in the bulk liquid phase;
* species in solution are: I2, OH-, I-, I3-, I2OH- and HOI;
* I2gas is the concentration of iodine in the gas phase (M);
VARIABLE      I2bulk I-bulk I3-bulk OH-bulk 1E-6 I2OH-bulk
              HOIbulk I2gas 5e-9 I2TRAP;
VARIABLE <#nzone> I2 I- I3- OH- I2OH- HOI;

* DIMENSIONAL PARAMETERS;
* s is height of a zone (dm);
* BL is thickness of the liquid film (dm);
* Vgas and Vliq are the volumes of the gas and liquid phases (dm3);
* A is the surface area of solution (dm2);
* flow is the flowrate of air (dm3/s), Kvent = flow/Vgas (s-1);
* Kgas and Kliq are the gas and liquid phase mass transfer coefficients (dm/s);
* H is the air/water iodine equilibrium partition constant;
PARAMETER     s Kliq 2E-5 BL flow 0.0186 Kgas 0.036 Kvent Vliq 0.1 pH
              A 0.42 Vgas 0.2 H 80 I2gasin 5E-9;

* dX is the diffusion coefficient of species X in water (dm2/s);
PARAMETER     dI2 1.2e-07 dI- 1.8e-07 dI3- 9.0e-08 dOH- 3.4e-07
              dHOI 1.5e-07 dI2OH- 1.1e-07;

* X0 is the initial concentration of species X (M);
PARAMETER I20 I-0 I3-0 HOI0 I2OH-0 OH-0 1E-6;

* kf# and kb# are forward and reverse rate constants for rxn#;
PARAMETER     kf1 8.0e08 kb1 5.0e04 kf2 1.4e06 kb2 4e08
              kf3 5.6e09 kb3 7.5e06 Kps 260;
* coefficients of transport;
PARAMETER fI2 fI- fI3- fOH- fI2OH- fHOI;

* workspace array for array code;
PARAMETER <200> WORK;

* parameters needed for output;
* Xend is the conc. of species X in the last zone;
PARAMETER I2end OH-END I2OH-END HOIEND I-END I3-END;
```

```
PARAMETER K1 K2 K3;

COMPILE INSTANT;
OPEN 11 "OH-ABS1.out";
OPEN 6 "OH-ABS.log";

* calculate height, s, of each zone;
BL = dI2/Kliq;
s = BL/(FLOAT(#nzone) - 1.0);
Kvent = flow/Vgas;
* calculate pH;
pH = 14 + LOG10(OH-0);
* define transport coefficients;
fI2      = dI2/(s*s);
fI-      = dI-/(s*s);
fI3-     = dI3-/(s*s);
fOH-     = dOH-/(s*s);
fI2OH-   = dI2OH-/(s*s);
fHOI     = dHOI/(s*s);
**;

* initialization of variables;
COMPILE INITIAL;
DO 1 FOR #1 = 0 (1) (#NZONE - 1);
I2<#1>          = I20;
I-<#1>          = I-0;
I3-<#1>         = I3-0;
OH-<#1>         = OH-0;
I2OH-<#1>       = I2OH-0;
HOI<#1>         = HOI0;
LABEL 1;
I-<0>           = I-0;
I3-<0>          = I3-0;
I2<0>           = I20;
OH-<0>          = OH-0;
I2OH-<0>        = I2OH-0;
HOI<0>          = HOI0;
**;


COMPILE EQUATIONS;
* set index register for last element in arrays;
FOR #1=#nzone - 1;
* reaction equation for each zone;
ARRAY <#nzone> WORK;
R1 % kf1  % kb1 : I2   + OH- = I2OH-    ;
R2 % kf2  % kb2 : I2OH-      = HOI   + I-;
R3 % kf3  % kb3 : I2   + I-  = I3-      ;
* % kps : I2 + OH- = I2OH-;
ARRAY END;
* add diffusion terms;
TRANSPORT <#nzone> I2 fI2 fI2;
* inlet condition at gas/liquid interface;
% Kgas*A*(I2<0> - H*I2gas)/(H*Vgas) : = I2gas;
```

```
% Kvent*(I2gasin - I2gas)  : = I2gas;
* outlet condition at film/bulk interface;
% fI2*1e06*(I2<#1> - I2bulk)/(Vliq) : = I2bulk;
% fI2*1e06*(I2bulk - I2<#1>)/(s*A) : = I2<#1>;
TRANSPORT <#nzone> HOI fHOI fHOI;
* no inlet condition at gas/liquid interface;
* outlet condition at film/bulk interface;
% fHOI*1e06*(HOI<#1> - HOIbulk)/(Vliq) : = HOIbulk;
% fHOI*1e06*(HOIbulk - HOI<#1>)/(s*A) : = HOI<#1>;
TRANSPORT <#nzone> I- fI- fI-;
* no transfer across the gas/liquid interface;
* outlet condition at film/bulk interface;
% fI-*1e06*(I-<#1> - I-bulk)/(Vliq) : = I-bulk;
% fI-*1e06*(I-bulk - I-<#1>)/(s*A) : = I-<#1>;
TRANSPORT <#nzone> I3- fI3- fI3-;
* no transfer across the gas/liquid interface;
* outlet condition at film/bulk interface;
% fI3-*1e06*(I3-<#1> - I3-bulk)/(Vliq) : = I3-bulk;
% fI3-*1e06*(I3-bulk - I3-<#1>)/(s*A) : = I3-<#1>;
TRANSPORT <#nzone> OH- fOH- fOH-;
* no transfer across the gas/liquid interface;
* outlet condition at film/bulk interface;
% fOH-*1e06*(OH-<#1> - OH-bulk)/(Vliq) : = OH-bulk;
% fOH-*1e06*(OH-bulk - OH-<#1>)/(s*A) : = OH-<#1>;
TRANSPORT <#nzone> I2OH- fI2OH- fI2OH-;
* no transfer across the gas/liquid interface;
* outlet condition at film/bulk interface;
% fI2OH-*1e06*(I2OH-<#1> - I2OH-bulk)/(Vliq) : = I2OH-bulk;
% fI2OH-*1e06*(I2OH-bulk - I2OH-<#1>)/(s*A) : = I2OH-<#1>;
**;

PSTREAM 5 11;
time I2end OH-end I2OH-end HOIend I-end I3-end PH I2gas;
**;

COMPILE TABLE;
* set up tables of results;
FOR #3=#NZONE - 1;
I2end          = I2<#3>;
OH-end         = OH-<#3>;
I2OH-end       = I2OH-<#3>;
HOIend         = HOI<#3>;
I-end          = I-<#3>;
I3-end         = I3-<#3>;
PSTREAM 5;
**;

WHENEVER time = 0.0 + 100.0 * 36 % CALL TABLE;
**;

BEGIN;
STOP;
```

LISTING FOR THE MODEL SIMULATING THE EVAPORATION OF IODINE IN THE PRESENCE OF RADIOLYTIC REACTIONS

```
* model of the evaporation of iodine from solution in the presence of a radiation field;
* the liquid film is divided into #NZONE zones, the #NZONE +1 being the bulk layer;

* SIMPLIFIED LIRIC DATA BASE IN FACSIMILE FORM (5/94)
* INPUT pH, I-
* NO THERMAL OXIDATION OF I-, DUSHMAN, RH, ADSORPTION
* BASED ON GEOMETRY OF EXPERIMENTAL APPARATUS
* NO TEMPERATURE VARIATION;

* RADIOLYSIS OF WATER
* BASED ON WATER SET IN LIRIC 2
* EDITED Oct 5 1995 BY G.EVANS;

COMPILE INSTANT;
OPEN 6  "RADEVP.LOG";
OPEN 10 "RADEVP1.OUT";
OPEN 11 "RADEVP2.OUT";
OPEN 12 "RADEVP3.OUT";

* ************************************************************;
* ************************************************************;
* **                                                        **;
* **     DON'T RUSH ME, I'M  THINKING                       **;
* **                                                        **;
* ************************************************************;
* ************************************************************;
**;

PERMIT + - ;
INTEGER #nzone 20;
* XBULK is the concentration of species X in the BULK liquid phase (M);
VARIABLE      I2BULK I-BULK 1e-4 I3-BULK OI-BULK HOIBULK IBULK I2-BULK
              IO-2BULK IO2HBULK HO2BULK O-BULK H+BULK HBULK
              H2BULK OHBULK O2-BULK I2OH-BULK OH-BULK O2BULK
              HO2-BULK H2O2BULK S2O3-2BULK I2S2O3-2BULK
              IS2O3-BULK S4O6-2BULK O2Gin;

VARIABLE <#NZONE>  I2 I- I3- OI- HOI I I2- IO-2 PROD IO2H
                   HO2 O- H H2 OH O2- I2OH- OH- O2
                   HO2- H2O2  H+ S2O3-2 I2S2O3-2 IS2O3- S4O6-2;

* XG is the concentration of species X in the gas phase;
VARIABLE      E- I2G IG O2G H2G;

* s is height of each zone (dm);
* BL is thickness of the liquid phase film (dm);
* AGL is the surface area of solution (dm2);
* X0- is the initial concentration of species X;
* FLOW is the flow rate of air through the system (dm3/s);
* VG and VL are the volumes of the gas and liquid phases (dm3);
PARAMETER   s  BL  AGL 0.42  I0- 1e-04  S2O3-20 0
```

```
* dX is the diffusion coefficient of species X in water (dm2/s);
PARAMETER   dI2 1.2e-07  dI- 1.8e-07  dI3- 9.0e-08 dOI- 1.5E-07 dHOI 1.5E-07
            dI 1.8E-07 dI2- 1.2E-07 dIO-2 1.5E-07 dIO2H 1.3E-07 dHO2 2.1E-07
            dO- 3.3E-07 dH 6.0E-07 dH+ 6.0E-07 dH2 4.2E-07 dOH 2.8E-07
            dO2- 2.3E-07 dI2OH- 1.1E-07 dOH- 2.8E-07 dO2 2.3E-07 dHO2- 2.1E-07
            dH2O2 2.0E-07 dS2O3-2 1.2E-07 dI2S2O3-2 7.7E-08 dIS2O3- 9.2E-08
            dS4O6-2 7.6E-08;

* coefficients of transport;
PARAMETER   fI2 fI- fI3- fOI- fHOI fI fI2- fIO-2 fIO2H fHO2 fO-
            fH fH2 fOH fO2- fI2OH- fOH- fO2 fHO2- fH2O2  fS2O3-2
            fI2S2O3-2 fIS2O3- fS4O6-2 fH+;

* workspace array for array code;
PARAMETER <200> WORK;

* parameters needed for OUTput;
* XOUT is the concentration of species X in the last zone (M);
* XALL refers to the concentration of species X in ALL the zones (M);
* zone is the zone number;
PARAMETER   I2OUT  I-OUT  I3-OUT S2O3-2OUT S4O6-2OUT;
PARAMETER   ZONE 0.0  I2ALL I-ALL I3-ALL;
PARAMETER   OI-OUT HOIOUT IOUT I2-OUT IO-2OUT IO2HOUT HO2OUT O-OUT
            H+OUT HOUT H2OUT OHOUT O2-OUT I2OH-OUT OH-OUT O2OUT
            HO2-OUT H2O2OUT I2S2O3-2OUT IS2O3-OUT;

* rates of reactions;
PARAMETER R1 R2 R3 R4 R5 R6;
* DO is dissolved oxygen, PH is pH of solution;
PARAMETER  H2O 55.51 DO 8 PH 6;
* AN is Avogadro's number, DR is dose rate (kGRAY/h);
PARAMETER  AN 6.023E23 DR 1 PR;
PARAMETER  GE- 2.7 GH 0.6 GH2 0.45 GOH 2.7 GH2O2 0.7 GH+ 2.7;

* HEX is the equilibrium partition ceofficient of species X;
PARAMETER  HEO2 2.6354E-2 HEH2 1.7569E-2  HEI2 80  HEI 1.85 ;
* K values are the mass transfer coefficients;
* KVENT = volumetric flow rate of air / volume (s-1);
PARAMETER KTL 2E-05 KTG 3.6E-02 KVENT;

* initialization of variables;
COMPILE INITIAL;
O2Gin = DO*2.5E-04/(8*HEO2) ;
DO 1 FOR #I = 0 (1) (#NZONE - 1);
I2<#1>          = 0.0;
I-<#1>          = I0-;
I3-<#1>         = 0.0;
H+<#1>          = 10.@(- PH);
OH-<#1>         = 1.0E-14/(10.@(- PH));
O2<#1>          = DO*2.5E-4/8;
S2O3-2<#1>      = S2O3-20;
LABEL 1;
I-<0>           = I0-;
```

```
H+<0>           = 10.@(- PH);
OH-<0>          = 1.0E-14/(10.@(- PH));
O2<0>           = DO*2.5E-4/8;
S2O3-2<0>       = S2O3-20;
**;

COMPILE INSTANT;
* calculate height, s, of each zone;
BL = dl2/KTL;
s = BL/(FLOAT(#nzone) - 1.0);
* define transport coefficients;
fl2             = dI2/(s*s);
fI-             = dI-/(s*s);
fI3-            = dI3-/(s*s);
fOI-            = dOI-/(s*s);
fHOI            = dHOI/(s*s);
fI              = dI/(s*s);
fI2-            = dI2-/(s*s);
fIO-2           = dIO-2/(s*s);
fIO2H           = dIO2H/(s*s);
fHO2            = dHO2/(s*s);
fO-             = dO-/(s*s);
fH              = dH/(s*s);
fH+             = dH+/(s*s);
fH2             = dH2/(s*s);
fOH             = dOH/(s*s);
fO2-            = dO2-/(s*s);
fI2OH-          = dI2OH-/(s*s);
fOH-            = dOH-/(s*s);
fO2             = dO2/(s*s);
fHO2-           = dHO2-/(s*s);
fH2O2           = dH2O2/(s*s);
* fE-           = dE-/(s*s);
fS2O3-2         = dS2O3-2/(s*s);
fI2S2O3-2       = dI2S2O3-2/(s*s);
fIS2O3-         = dIS2O3-/(s*s);
fS4O6-2         = dS4O6-2/(s*s);
**;

COMPILE GENERAL;
KVENT=FLOW/VG;
PR  =DR*1E3/(1.6E-19*3600*AN*100.);
**;


COMPILE EQUATIONS;
* set index register for last element in arrays;
FOR #1=#nzone - 1;
* reaction equations for each zone;
ARRAY <#nzone> WORK;
* REACTIONS OF OH;
* ----------------------------;
% PR*GOH          :       = OH        ;
```

```
% 4.2E7          : OH + H2  = H   + H2O ;* B,G,H&R;
% 2.7E7          : OH + H2O2 = HO2  + H2O ;* B,G,H&R;
% 8.000E+09      : OH + O2-  = O2   + OH- ;* B,G,H&R;
% 6.000E+09      : OH + HO2  = H2O  + O2  ;* B,G,H&R;
% 5.500E+09      : OH + OH   = H2O2       ;* BOYD;
% 1.3E+10 % 1.8E+06 : OH + OH-  = H2O  + O-  ;* B,G,H&R;
% 7.000E+09      : H  + OH   = H2O        ;* B,G,H&R;

* REACTIONS OF e- ;
* -------------------------;
% PR*GE-         :          = E-        ;
% 1.900E+10      : E- + O2    = O2-       ;* BOYD;
% 1.100E+10      : E- + H2O2  = OH   +OH-  ;* B,G,H&R;
% 1.300E+10      : E- + O2-   = HO2- + OH- ;* BOYD;
% 2.300E+10      : E- + H+    = H         ;* B,G,H&R;
% 1.9E+01 % 2.2E+07 : E- + H2O  = H    + OH- ;* B,G,H&R;
% 3.500E+09      : E- + HO2-  = O-   + OH- ;* BOYD;
% 2.500E+10      : E- + H     = H2   + OH- ;* BOYD;


* REACTIONS OF H ;
*-------------------------------;
% PR*GH    :       = H      ;
% PR*GH2   :       = H2     ;
% 2.100E+10 : H + O2   = HO2     ;* B,G,H&R;
% 2.000E+10 : H + O2-  = HO2-    ;* BOYD;
% 1.000E+10 : H + HO2  = H2O2    ;* B,G,H&R;
% 9.000E+07 : H + H2O2 = H2O + OH ;* BOYD;
% 7.750E+09 : H + H    = H2      ;* B,G,H&R;


* OTHER REACTIONS ;
* -------------------------------;
% PR*GH2O2          :          = H2O2      ;
% PR*GH+            :          = H+        ;
% 8.900E+07         : HO2 + O2-  = O2   + HO2- ;* BOYD;
% 2.000E+06         : HO2 + HO2  = H2O2 + O2   ;* BOYD;
% 4.5E+10 % 8.0E+05    : H+  + O2-  = HO2        ;* BOYD;
% 2.0E+10 % 3.56E-02   : H+  + HO2- = H2O2       ;* BOYD;
% 4.000E+08         : O-  + H2O2 = H2O  + O2-  ;* B,G,H&R;
% 1.438E+11 % 2.596E-05 : H+  + OH-  = H2O        ;* BOYD;

*THERMAL IODINE REACTIONS
*-------------------------------;
% 5.600E+09 % 7.500E+06  : I2  + I-  = I3-          ;
* % 4.000E-02 % 4.400E+12 : I2  + H2O = HOI  + I- + H+ ;
% 5.76E-02  % 2.0E+10    : I2  + H2O = I2OH- + H+     ;* KUSTIN;
% 1.36E+06  % 4.0E+08    : I2OH-     = HOI  + I-      ;* KUSTIN;
% 1.000E+10 % 1.000E-01  : H+  + OI-  = HOI          ;

*IODINE REACTIONS WITH OH
*-------------------------------;
%  1.100E+10 : I2  + OH = HOI  + I  ;* SCHWARZ;
%  1.80E+10  : I-  + OH = I    + OH- ;* SIMPLIFIED;
```

```
% 3.800E+10 : I2- + OH = I2 + OH- ;* BURNS28;
% 2.140E+09 : I- + O- = IO-2 ;
% 5.000E+10 : IO-2 + H+ = I + OH- ;* MODIFIED HOI-;

*IODINE REACTIONS WITH H
*--------------------------------;
% 2.700E+10 : H + I = I- + H+ ; * BURNS15;

*IODINE REACTIONS WITH e-
*--------------------------------;
% 2.400E+10 : I + E- = I- ;* BURNS14;
% 2.000E+10 : E- + OI- = IO-2 ;* BUXTON;

*IODINE REACTIONS WITH O2-/HO2
*--------------------------------;
% 1.800E+07 : HO2 + I2 = H+ + O2 + I2- ;* BURNS16;
% 1.000E+10 : HO2 + I2- = I2 + HO2- ;* BURNS1;
% 5.000E+08 : O2- + I2- = I- + I- + O2 ;* BURNS26;
% 6.000E+09 : O2- + I2 = I2- + O2 ;* BURNS19;
% 2.00E+09 : O2- + I = I- + O2 ;
% 2.500E+08 : O2- + I3- = O2 + I- + I2- ;* BURNS22;

*IODINE REACTIONS WITH H2O2
*--------------------------------;
* * R44 % 37 : H2O2 + HOI = I- + H+ + H2O + O2 ;* BURNS29;
* * R45 % 1.600E+09 : H2O2 + OI- = I- + H2O + O2 ;* BURNS24;
% 8.0E+08 % 5.0E+04: I2 + OH- = I2OH- ; * KUSTIN ;
% 2.02E+06 % 1.3E+07/55.5: I2OH- + H2O2 = I- + IO2H + H2O; * BALL;
% 3.0E+09 : IO2H + OH- = O2 + H2O + I- ;* BALL;
* * R44 % 3.0E+8 % 2.1E-07 : I2 + HO2- = I- + IO2H ; * BALL;
* * R45 % 1.0E+10 : IO2H + OH- = O2 + H2O + I- ;* BALL;
% 1.000E-02 : H2O2 + I- = H2O + OI- ;* BURNS25;
% 3.000E+03 : H2O2 + I = I- + HO2 + H+ ;* BURNS13;

*IODINE-IODINE REACTIONS
*--------------------------------;
% 1.100E+05 % 1.2E10 : I2- = I + I- ;* BURNS7,8;
% 4.500E+09 : I + I2- = I3- ;* BURNS17;
% 1.000E+10 : I + I = I2 ;* BURNS18;
% 4.500E+09 : I2- + I2- = I3- + I- ;* BURNS12;
* % 1.1E-14 % 2.9E8 : I2G = IG + IG ;* BARNES;

*THIOSULPHATE REACTIONS
*--------------------------------;
% 7.8E09 % 2.5E06 : I2 + S2O3-2 = I2S2O3-2 ;
% 4.2E08 % 9.5E03 : I3- + S2O3-2 = I2S2O3-2 + I- ;
% 2.5E02 % 1.02E03 : I2S2O3-2 = IS2O3- + I- ;
% 1.29E06 : IS2O3- + S2O3-2 = S4O6-2 + I- ;
* % 1.29E05 : I2 + S2O3-2 + S2O3-2 = S4O6-2 + I- + I- ;
* % 1.29E05 : I3- + S2O3-2 + S2O3-2 = S4O6-2 + I- + I- + I- ;
ARRAY END;

* add diffusion terms;
TRANSPORT <#nzone> I2 fI2 fI2;
```

```
R1 % KTG*AGL*(I2<0> - I2G * HEI2)/(VG*HEI2) := I2G;
R2 % KTG*AGL*(I2G * HEI2 - I2<0>)/(s*AGL*HEI2) := I2<0>;
R3 % KVENT*(0 - I2G) : = I2G ;
* outlet condition at film/BULK interface;
R5 % fI2*1e06*(I2<#1> - I2BULK)/VL : = I2BULK;
R6 % fI2*1e06*(I2BULK - I2<#1>)/(s*AGL) : = I2<#1>;
TRANSPORT <#nzone> I- fI- fI-;
* no transfer across gas/liquid interface;
* outlet condition at film/BULK interface;
% fI-*1e06*(I-<#1> - I-BULK)/VL : = I-BULK;
% fI-*1e06*(I-BULK - I-<#1>)/(s*AGL) : = I-<#1>;
TRANSPORT <#nzone> I3- fI3- fI3-;
* no transfer across gas/liquid interface;
* outlet condition at film/BULK interface;
% fI3-*1e06*(I3-<#1> - I3-BULK)/VL : = I3-BULK;
% fI3-*1e06*(I3-BULK - I3-<#1>)/(s*AGL) : = I3-<#1>;
TRANSPORT <#nzone> OI- fOI- fOI-;
* no transfer across gas/liquid interface;
* outlet condition at film/BULK interface
% fOI-*1e06*(OI-<#1> - OI-BULK)/VL : = OI-BULK;
% fOI-*1e06*(OI-BULK - OI-<#1>)/(s*AGL) : = OI-<#1>;
TRANSPORT <#nzone> I2- fI2- fI2-;
* no transfer across gas/liquid interface;
* outlet condition at film/BULK interface;
% fI2-*1e06*(I2-<#1> - I2-BULK)/VL : = I2-BULK;
% fI2-*1e06*(I2-BULK - I2-<#1>)/(s*AGL) : = I2-<#1>;
TRANSPORT <#nzone> IO-2 fIO-2 fIO-2;
* no transfer across gas/liquid interface;
* outlet condition at film/BULK interface;
% fIO-2*1e06*(IO-2<#1> - IO-2BULK)/VL : = IO-2BULK;
% fIO-2*1e06*(IO-2BULK - IO-2<#1>)/(s*AGL) : = IO-2<#1>;
TRANSPORT <#nzone> O- fO- fO-;
* no transfer across gas/liquid interface;
* outlet condition at film/BULK interface;
% fO-*1e06*(O-<#1> - O-BULK)/VL : = O-BULK;
% fO-*1e06*(O-BULK - O-<#1>)/(s*AGL) : = O-<#1>;
TRANSPORT <#nzone> O2- fO2- fO2-;
* no transfer across gas/liquid interface;
* outlet condition at film/BULK interface;
% fO2-*1e06*(O2-<#1> - O2-BULK)/VL : = O2-BULK;
% fO2-*1e06*(O2-BULK - O2-<#1>)/(s*AGL) : = O2-<#1>;
TRANSPORT <#nzone> I2OH- fI2OH- fI2OH-;
* no transfer across gas/liquid interface;
* outlet condition at film/BULK interface;
% fI2OH-*1e06*(I2OH-<#1> - I2OH-BULK)/VL : = I2OH-BULK;
% fI2OH-*1e06*(I2OH-BULK - I2OH-<#1>)/(s*AGL) : = I2OH-<#1>;
TRANSPORT <#nzone> OH- fOH- fOH-;
* no transfer across gas/liquid interface;
* outlet condition at film/BULK interface;
% fOH-*1e06*(OH-<#1> - OH-BULK)/VL : = OH-BULK;
% fOH-*1e06*(OH-BULK - OH-<#1>)/(s*AGL) : = OH-<#1>;
TRANSPORT <#nzone> HO2- fHO2- fHO2-;
* no transfer across gas/liquid interface;
* outlet condition at film/ BULK interface;
```

```
% fHO2-*1e06*(HO2-BULK - HO2-<#1>)/(s*AGL) : = HO2-<#1>;
TRANSPORT <#nzone> HOI fHOI fHOI;
* no inlet condition at gas/liquid interface;
* outlet condition at film/BULK interface;
% fHOI*1e06*(HOI<#1> - HOIBULK)/VL : = HOIBULK;
% fHOI*1e06*(HOIBULK - HOI<#1>)/(s*AGL) : = HOI<#1>;
TRANSPORT <#nzone> I fI fI;
* inlet condition at gas/liquid interface;
% KTG*((dI/dI2)@0.6)*AGL*(IG * HEI - I<0>)/(s*AGL*HEI):=I<0>;
% KTG*((dI/dI2)@0.6)*AGL*(I<0> - IG * HEI)/(VG*HEI)    :=IG;
% KVENT*(0 - IG):=IG;
* outlet condition at film/BULK interface;
% fI*1e06*(I<#1> - IBULK)/VL : = IBULK;
% fI*1e06*(IBULK - I<#1>)/(s*AGL) : = I<#1>;
TRANSPORT <#nzone> IO2H fIO2H fIO2H;
* no transfer across gas/liquid interface;
* outlet condition at film/BULK interface;
% fIO2H*1e06*(IO2H<#1> - IO2HBULK)/VL : = IO2HBULK;
% fIO2H*1e06*(IO2HBULK - IO2H<#1>)/(s*AGL) : = IO2H<#1>;
TRANSPORT <#nzone> HO2 fHO2 fHO2;
* no transfer across gas/liquid interface;
* outlet condition at film/BULK interface;
% fHO2*1e06*(HO2<#1> - HO2BULK)/VL : = HO2BULK;
% fHO2*1e06*(HO2BULK - HO2<#1>)/(s*AGL) : = HO2<#1>;
TRANSPORT <#nzone> H fH fH;
* no transfer across gas/liquid interface;
* outlet condition at film interface;
% fH*1e06*(H<#1> - HBULK)/VL : = HBULK;
% fH*1e06*(HBULK - H<#1>)/(s*AGL) : = H<#1>;
TRANSPORT <#nzone> H+ fH+ fH+;
* no transfer across gas/liquid interface;
* outlet condition at film interface;
% fH+*1e06*(H+<#1> - H+BULK)/VL : = H+BULK;
% fH+*1e06*(H+BULK - H+<#1>)/(s*AGL) : = H+<#1>;
TRANSPORT <#nzone> H2 fH2 fH2;
* inlet condition at gas/liquid interface;
% KTG*((dH2/dI2)@0.6)*AGL*(H2G * HEH2 - H2<0>)/(s*AGL*HEH2):=H2<0>;
% KTG*((dH2/dI2)@0.6)*AGL*(H2<0> - H2G * HEH2)/(VG*HEH2)    :=H2G;
% KVENT*(0 - H2G):=H2G;
* outlet condition at film/BULK interface;
% fH2*1e06*(H2<#1> - H2BULK)/VL : = H2BULK;
% fH2*1e06*(H2BULK - H2<#1>)/(s*AGL) : = H2<#1>;
TRANSPORT <#nzone> OH fOH fOH;
* no transfer across gas/liquid interface;
* outlet condition at film/BULK interface;
% fOH*1e06*(OH<#1> - OHBULK)/VL : = OHBULK;
% fOH*1e06*(OHBULK - OH<#1>)/(s*AGL) : = OH<#1>;
TRANSPORT <#nzone> O2 fO2 fO2;
* inlet condition at gas/liquid interface;
% KTG*(dO2/dI2)@0.6*AGL*(O2G * HEO2 - O2<0>)/(s*AGL*HEO2):=O2<0>;
% KTG*(dO2/dI2)@0.6*AGL*(O2<0> - O2G * HEO2)/(VG*HEO2)   :=O2G;
% KVENT*(O2Gin - O2G):=O2G;
* outlet condition at film/BULK interface;
% fO2*1e06*(O2<#1> - O2BULK)/VL : = O2BULK;
```

```
TRANSPORT <#nzone> H2O2 fH2O2 fH2O2;
* no transfer across gas/liquid interface;
* outlet condition at film/BULK interface;
% fH2O2*1e06*(H2O2<#1> - H2O2BULK)/VL : = H2O2BULK;
% fH2O2*1e06*(H2O2BULK - H2O2<#1>)/(s*AGL) : = H2O2<#1>;
TRANSPORT <#nzone> S2O3-2 fS2O3-2 fS2O3-2;
* no transfer across gas/liquid interface;
* outlet condition at film/BULK interface;
% fS2O3-2*1e06*(S2O3-2<#1> - S2O3-2BULK)/VL : = S2O3-2BULK;
% fS2O3-2*1e06*(S2O3-2BULK - S2O3-2<#1>)/(s*AGL) : = S2O3-2<#1>;
TRANSPORT <#nzone> I2S2O3-2 fI2S2O3-2 fI2S2O3-2;
* no transfer across gas/liquid interface;
* outlet condition at film/BULK interface;
% fI2S2O3-2*1e06*(I2S2O3-2<#1> - I2S2O3-2BULK)/VL : = I2S2O3-2BULK;
% fI2S2O3-2*1e06*(I2S2O3-2BULK - I2S2O3-2<#1>)/(s*AGL) : = I2S2O3-2<#1>;
TRANSPORT <#nzone> IS2O3- fIS2O3- fIS2O3-;
* no transfer across gas/liquid interface;
* outlet condition at film/BULK interface;
% fIS2O3-*1e06*(IS2O3-<#1> - IS2O3-BULK)/VL : = IS2O3-BULK;
% fIS2O3-*1e06*(IS2O3-BULK - IS2O3-<#1>)/(s*AGL) : = IS2O3-<#1>;
TRANSPORT <#nzone> S4O6-2 fS4O6-2 fS4O6-2;
* no transfer across gas/liquid interface;
* outlet condition at film/BULK interface;
% fS4O6-2*1e06*(S4O6-2<#1> - S4O6-2BULK)/VL : = S4O6-2BULK;
% fS4O6-2*1e06*(S4O6-2BULK - S4O6-2<#1>)/(s*AGL) : = S4O6-2<#1>;
**;


PSTREAM 4 10;
time I2OUT I-OUT I-BULK I3-OUT OI-OUT HOIOUT IOUT I2-OUT IO-2OUT;
**;

PSTREAM 5 11;
TIME R1 R2 R3 R4 R5 R6;
**;

PSTREAM 6 12;
time IO2HOUT I2OH-OUT I2S2O3-2OUT IS2O3-OUT I2G O2G;
**;

COMPILE TABLE;
* set up tables of results;
FOR #3=#nzone - 1;
I2OUT          = I2<#3>;
I-OUT          = I-<#3>;
I3-OUT         = I3-<#3>;
S2O3-2OUT      = S2O3-2<#3>;
S4O6-2OUT      = S4O6-2<#3>;
OI-OUT         = OI-<#3>;
HOIOUT         = HOI<#3>;
IOUT           = I<#3>;
I2-OUT         = I2-<#3>;
IO-2OUT        =  IO-2<#3>;
IO2HOUT        = IO2H<#3>;
```

```
O-OUT          = O-<#3>;
H+OUT          = H+<#3>;
HOUT           = H<#3>;
H2OUT          = H2<#3>;
OHOUT          = OH<#3>;
O2-OUT         = O2-<#3>;
I2OH-OUT       = I2OH-<#3>;
OH-OUT         = OH-<#3>;
O2OUT          = O2<#3>;
HO2-OUT        = HO2-<#3>;
H2O2OUT        = H2O2<#3>;
I2S2O3-2OUT    = I2S2O3-2<#3>;
IS2O3-OUT      = IS2O3-<#3>;
PSTREAM 4;
PSTREAM 6;
PSTREAM 5;
**;

WHENEVER time = 0.0 + 200.0 * 50 % CALL TABLE;
**;

BEGIN;
STOP;
```

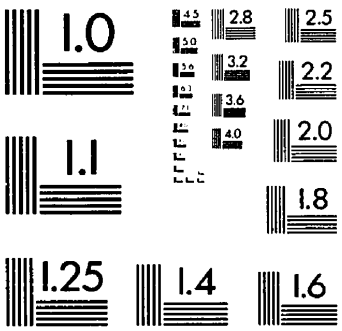

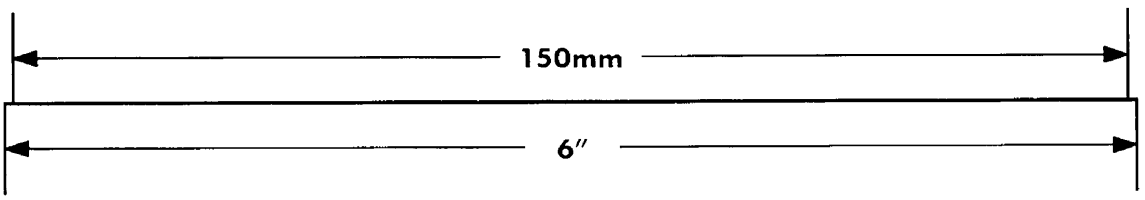

APPLIED IMAGE, Inc
1653 East Main Street
Rochester, NY 14609 USA
Phone: 716/482-0300
Fax: 716/288-5989